CZECH TECHNICAL UNIVERSITY IN PRAGUE

FACULTY OF MECHANICAL ENGINEERING

DEPARTMENT OF PROCESS ENGINEERING

COFFEE BEANS DRYER FOR DECENTRALIZED PURPOSES

DIPLOMA THESIS

Author: Eduardo Duque Dussán

Supervisor: Ing. Jan Skočilas, Ph.D.

Prague, June 2019

Annotation sheet

Name: Eduardo

Surname: Duque Dussán

Title Czech: Sušárna kávových zrn pro decentralizované účely

Title English: Coffee beans dryer for decentralized purposes

Scope of work: Number of pages: 130

Number of figures: 103

Number of tables: 5

Academic year: 2018/2019

Language: English

Department: Process Engineering

Supervisor: Ing. Jan Skočilas, Ph.D.

Submitter: Czech Technical University in Prague, Faculty of Mechanical Engineering, Department of Process Engineering.

Annotation: Local producers of coffee use a small convective dryer for product drying. This dryer has a lot of problems when it comes to engineering design and functioning. Therefore, the state of art of the local dehydration system of the coffee beans must be done and furthermore, an optimal design of a simple dryer shall be done fur such application.

Keywords: Coffee parchment, coffee benefit, drying air, humidity.

Utilization: Academical purposes and future projects from the Department of Process Engineering. Czech Technical University in Prague.

Declaration

Hereby I confirm that this master thesis was disposed by myself and independently, under leading of my supervisor. I stated all sources of documents and literature.

In Prague 7/06/2019

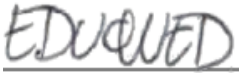

Signature

1. Introduction

Nowadays a small convective coffee dryer is used by the coffee growers to accomplish their needs. This coffee dryer, from the engineering point of view has a lot of problems when it comes to performance and design: the air is poorly distributed, the shape could be better displayed, the drying time is high and more. Therefore, the main focus of this work is to develop a new coffee dryer, using the same working principles as the actual and keeping it on a budget so the coffee grower is able to afford it, but, ensuring for him some benefit either on drying time, air distribution, energy cost reduction, etc.

We must gather then gather most of all the knowledge acquired during the whole master's program, hence we will be designing an optimal apparatus containing all the required parameters and demanded performance.

2. Coffee benefit (wet)

The coffee benefit is the process in which the transformation of the coffee bean to dried parchment coffee is achieved by separating the parts of the fruit and drying the grains, in order to preserve their physical, organoleptic and sanitary quality.

The coffee benefit process consists of a set of operations to transform the coffee fruits into high quality parchment coffee as for its physical properties and cup (taste) tests, which because of its stability in a wide range of environmental conditions, is the state in which this product is commercialized internally in Colombia.

The coffee benefit process is carried out by coffee farmers, mostly in the facilities they have in their farms, where they basically perform the receipt of the raw material (coffee beans), pulping, removal of mucilage, washing, various classifications (types of coffee or varieties) and drying.

In Colombia, the benefit is done by wet path, which includes the following main stages: Pulping, Removal of the mucilage (by natural fermentation or mechanical removal), Washing and Drying.

This type of benefit allows to obtain dry parchment coffee (dpc), of high quality, the qualities described by the Colombian coffee will after ensure a good cup rating, holding the world record in equilibrium, body, aroma and of course taste [25]. Dpc is the way which is sold by coffee growers in cooperatives or private traders. Then, the parchment coffee is threshed to extract the almond that is exported.

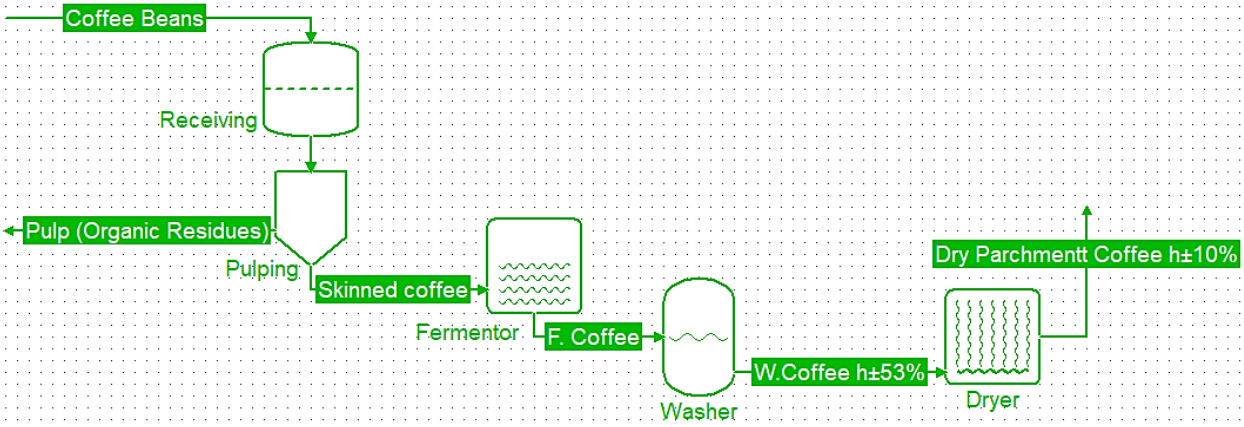

Figure 1. Coffee benefit process flow diagram (drawn in COFE Simulator).

The stages of coffee benefit in Colombia are described below:

Receive of coffee beans: In farms with productions of less than 300 arrobas of dry parchment coffee per year, the cherry coffee is received in the pulper's hopper. In farms with higher production, dry hoppers can be used, where coffee is received and transported by gravity to the pulper. Water should not be used in this stage.

Figure 2. Receive of coffee beans taken from http://www.tecapa.com/assets/img/beneficio/prochumedo01.jpg

Pulped: It consists in removing the pulp from the cherry by means of pressure exerted by the pulper's jacket, and it must be started immediately after the fruits are harvested. The delay for more than 6 hours affects the quality of the drink and can cause the defect called "ferment". The ripe coffee contains mucilage, which allows the pulping with just pressing the cherry. Therefore, no use of water is required to pulp off the coffee.

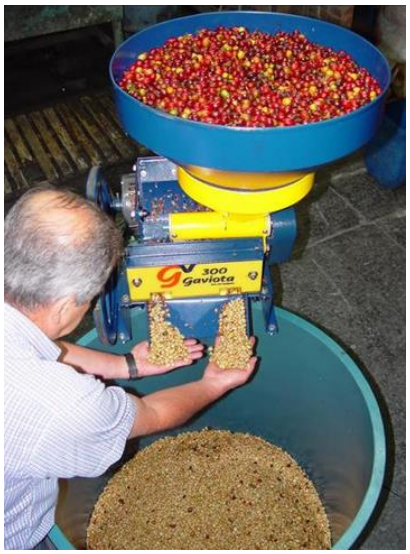

Figure 3. Process of pulping taken from http://cafemotilonazul.blogspot.com/2012/05/despulpado-del-cafe.html.

Afterwards, the retired pulp (skin) of the coffee is usually used as composting material or organic fertilizer.

Removal of the mucilage: The mucilage is the slime that covers the pulped grain. The mucilage must be removed by means of the natural or mechanical fermentation process.

The fermentation process is carried out in tanks (at least 2, each one with capacity to store the peak day coffee) where the pulped grain is received. In natural fermentation, its demanded time control ensure the final quality of the grain, because if the coffee is over-fermented non-desired flavours will be printed to the grain. If pulped coffee is mixed on different days, there may be over-fermentation as well.

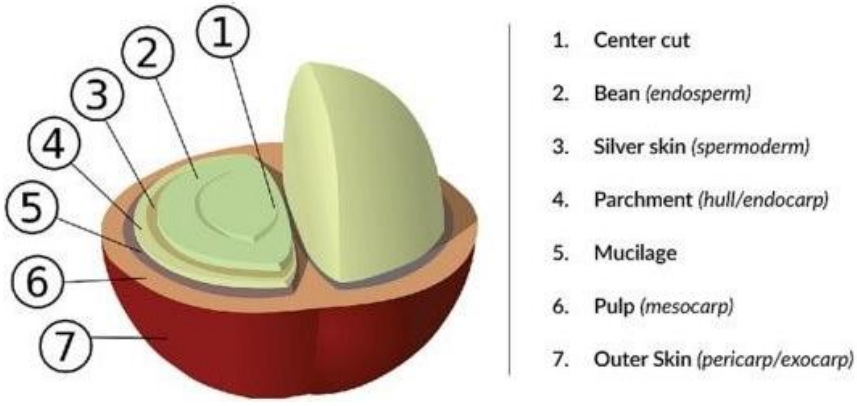

Figure 4. Anatomy of a coffee bean by layers. Taken from http://redberrycoffee.co.id/anatomy-of-a-coffee-bean/

The time of fermentation should be between 12 and 18 hours, depending on the ambient temperature (the higher temperature the lower fermentation time should be performed). Once the fermentation is finished, the coffee is washed.

Washed: The washing allows to completely remove the fermented mucilage from the grain. It must be used clean water to avoid defects such as grain staining, dirty grain, ferment taste and contamination.

Figure 5. Coffee washing tank. Taken from https://hectorellector.wordpress.com/2014/12/09/serie-cafe-sierra-nevada-de-santa-marta/

To facilitate washing, stirring blades are usually used. The washing of the fermented coffee is usually carried out in tub tanks by doing four rinses as follow:

- The first washing involves adding water and softly but deeply stirring the dough, draining the residue from the wash.

- In the second and third rinse, water is again supplied until the coffee mass is covered, stirred vigorously and the residue is again drained.

- In fourth step, water is added until it is above the coffee approximately five centimeters, it is stirred, it is held for a while to be able to remove the floating grains.

Drying: The drying of agricultural products is a practice used to conserve its nutritional value, physical quality, organoleptic and innocuousness for indefinite periods of time. By drying an agricultural product to the levels required in commercialization (10% to 12%, in most of them), the water activity is reduced to levels that impede the development of microorganisms and markedly decrease their metabolic activity [22].

At this stage the coffee benefit is finished, after some procedures as threshing, toasting and grinding are performed, but they do not form strictly part of the benefit.

3. Coffee drying

In the process of wet profit used in Colombia and other coffee producer countries, washed coffee parchment is obtained, with an average humidity of 53% [9] on wet basis w.b. Withdrawing from the fruit two structures that cover the grain, the epicarp or pulp and the mesocarp or mucilage, which represent the 44.75% and 16.06% in fresh weight of the fruit [11] respectively.

To preserve the quality of the coffee, the drying process must be started immediately. When the washed coffee parchment is left for more than 48 h with the initial humidity due to delay in the drying process or when stored with moisture contents higher than 12% w.b. (due to a deficient drying process), the risk of being attacked by fungi or contaminated with mycotoxins is very high. Fungal or OTA (Ochratoxin A) [4] contamination might be common as well if a bad practice in the benefit or drying process is performed (. The OTA is a toxin produced by certain fungi in the grain, it is a carcinogenic substance with nephrotoxic potential (it can produce renal tissue toxicity) [21]. These problems make the grain lose its quality and innocuousness, causing its rejection in national markets and international markets, which affects the country and coffee growers income.

In consideration of the above, the technology and technical developments in terms of drying are then considered as the most accurate response in terms of quality and economy for the grain drying process, in order to ensure the moisture content reduction up to 10% - 12%, allowing storage for extended periods.

In Colombia, mainly two drying methods are used: solar drying and mechanical drying systems.

3.1 Solar drying

This drying method is employed as only option mainly on farms with an annual production lower than 3,500 kg of dry coffee. Sun drying is also used on farms with higher production in days of lower flow of harvest. It has been developed relatively inexpensive and easy technologies to build and operate, which are successfully used in many of the coffee growing zones. Among the most used solar dryers used in Colombia we can speak about the parabolic sun dryer (Figure 6) [17], and the tunnel sun dryer type (Figure 7) [13].

Figure 6. Parabolic sun dryer. Taken from http://www.rufepa.com/invernadero/familia-productos/1/invernaderos/62/invernaderos-tipo-tunel/149/tunel-secadero-solar.html

Natural drying is done by free convection, taking advantage of natural energy of the ambient air and solar radiation that hits the surface of the grains, which is presented in layers with a maximum height of 2.5 cm, which when mixed during the day and while being picked up in the afternoon, ensure that the amount of grains receive as much as they can the same radiation and convection,

like this the desired uniformity and the highest efficiency energy of the global solar drying process is achieved.

Figure 7. Tunnel sun dryer. Taken from http://www.rufepa.com/invernadero/familia-productos/1/invernaderos/62/invernaderos-tipo-tunel/149/tunel-secadero-solar.html

In a 2.5 cm height coffee layer, the area that receives solar radiation direct is only 2.71% of the total area of the surface of the grains [17].

The capacity, the drying time (usually prolonged) and the final quality of the product depend mainly on the climatic conditions, which vary from one place to another and from time to time around the whole country, making this drying technique highly unpredictable, with high risk of seriously compromising its quality.

This situation is especially critical in the coffee growing zone, where rains are mostly permanent and few solar radiation is present during the harvest season and benefit of the grain. Even though in Colombia it has become trendy to produce export coffee type using natural drying systems, it is necessary to take into account its limitations, mainly in times where the climatic phenomena known as “La Niña” is present, this event is characterized by the increase of the precipitations by 20% and 40%, as well as the decrease in solar brightness and temperature in the coffee producing regions [8].

Also, when the coffee production in the farm increases because of coffee plantation renewal, better management of plantation density or increase of the plantation itself (number of trees per hectare). With the use of mechanical drying, especially in the days of greater flow of the crop, advantages are obtained such as reduction of labor, reduction of drying time and preservation of quality, with less risk to the quality and safety of coffee [23].

There is no updated information available of the number of coffee dryers used in Colombia, the technology used or the capacity of the equipment. However, as an approximation, it can be estimated that mechanical drying is used in 27,650 farms with an area planted in coffee of more than 5 ha, which in Colombia represent 5% of coffee growers [6], which account for 31% of annual national production.

In mechanical coffee drying systems, the moisture content of the coffee can be reduced from 52% -55% to 10% -12% (h.b), in a relatively short period of time (18 to 32 h, depending of the type of

dryer and the operating conditions of the system), thus reducing the risk of deterioration caused by the attack of fungi and microorganisms. However, if the dryer is not designed and operated properly, for instance, if a certain thickness of grain layer is not supplied with the necessary and required amount of air at the right temperature, the dryer will not efficiently perform the removal of moisture, compromising the quality of the grain, it also might increase the energy requirement (thermal and electrical) and the cost of working labor, plus increasing the costs of the drying process .

Research results performed by the National Coffee Research Center of Colombia (Cenicafé) indicate that for dryers in static layer, the minimum recommended flow is 38 m3.min-1.m-3 of parchment coffee (that is, 100 m3. min-1.t-1 of dry coffee parchment-dcp) and maximum temperature of drying air of 50 °C [15, 16].

3.2 Mechanical drying

As we already said, since the beginning of coffee growing in Colombia, solar dryers have been used, in which, the irradiated energy of the sun and the convection of the air is used to reduce coffee moisture from an average of 53% h.b. up to the required range in its commercialization (10% to 12% h.b.). However, the increase in productivity as a result of research and the coincidence of the harvest season with the rainy season, led to the use of mechanical dryers, with which the drying capacity is increased, drying time decreases, and the process control is improved.

Figure 8. Rotative drum dryer. Taken from https://fundidoradelnorte.com/wp-content/uploads/2014/10/2-secadora-rotativa-pa-sr7.jpg

One of the mostly known technologies is the rotative drum dryer (Figure 8), this system consists on a large perforated drum, which rotates very slowly on its axis (<2 rpm), with a fixed central tunnel, which is drilled, through which hot air enters the drying chamber that is formed between the pipeline center and the drum housing [24]. The coffee is deposited inside the drum, without filling it completely, while the rotation favors the movement and mixing of the grains. Finally, the exhaust air exits to the environment through the perforations of the drum. Although some dryers are still used because users argue good final uniformity of humidity, it has disadvantages such as

prolonged drying time, low thermal efficiency, high maintenance requirement, complexity in handling and pre-drying need, among others.

The first dryer developed for coffee in Colombia, which has been reported, was the so-called “Silo Secador Cenicafé” (Figure 9), which was designed in the mid-1970s by the Postharvest Discipline of the National Coffee Research Center. The dryer is constituted by a central tunnel where it counts with the opening and closing of eight gates, allowing the air distribution to be even into two drying chambers arranged in the same plane, as indicated in Figure 10. The gates also allow to change the direction of the Air flow in each drying chamber, ascending or descending, in order to achieve a better uniformity of the final moisture of the product.

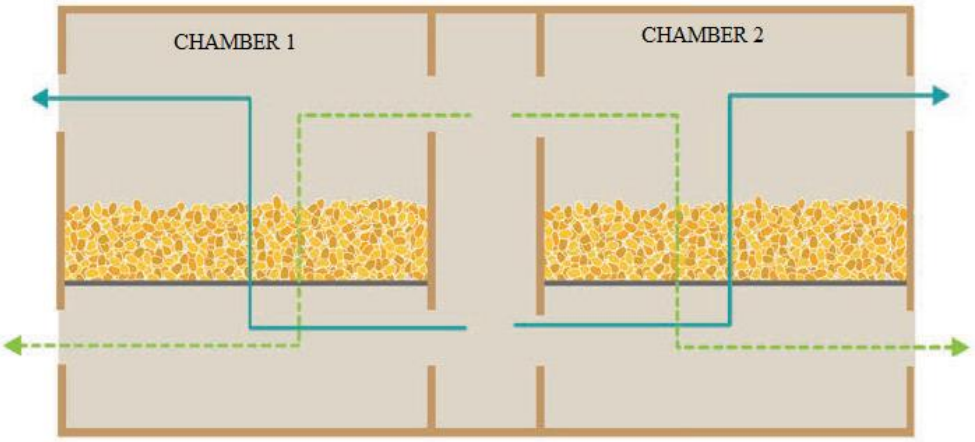

Figure 9. Diagram of operation of a Central Tunnel Cenicafé Dryer. The arrows in continuous line indicate the ascending air flow, which after a few hours and with the help of the floodgates, is reversed to have downward air flow (lines with points).

In these dryers it was difficult to operate the hatches because the operator had to enter the tunnel, which was narrow and hot. Additionally, the flow of drying air increased markedly when there was only one chamber with coffee, which increased the consumption of fuel and electrical energy in the drying and it was difficult to determine the completion of the process. To overcome the mentioned limitations and increase the energy efficiency in the process, taking advantage of the drying capacity of the exhaust air, the Cenicafé Drying Silo was modified to work in series with one layer in drying and another in pre-drying, operating as follows: The hot air enters initially through the upper part of the coffee mass located in chamber 1, as shown by line A of in the Figure 10, initiating drying; if it is desired to obtain a greater uniformity in the moisture content of the grain, the air flow must be reversed periodically every 6 to 12 hours (line B) until obtaining the desired final moisture content; Once the grain is dry, it is removed from chamber 1. If more wet coffee is available, chamber 1 is filled and the drying air is passed, first through chamber 2, periodically inverting the air flow, as it is indicated by lines C and D, until the coffee in chamber 2 is dry.

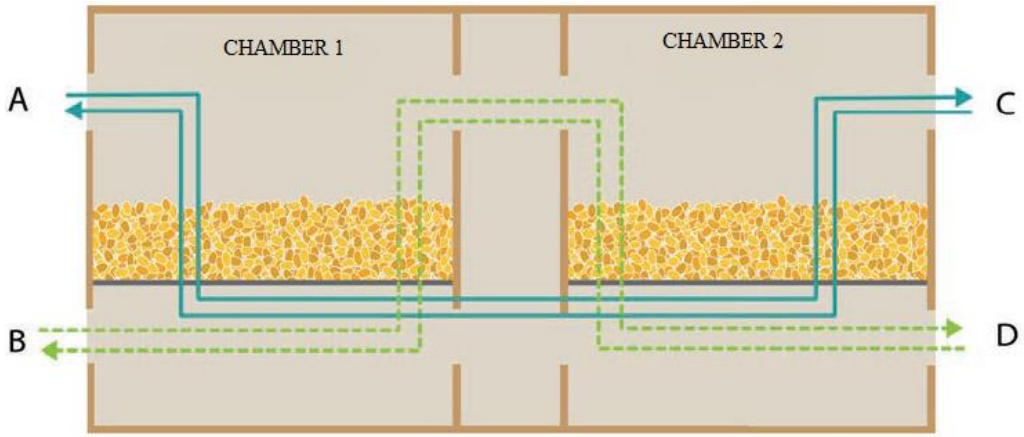

Figure 10. Outline of operation of a Silo Cenicafé modified dryer. The arrows in continuous line indicate the ascending air flow, which after a few hours and with the help of the floodgates, is reversed to have downward air flow (lines with points).

If there is more coffee to dry, it is taken to chamber 2 and the drying process is started again, reversing the direction of air flow; the process is repeated as many times as necessary. Although the modification required two additional gates, the handling of these was facilitated using levers operated externally. This technology was built in masonry and with materials available in the coffee zone, has been widely used in Colombia (Figure 11). From the modified Cenicafé Silo Dryer, the national industry has designed new technologies, looking for simple construction equipment to reduce production costs, to obtain better uniformity of dry coffee moisture. The simplest option is a small single layer dryer, which has an air flow reversal system, to improve the uniformity of the final moisture as shown in the Figure 12.

Figure 11. Silo Secador Cenicafé Dryer.

Other technologies manufactured in Colombia are the two or three layer dryers, arranged vertically. Figure 13 shows a diagram of a dryer with two vertical chambers, in which the inversion of air flow is made only in the lower one. Once the coffee in the lower chamber is dry, it is removed from the dryer and the coffee is passed from the upper chamber to the lower chamber, unloading

it with the help of a wooden ruler and using a central opening in the floor that holds the coffee, which is usually covered with a mesh, first the coffee of the highest part of the layer, which has more humidity, and finally the lower coffee that is drier. In this way it is possible to invert the order of the coffee in the unloaded layer, which facilitates obtaining the highest final uniformity of the coffee. Subsequently, the upper chamber is again charged with washed coffee to establish the drying cycle. The system requires an external duct and gates to direct the air to the pre-drying chamber.

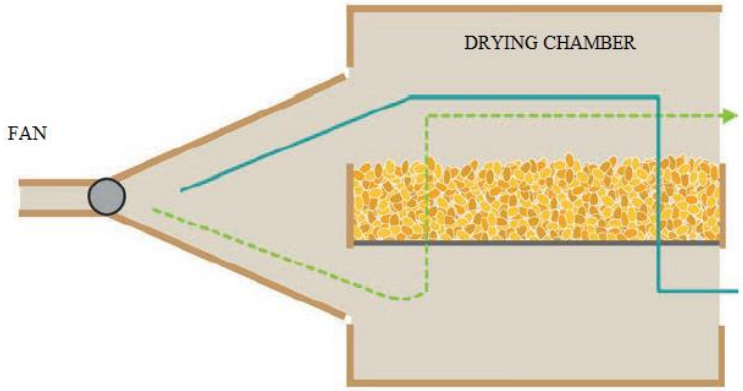

Figure 12. Diagram of operation of a single-layer dryer with reversal of air flow. The continuous line arrow indicates the descending air flow, which after a few hours and with the help of the floodgates, is inverted to have upward air flow (dashed line).

The three-floor dryer is offered with two options: with reversal of the air flow in the lower chamber or without reversal of air flow. The first option also requires an external duct and gates, a sliding plate to remove it when the air flow is up in the drying chamber (Figure 14).

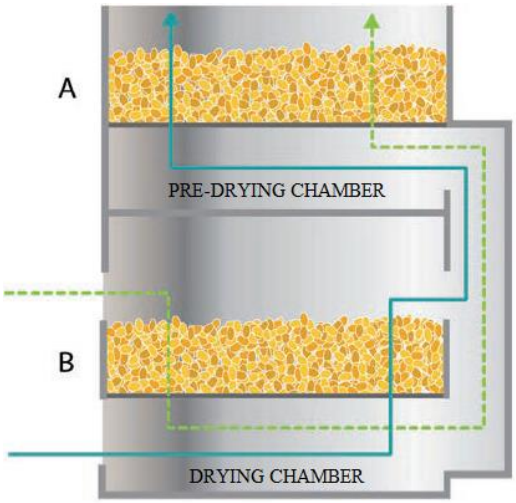

Figure 13. Scheme of operation of a dryer of two floors with inversion of air flow in the lower chamber. Direction of air flow at the start of drying (arrow in solid line), which is reversed after a few hours (arrow in dashed line).

The second option does not have an external duct, or gates, or sliding plates and bases the uniformity of the drying in an orderly passage of coffee from one chamber to another, just as the

procedure was described in the two-layer dryer. This last provision is the most economical in terms of initial investment, but it is the one that requires the most labor.

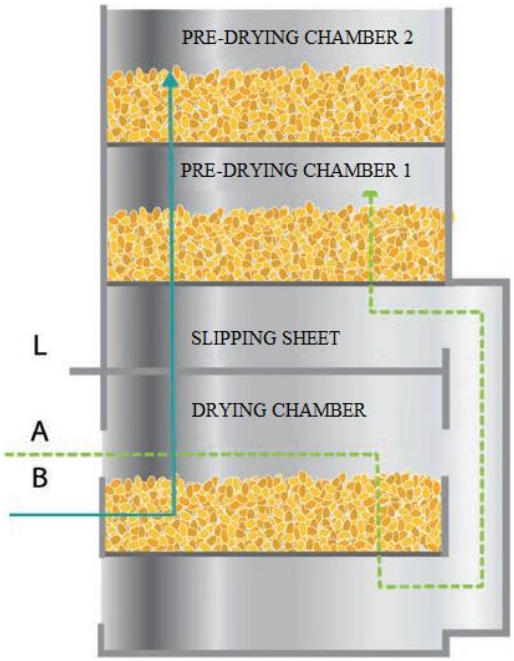

Figure 14. Diagram of operation of a dryer with three fixed layers arranged vertically, with inversion of air flow in the lower chamber. Direction of air flow at the start of drying (arrow in solid line), which is reversed after a few hours (arrow in dashed line).

Figure 15 shows some example equipment manufactured by the Colombian industry to meet the needs of coffee drying, in a wide range of annual production. The equipment consists of three drying chambers. For farms with production of 2,500 to 3,750 kg of dry coffee / year, with a static capacity of 178 kg of washed coffee (approximately 94 kg of dried parchment coffee), using propane gas in direct combustion to heat the drying air to an average of 50 ° C. For farms with production of up to 10,000 kg of dry coffee / year, equipment is manufactured with the capacity to dry 500 kg of washed coffee (approximately 262 kg of dry parchment coffee), with heat exchanger, using as fuel generally leftover parchment or coffee husks, with mechanical or gravity feed. They are intended mostly for top harvest or for drying during the raining season, so the farmer would not be stuck up with wet coffee waiting to be dried.

For greater drying needs, the industry offers dryers with a static capacity of 10,600 kg of washed coffee (approximately 5,625 kg of dry parchment coffee), with automatic mechanical agitation for the coffee in each drying chamber, mechanical unloading of coffee between chambers and removal of dry coffee using auger.

In order to obtain a better quality product, with greater uniformity in humidity at the end of the process and greater energy efficiency, a parchment coffee dryer was designed and evaluated in Cenicafé, with the characteristics presented in Figure 16. The equipment consists of a resting chamber in the upper part, connected to a drying chamber by means of hoppers designed to restrict the upward flow of the drying air; It also allows the mixture of the coffee mass, helping to

uniformize its moisture content. The coffee and the drying air flow downwards in the drying chamber.

Figure 15. Dryer with mechanical agitation of the coffee in the chambers and discharge with screw.

The exhaust air is removed from the drying chamber by means of ducts. The coffee passes from the drying chamber to the discharge hopper by means of smaller internal hoppers, designed to allow a similar speed of the grains in the section of the dryer and thus prevent the grains from adhering to the internal surface of the dryer. dryer walls in this section, especially in the early stages of the drying process, by the presence of moisture film on its surface. In the parts of the dryer where the grains are not in contact with the drying air, called resting, the grains undergo moisture diffusion from the interior to the exterior, facilitating their removal when passing through the drying stage. This dryer is called intermittent flow of concurrent (grain and drying air), taking into account the direction of air and of the grains in the drying chamber and the intermittency in the energy supply for drying.

In fact, according to the physical laws that govern the drying phenomenon, the process begins by creating dis-uniformities of moisture in the coffee layers, and only through the good management recommended for each type of dryer these differences can be gradually diminished, until that at the end of the process it is possible to obtain the required moisture values.

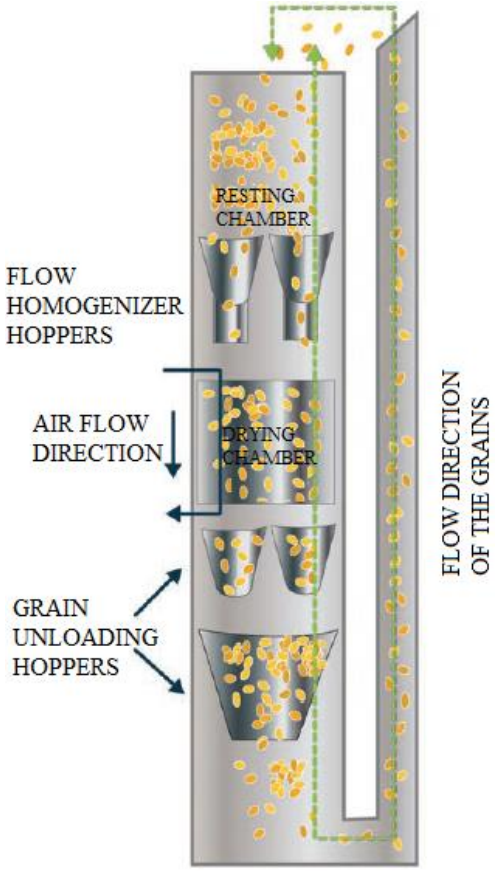

Figure 16. Diagram of an intermittent concurrent flow coffee dryer (ICF).

Therefore, it is necessary to know each type of dryer well, to detect when it is malfunctioning and what must be done to correct the problems of the dryer and/or its operation. The most appropriate, for all cases, is that the solution is always achieved by following the essential procedures, simple but necessary, as indicated.

4. Mathematical models for the mechanical drying of grains

The models proposed to predict the behavior of grain drying are classified as: non-equilibrium, equilibrium and logarithmic; however, this classification cannot be defined in an exact way, so it must be taken in approximate form.

The drying models of non-equilibrium grains are more accurate and more elaborated. In these the drying model is developed as a system of partial differential equations from the heat transfer and mass balances.

In the equilibrium models for grain drying or simplified models, the basic approach for the simulation is to calculate the drying in a thin layer of grains by means of heat and mass balances (equilibrium model), and by an iterative process, many thin layers are combined to form the thick layer. The heat transfer between the grain and the surrounding air occurs fast, therefore, the temperature of the grain is assumed equal to the temperature of the air that is close to it; In addition,

the grain reaches the moisture content in equilibrium with the psychrometric conditions (temperature and relative humidity) of the surrounding air. The equilibrium moisture content is one of the factors that determine the removal of moisture from the grain layer.

The logarithmic models of grain drying are based on the direct relationship between the rate of drying of a grain layer,

$$\frac{\partial M}{\partial T}$$

and the air temperature gradient that goes through it,

$$\frac{\partial T}{\partial x}$$

Even though these models have a low prediction of the drying phenomenon, they have been used by many researchers, in some applications, due to their simplicity since long time ago, plus predicting is better than non-predicting, so even if they accuracy is questionable, they provide a real approach for the process itself.

On the other hand, even when several models have been developed for the simulation of grain drying, the most used are the Thompson model [18] and the MSU model (Michigan State University) developed by Bakker- Arkema et al. [1].

4.1 Thompson model:

The Thompson model is a semiempirical equilibrium model that was originally developed to simulate the drying of husked corn [5, 14, 15, 19]. In this model it is considered a thin layer of grains, each formed by layers of 2.5 cm thick, placed one on top of the other. The basic approach for the simulation is to calculate the drying in a thin layer of grains by means of heat and mass balances (equilibrium model), and by means of an iterative process extend it to more thin layers until it is reached the same dimensions of the layer thickness as the one of the products in the dryer. The drying of a thin layer can normally be represented by means of equations representing the change of the humidity of the grains of the layer with respect to time, according to the different temperatures and humidity of the drying air.

As it is seen in the Figure 12, the air flow initially at a temperature (T) and at a moisture ratio (H), goes through the first thin layer of grains having an initial humidity (M_1) and an initial temperature (Tg_1). After some time-lapse (Δt), a certain amount of humidity (ΔM_1) evaporates from the grains, being transported by the air, which happens to have a higher humidity ratio ($H + \Delta H_1$). At the same time, the air decreases its temperature at ($T - \Delta T_1$) proportionally to the increase in temperature of the grain ($Tg_1 + \Delta Tg_1$). The released air conditions of the first thin layer of grain (thin layer 1), are the conditions of entry for the next layer (thin layer 2), and so on the layers are

augmented, with the same mathematical analysis, until completing the thick layer of grain (real layer, in the dryer chamber).

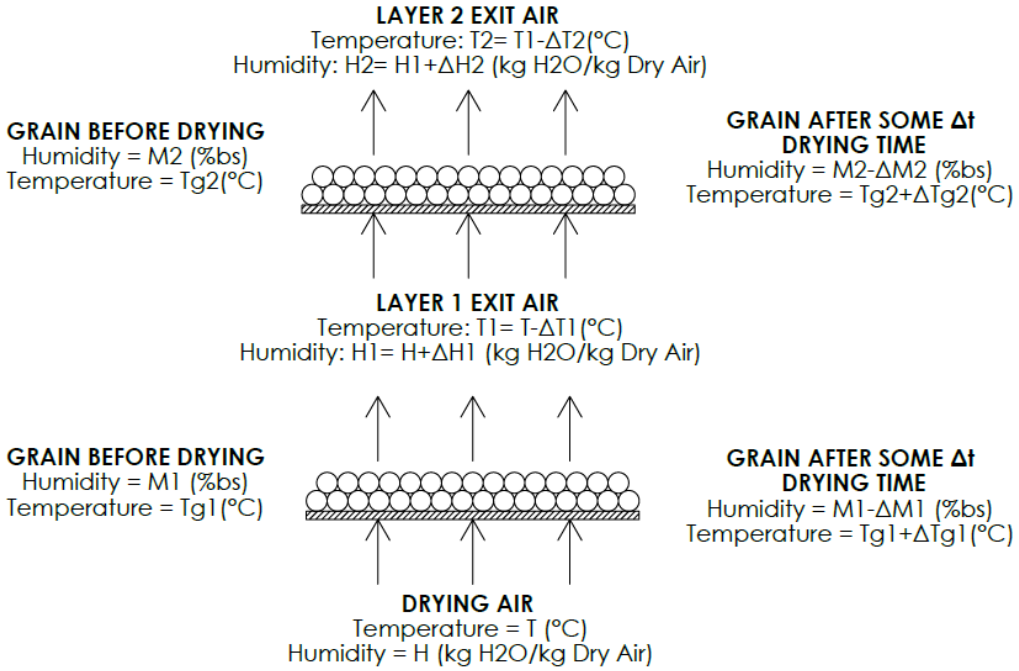

Figure 17. Schematic of Thompson's thin-film drying simulation model. Drawn in solidworks by the author.

The model predicts the final drying of the grain layer by using equilibrium equations (balance before and after drying) and semi-empirical equations such as equilibrium moisture content, specific heat, latent heat of vaporization of contained water in the grain and the thin-layer drying equation, for which the initial air and grain conditions must be considered. The heat balance is completed by predicting the final air and grain conditions. The model is flexible and allows to integrate in it all the variables and parameters necessary to simulate the drying process. Once the complete model is available it is especially useful for the study of different drying systems and for the design of equipment.

4.1.1 Before drying balance:

In Thompson's model, a sensible heat balance is made before starting the drying process, which consists in determining the equilibrium temperature between air and grain. The equilibrium temperature (T_e) is determined from the humidity ratio and the temperature of the drying air (H and T respectively), and from the temperature and specific heat of the grain (T_g and c_p respectively), as indicated in the Equation 1

$$T_e = \frac{(0.24 + 0.45H)T + c_p T_g}{0.24 + 0.45H + c_p} \qquad (1)$$

4.1.2 After drying balance:

The simulation of the grain layer drying is done using the equations of equilibrium moisture content and thin layer drying; In addition, the synchrometric balances of the drying air are made. The balance after the drying of a thin layer consists in determining the air and grain temperature (T_f) once the time interval Δt has elapsed; for this, the latent heat of vaporization of the water contained in the grain, L., is considered. The grain will have lost moisture (ΔH), which will have been removed by the air (increasing its humidity ratio to H_f. The heat balance after drying is presented in Equation 2

$$T_f = \frac{(0.24 + 0.45H_0)T_e - \Delta H(587.9 + L - T_e) + c_p T_e}{0.24 + 0.45H_f + c_p} \qquad (2)$$

In continuous dryers of concurrent flow, the grains and air move in the same direction. The grain in the dryer is considered as a set of thin layers, with the drying air flowing down through the grain layers. For each time interval, a new grain layer is located on top of the dryer and a layer is removed from the bottom. The procedure to simplify the simulation consists of calculating the humidity changes of a layer as it moves through the dryer. In other words, if the time interval is appropriately selected, the output air of one layer in the first position during the first period of time, is the input air for the same layer, which is in the second position during the second period of time and so on, until the desired depth is obtained. This simulation represents equilibrium or steady state in concurrent flow drying processes, with the initial air and grain conditions known, and for a preset grain flow rate. For a given depth, the flow rate of the grains will determine the final moisture content.

The variables used in the equations of the Thompson models are the following:

- c_p: Specific heat of the grain, $\left[\frac{kJ}{kgK}\right]$
- ΔH: Moisture removed by air during time Δt $\left[\frac{kg}{h}\right]$ of water.
- H: Ratio of air humidity, $\left[\frac{kg_{steam}}{kg_{dry\ air}}\right]$
- H_0: Ratio of air humidity before passing through the grain layer, $\left[\frac{kg_{steam}}{kg_{dry\ air}}\right]$
- H_f: Ratio of air humidity after passing through the grain layer, $\left[\frac{kg_{steam}}{kg_{dry\ air}}\right]$
- L: Latent heat of vaporization of grain water, $\left[\frac{kJ}{kg}\right]$
- T: Drying air temperature, $[°C]$
- T_g: Grain temperature, $[°C]$

- T_f: Final temperature of drying air and grain, $[°C]$
- T_e: Equilibrium temperature of drying air and grain, $[°C]$

4.2 MSU Model (Michigan State University):

The MSU model, developed by Bakker-Arkema et al. [1, 2, 3, 5, 12, 14, 15] is a theoretical non-equilibrium model, and is based strictly on the laws of heat transfer and mass. The MSU model has the same basic approach as the Thompson model, since it divides the drying process into small increments of time and grain thickness, using the conditions of air output from one layer as input conditions for the next; calculates the air and grain conditions in each increment of time and layer thickness by making four balances:

- Balance for the enthalpy of the air
- Balance for air humidity.
- Balance for the enthalpy of the grain.
- Balance for grain moisture.

These balances originate partial differential equations that are solved simultaneously by numerical integration, using in our case finite differences, starting from initial and frontier conditions [1]. With this model, the operation of stationary dryers, crossed flows, concurrent flows and countercurrent can be simulated.

4.2.1 Simulation process in static dryers using the MSU Model:

The MSU model performs the mass and energy balances on a differential volume (Sdx), located at an arbitrary position within the stationary dryer. The unknown variables in the model are the moisture content and the temperature of each grain, the humidity ratio and the drying air temperature in the dryer.

As a result, the model for a fixed layer dryer consists of four partial differential equations, coming from the mass and energy balances of the grain and drying air and a thin layer drying equation for the grain, namely:

- Balance for the enthalpy of the air: The energy that comes out is equal to the energy that enters less the energy transferred by convection:

$$\frac{\partial T_a}{\partial x} = \frac{-h_a}{G_a c_a + G_a c_v H}(T_a - T) \qquad (3)$$

- Balance for the enthalpy of the product: The energy transferred is equal to the change in internal energy of the product minus the energy for evaporation:

$$\frac{\partial T}{\partial t} = \frac{h_a}{\rho_p c_p + \rho_p c_w M}(T_a - T) + \frac{h_{fg} + c_v(T_a - T)}{\rho_p c_p + \rho_p c_w M} G_a \frac{\partial M}{\partial x} \qquad (4)$$

- Balance for the humidity ratio of the air: The humidity transferred is equal to the humidity that enters minus the humidity that leaves:

$$\frac{\partial H}{\partial x} = -\frac{\rho_p}{G_a}\frac{\partial M}{\partial t} \qquad (5)$$

- The thin-film drying equation of the product or grain moisture balance, for which a suitable thin-film equation should be used. It should be as follows:

$$\frac{\partial M}{\partial t} = f(M, M_e, M_o, T, \dots t) \qquad (6)$$

The previous equations constitute the simulation model for fixed layer drying. However, an analytical solution of the system of equations is not known, so approximate solution techniques, by differences or finite elements, should be used.

4.2.2 Simulation process in concurrent flow dryers using the MSU Model:

Similar to the model for static layer dryers, the model for concurrent flow dryers performs the mass and energy balances on a differential volume (Sdx). The following equations are the result from the indicated balances:

$$\frac{\partial T_a}{\partial x} = \frac{-h_a}{G_a c_a + G_a c_v H}(T_a - T) \qquad (7)$$

$$\frac{\partial T}{\partial x} = \frac{h_a}{G_p c_p + G_p c_w M}(T_a - T) - \frac{h_{fg} + c_v(T_a - T)}{G_p c_p + G_p c_w M} G_a \frac{\partial H}{\partial x} \qquad (8)$$

$$\frac{\partial H}{\partial x} = \frac{G_p}{G_a}\frac{\partial M}{\partial x} \qquad (9)$$

For thin layer, some equation stating the following should be used,

$$\frac{\partial M}{\partial x}$$

Which represents a general form from the presented in Equation 6.

The differential equations in the concurrent flow dryer model are ordinary differential equations (ODE), while in the static dryers model they are partial differential equations [1].

The numerical solution of the MSU models requires knowing the initial and edge or boundary conditions of the grain and drying air. Between the initial conditions of the grain and the air we can have: initial temperature and moisture content of the grain; temperature and humidity ratio of the drying air at the entrance.

The variables used in the equations of the MSU models are the following:

- a: Specific area of the product, $\left[\frac{m^2}{m^3}\right]$
- c_a: Specific heat of air, $\left[\frac{kJ}{kgK}\right]$
- c_p: Specific heat of the grain, $\left[\frac{kJ}{kgK}\right]$
- c_v: Specific steam heat, $\left[\frac{kJ}{kgK}\right]$
- c_w: Specific heat of water, $\left[\frac{kJ}{kgK}\right]$
- G_a: Air mass flow per unit area, $\left[\frac{kg}{hm^2}\right]$
- G_p: Mass flow of grain per unit area, $\left[\frac{kg}{hm^2}\right]$
- H: Ratio of air humidity, $\left[\frac{kg_{water}}{kg_{dry\ air}}\right]$
- h: Coefficient of heat transfer by convection, $\left[\frac{kJ}{hm^2K}\right]$
- h_{fg}: Latent heat of vaporization, $\left[\frac{kJ}{kg}\right]$
- M: Local moisture content of the grain, decimal bs.
- ρ_p: Density expressed on the basis of the dry weight of the grain, $\left[\frac{kg}{m^3}\right]$
- t: Time, $[h]$
- S: dryer section perpendicular to the air flow, $[m^2]$
- T_a: Air temperature, $[°C]$
- T: Grain temperature, $[°C]$
- x: Coordinate within the deep layer of grain, $[m]$

5. Parameters of coffee drying simulation models

For the mathematical simulation of drying it is necessary to know the physical characteristics of the grain and the psychrometric properties of the drying air. Regarding the physical characteristics of the grain, it is necessary to know the apparent specific weight (bulk density), as well as the equations of moisture content in equilibrium, specific heat, latent heat of vaporization and thin layer drying. The temperature and relative humidity or humidity ratio must be established for the drying air. The equations and characteristics of the grain were determined by the National Coffee Research Center of Colombia (Cenicafé) in different research development [7, 10, 12, 14, 15, 20]

5.1 Heat transfer coefficient by convection between the air and the grain:

Brooker et al. [2] developed the following equation, which describe the approach for the calculation of the convective heat transfer coefficient in grains, which is used in the mathematical simulation drying models of the Michigan State University (MSU) the constants A, B, C and D are calculated by the MSU developers for the grain drying and are used here as follows.

$$h_c = Ac_a G_a \left(\frac{2r_0 G_a}{C + DT}\right)^B \qquad (10)$$

Where:

- h_c: Convection heat transfer coefficient, $\left[\frac{W}{m^2 K}\right]$
- r_0: Equivalent radius of the particle (coffee bean), $[m]$
- c_a: Specific heat of air, $\left[\frac{kJ}{kgK}\right]$
- G_a: Air flow, $\left[\frac{kg}{hm^2}\right]$
- T: Air temperature, $[K]$
- A: 0.2755
- B: -0.34
- C: 0.06175
- D: 0.000165

5.2 Specific heat of parchment coffee:

Montoya et al. (12) used the method of mixtures to determine the specific heat of parchment coffee in the grain moisture range between 11% and 45% h.b, obtaining the following:

$$c_p = 1.3556 + 5.7859M \qquad (11)$$

Where:

- c_p: Specific heat, $\left[\frac{kJ}{kgK}\right]$
- M: Moisture content, decimal.

5.3 Moisture content in coffee parchment equilibrium:

Trejos [20] used the dynamic method, proposed by Rossi and Roa, for the determination of equilibrium moisture content for parchment coffee.

$$M_e = \left(P_1 H_R + P_2 {H_R}^2 + P_3 {H_R}^3\right) e^{\left(Q_1 H_R + Q_2 {H_R}^2 + Q_3 {H_R}^3\right)T} \qquad (12)$$

Where:

- M_e: Balance moisture content of parchment coffee, % humidity.
- H_R: Relative humidity, decimal.
- T: Air temperature, [$°C$]
- P_1 = 61.030848
- P_2 = -108,37141
- P_3 = 74.461059
- Q_1 = -0.03049
- Q_2 = 0.070114
- Q_3 = -0.035177

This equation is valid for a temperature range of 10 to 56 ° C and relative humidity between 0% and 100%.

5.4 Latent heat of vaporization of parchment coffee:

Trejos [20], from the hygroscopic equilibrium isotherms obtained for parchment coffee, Equation 12, and applying the Othmer method, determined the latent heat equation of vaporization of parchment coffee, which has the following form:

$$L = (2502.4 - 2.42958T)[1 + 1.44408e^{-21.5011M}] \qquad (13)$$

Where:

- L: Latent heat of vaporization of parchment coffee, $\left[\frac{kJ}{kgK}\right]$
- T: Coffee temperature, [$°C$]
- M: Coffee moisture content, decimal.

5.5 Thin-film drying equation:

López and Ospina [10], used the dynamic method for the determination of the coefficients (m, n and q) of the drying equation in thin layer of Roa, for coffee moisture contents from 55% h.b. up to moisture equilibrium. The coefficients of the following equation were determined for three ranges of drying air temperature.

$$\frac{\partial M}{\partial t} = -mq(M - M_e)(P_{vs} - P_v)^n t^{(q-1)} \qquad (14)$$

Where:

- M: Moisture content of the grain at any time, decimal, d.b.
- M_e: Balance moisture content, decimal, d.b.
- P_{vs}: Saturation vapor pressure, [kPa]

- P_v: Partial vapor pressure, $[kPa]$
- t: Drying time, $[h]$

Based on preliminary drying simulations carried out by Parra-Coronado, Roa determined the parameters m, n, and q for the unified thin-layer drying equation [14, 15], valid for the ranges of 10 to 70°C of temperature and from 5% to 55% humidity in h.b (Figure 18).

$$m = 0.0143;\ n = 0.87898;\ q = 1.06439$$

5.6 Humidity diffusion coefficient:

Montoya et al. [22], obtained an equation for the coefficient of moisture diffusion in parchment coffee as a function of moisture and grain temperature. The expression is valid for humidity contents less than or equal to 50% d.b. (33.33% h.b.) and is presented in the following equation:

$$D = 4.1582 \times 10^{-8} e^{\left[(0.1346\,T_g + 2.2055)M - \frac{1184}{T_g + 273.15}\right]} \qquad (15)$$

Where:

- D: Humidity diffusion coefficient, $\left[\frac{m^2}{min}\right]$
- M: Average moisture content of the grain, decimal, d.b.
- T_g: Grain temperature, $[°C]$

5.7 Specific area of the parchment coffee:

When considering the coffee bean as a sphere, Montoya et al. [22], obtained a specific area of $779.8\ \left[\frac{m^2}{m^3}\right]$ for parchment coffee, in the range of moisture content from 10% to 25.6 % h.b, which was applied in the MSU model for a concurrent flow IFC dryer.

5.8 Apparent density (apparent specific weight) of parchment coffee:

From the following equation, developed by Montoya et al. [22], the apparent density of the parchment coffee is estimated, as function of the moisture content:

$$\rho_a = 365.884 + 270.67M \qquad (16)$$

Where:

ρ_a: Apparent density, $\left[\frac{kg}{m^3}\right]$

M: Moisture content, decimal, d.b.

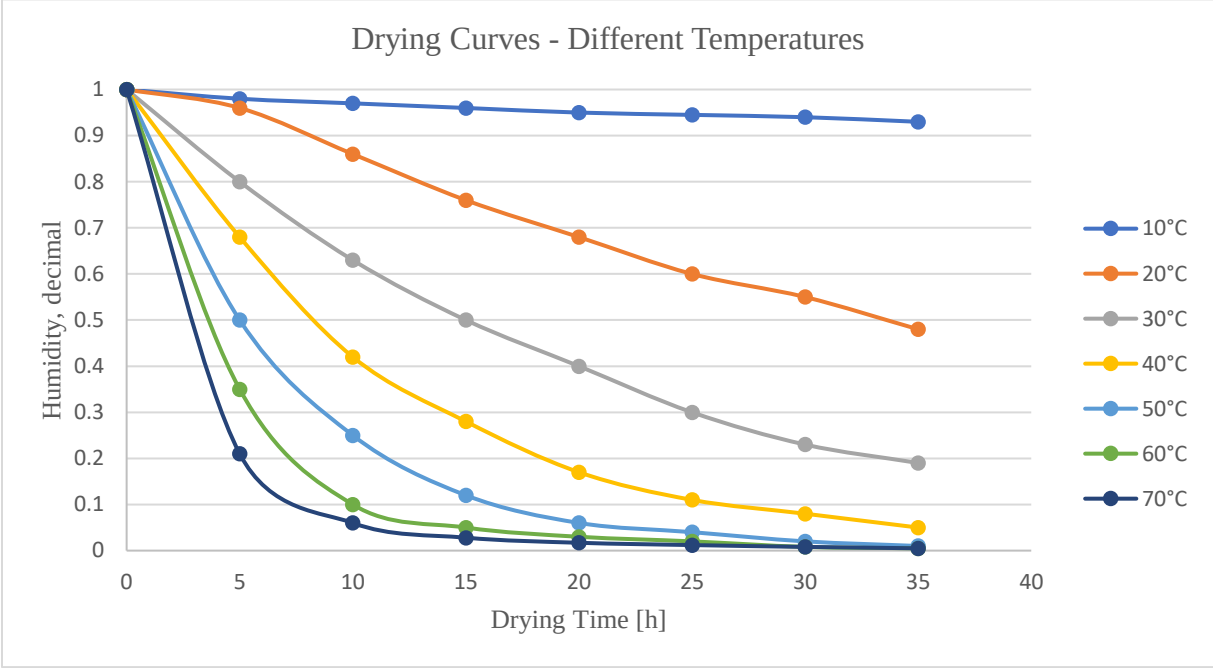

Figure 18. Thin layer curves for parchment coffee drying calculated with Equation 14 and with the given parameters. Given by Cenicafé.

6. Problem definition

In Colombia there are around 541000 coffee farmers, of which 521,000 are small coffee growers. Those who have between zero and five hectares sown in coffee are classified as small coffee farmers. In general, the small coffee grower is in low socioeconomic conditions and their income is not very high, since their land is limited and sometimes the price of coffee is not very favorable for them.

It should be remembered that in rainy seasons solar radiation and air convection are not optimal for drying coffee quickly (using solar drying techniques), leading to the product possibly being infected by fungi or unwanted microorganisms. If we add to this the fact that the small coffee grower is generally in unfavorable conditions, he would then be forced to sell the wet coffee (for which he would get less money) or pay a coffee-drying plant to safeguard their harvest, which is not very smart from an economic point of view because these plants normally charge high fees for their services.

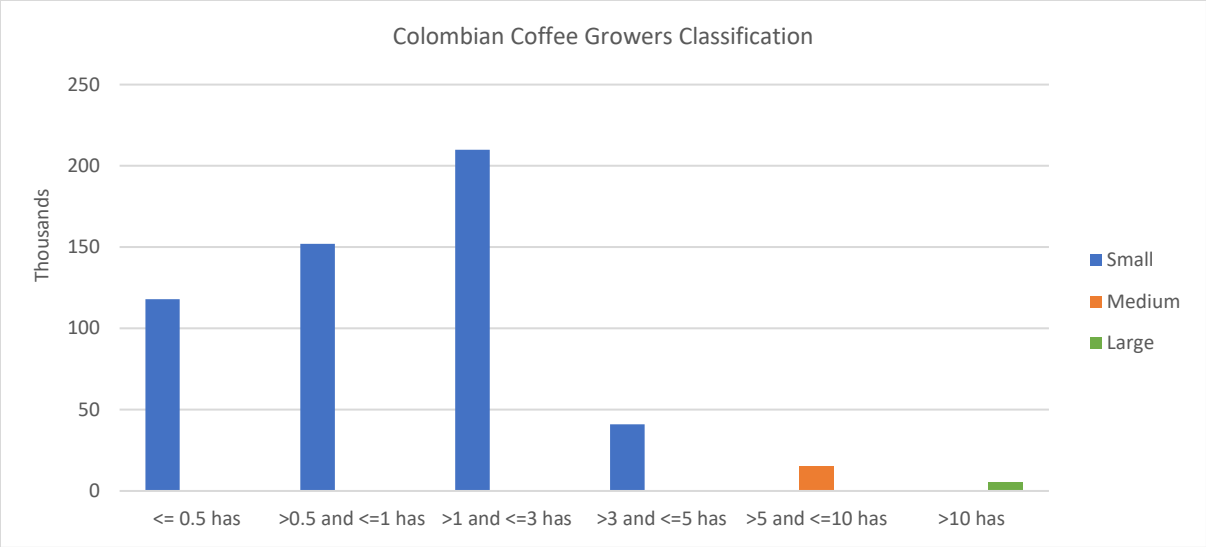

Figure 19. Coffee growers classification according to their sown coffee area. Data given by Cenicafé.

That is why the coffee research center representing the National Federation of Coffee Growers of Colombia along with some private companies have developed equipment that is within the reach of these coffee farmers to be able to dry their coffee effectively and quickly.

The most commonly used equipment for this task is a vertical dryer of capacity 93.75 kg (12.5@, arroba was a Portuguese and Spanish custom unit of weight, mass or volume, its symbol is @). 1@ equals to 12.5 kg, so the dryer has a net capacity of 93.75 kg.

The dryer is designed in a very simple form, a rectangular body is divided with three trays which hold the coffee (See Figure 20). These trays are perforated to let the incoming air flow through the coffee. The air is heated directly by a gas flame and fanned to the system through the bottom of the apparatus. The simplicity of the manufacture of this equipment focus on lower construction costs and therefore the selling price will be lower, which is favorable to the coffee grower, the less price he pays, the better.

Figure 20. 93.75 kg Vertical coffee dryer.

The startup of the process is triggered loading the tray I with wet coffee, with a humidity on wet basis of 53%, the whole dimensions of the volume at I (see Figure 23) will ensure a 2.5@ obtention in the end of the drying. An air stream at 50°C will start flowing at a rate of $\dot{V} \cong 9.8\, m^3/min$ and at a velocity $u = 1.3\, m/s$ through the apparatus, the air is heated by a gas burner installed parallelly to the fan (Figure 21-22), notice that by this time the two remaining trays II and III still empty. Seven hours after starting the procedure the coffee will have achieved a humidity of 30%, and it will be moved to the middle tray through the removable trays, and new wet coffee will be fed to the tray I. This input parameters are given by the manufacturer according to the data given by Cenicafé (National Center of Coffee Research of Colombia).

Figure 21. Gas burner for air heating.

Continuing the process, seven hours after, the coffee in tray II will go down to the tray III with a new humidity of 18%, then it will be moved to the bottom tray, number III; the coffee which was fed to the tray I will go to the middle tray with its new humidity of 30% and fresh coffee will be loaded into the first compartment. Lastly, seven hours after, the coffee which relays on the last tray will have the required humidity (12%), therefore it can be pulled out of the equipment and the coffee in the II tray will go down to the III one with a humidity of 18%, the one in the I tray will go to the middle compartment with a humidity of 18% and new coffee will be fed. Then, after 21 hours we have stabilized the system and we will have an output of 31.25 kg (31.25kg) of dry coffee each 7 hours.

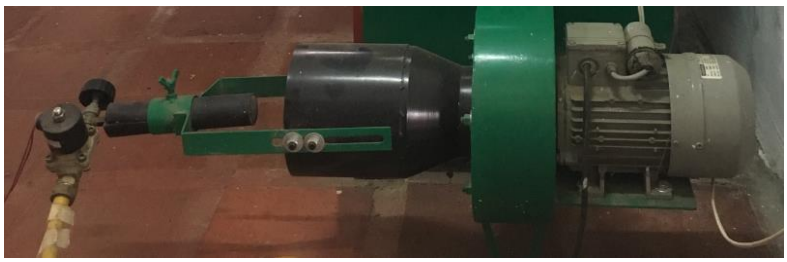

Figure 22. Burner-Fan setup.

As it can be interpreted in the description, it will take 21 hours to get 31.25kg of dry coffee; which is a decent amount for a small coffee grower, bigger dryers using the exact same principle are also used, for instance the same model has an expanded version of 10, 12, 15, 20, 25, 30 and 50@.

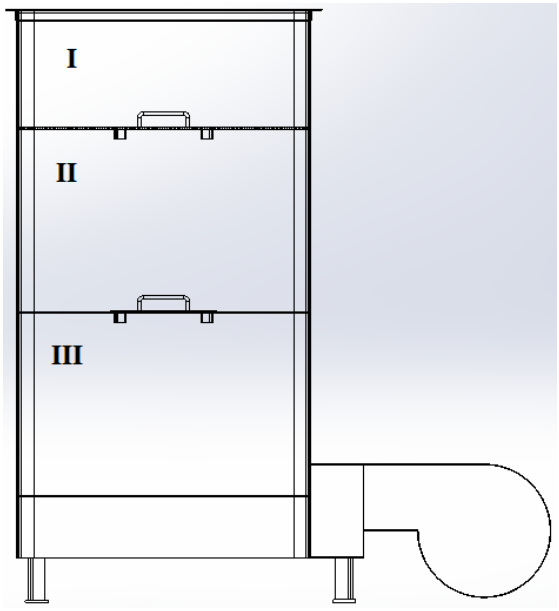

Figure 23. Schematic view of the 93.75 kg coffee dryer. Drawn in solidworks by the author.

At first glance, this dryer presents the necessary characteristics for a fast and efficient drying, but if we look a little more thoroughly, we can see that it presents too many problems from the engineering point of view. The main problems that it presents are:

- *Poor air distribution:* The air flows inside hitting at first a sheet metal (Figure 24) with the purpose of "reducing" the speed, but if the speed should be lowered then the fan should be changed instead, the internal geometry of the dryer has a very important effect on the process itself.

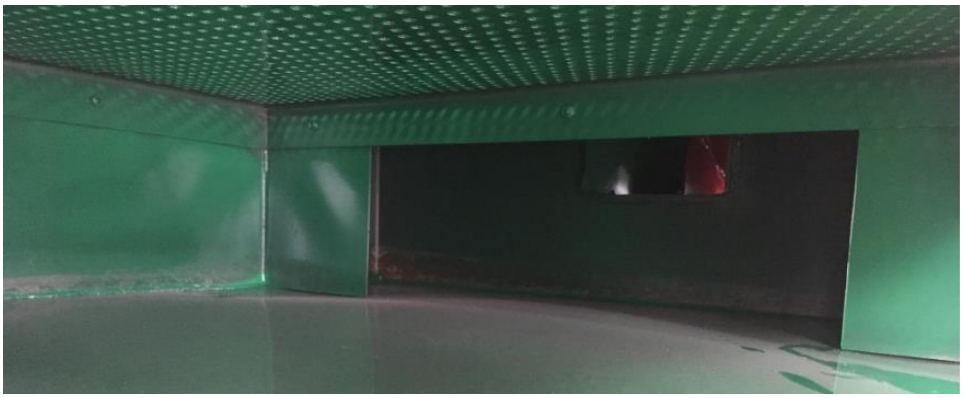

Figure 24. Air entrance to the dryer.

- *Ash:* Since the fanned air is coming from direct combustion some ash can be deposited in the lower chamber corners due to the tab where the air is directly hitting.

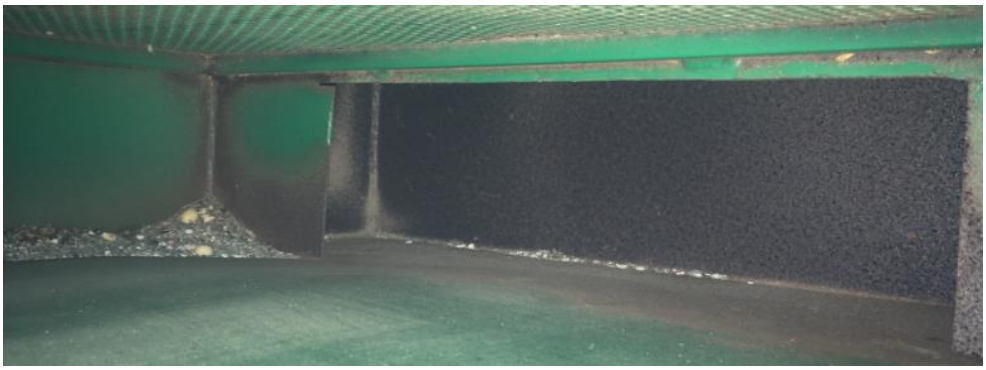

Figure 25. Dust and contaminating particles accumulation.

The Figure 25 was a snap done to an on-duty dryer, as it can be seen, the corners represent a place of concentration of non-desirable elements.

- *Product contamination:* Even though the most expert and recognized coffee tasters do not perceive any strange aroma or flavour in the product, we must realize that the coffee is being dried with direct gas combusted air, so as for sanitizing aspects it would be a quite good challenge to design some dryer which do not use the direct gas (Figure 21).

- *Geometry of the equipment:* The rectangular geometry of the equipment (Figure 26) generates corners where it is not clear if the air will flow properly or maybe will be filled with gaps or vortexes decreasing the efficiency of the dryer.

Figure 26. General on-duty dryer snap.

- *Air circulation:* There has been some energy already consumed in heating and fanning the air into the device, but all this air is been exhausted to the atmosphere. Some recirculation stream could be taken into account to improve the general performance.

As previously explained, the simplicity and ease of design of this equipment is mainly conceived by the need to manufacture a low-cost manufacturing device, in this way being able to offer it in the market at a low price for easy acquisition. The equipment is conformed by a folded sheet and one or another welding point, plus the hinges of the door, the bolts and other sheets forming the air route system.

But then a question arises that discerns in having an acceptable functioning as long as they have defects even when they are known. Or try to design something that meets the demands of the product and also provide more benefits to the coffee farmer.

That is why we have to develop a design that includes engineering and operational improvements considering that they should be coupled to a low manufacturing standard but with improvements in the points mentioned above, in this way apart from being more effective and efficient as such, it will also bring benefits in energy saving that obviously translates into money.

7. Objectives

7.1 Main objective

Design a coffee dryer which efficiently uses its drying air based on the geometry.

7.2 Specific objectives

Compare the performance of the new designed dryer vs the nowadays used regarding the drying air flux and distribution.

Perform suggestions to solve the direct combusted air pollution issues.

Compare the performance of the new designed dryer vs the nowadays used regarding the drying time.

8. Methodology

To be able to solve the proposed objectives, it is necessary to model the dryer including all the points of view, that is, a detailed calculation must be carried out taking into account the porosity of the elements inside it, change of temperature through the layers of coffee, amount of water removed, etc. Once we have all this information, we can then continue modeling in CAD to later simulate the drying with all the current operating parameters.

8.1 Porosity calculation:

The drying air flows through the support tray and through the coffee layer, this process will be repeated three times since the dryer has three layers of coffee. This is why we are faced with a problem of flow through a porous bed. the porosity of the trays will be the same since the three have the same dimensions and number and size of perforations. But for coffee you should then calculate the different porosities because they will not be the same because coffee reduces both its moisture and size, so the porosity in the three layers of coffee varies.

8.1.1 Coffee layer porosity:

It is known that the porosity can be calculated as follows:

$$\varepsilon = \frac{V_{Space}}{V_{Total}} \qquad (17)$$

The entire apparatus has a net capacity of 93.75 kg, and we also know that in the end of the process we will remove from the last tray roughly 31.25kg of dried coffee. It is also known that 1kg of dried coffee has between 4000 and 4400 coffee seeds, for our purpose we will use the mean average between both limits as our working amount of seeds as 4200.

With the mentioned above information and taking into account that the number of seeds do not change in time, we can establish then that the amount of seeds in the inlet is the same as in the outlet, and we can estimate the amount of coffee seeds per layer as follows.

$$Amount\ of\ seeds\ per\ layer = 4200\frac{seeds}{kg} * 31.25kg = 131250\ seeds\ per\ layer$$

We also have the average measures of an arabica coffee seed, which is the main type of harvested coffee in Colombian soils:

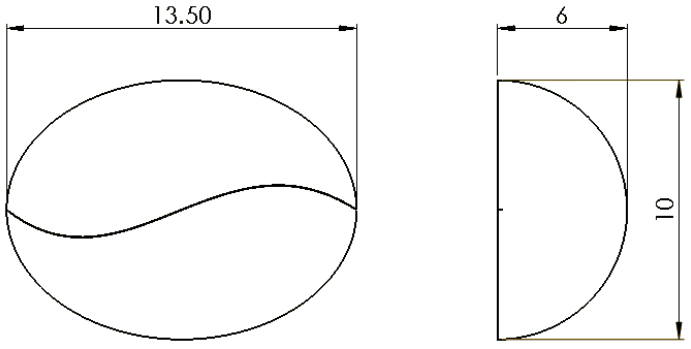

Figure 27. General dimensions of an arabica coffee seed. Drawn in solidworks by the author.

But, if we take a close look at the geometry of the coffee seed, we can put another half to it, which is the original disposition for the coffee bean, then we would have an ellipsoidal geometry which will ease our calculations.

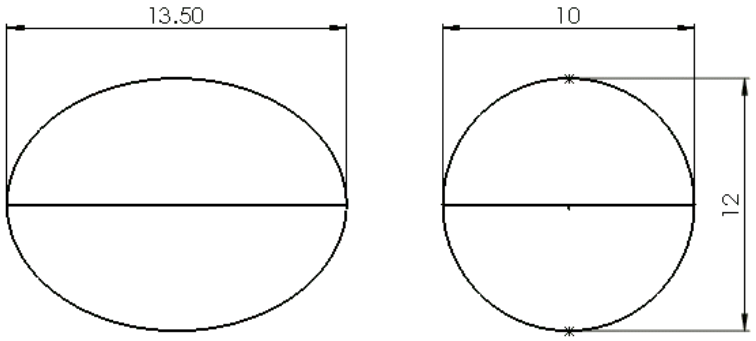

Figure 28. General dimensions of an arabica coffee assumed as ellipsoidal. Drawn in solidworks by the author.

Now, the volume of each seed assumed as ellipsoidal can be calculated by using the following formula:

$$V_{Seed} = \frac{4}{3} * \pi * a * b * c$$

Equation [17]

Where a, b and c are the radiuses of the seed:

- $a = \frac{13.5}{2} = 6.75\ [mm]$
- $b = \frac{10}{2} = 5\ [mm]$
- $c = \frac{12}{2} = 6\ [mm]$

So then, the volume of one coffee seed is:

$$V_{Seed} = \frac{4}{3} * \pi * 6.75mm * 5mm * 6mm$$

$$V_{Seed} = 848.23mm^3$$

$$V_{Seed} = 8.48 \times 10^{-7} m^3$$

And we already know the amount of seeds per layer as well calculating the total volume of coffee should be easy, but as we simplified the case using an ellipsoidal geometry, so the amount of seeds should be divided by half because there is another half implicit in the geometry.

$$V_{T\_Seeds} = V_{Seed} * \frac{number\ of\ seeds\ per\ layer}{2}$$

$$V_{T\_Seeds} = 8.48 \times 10^{-7} m^3 * \frac{131250}{2}$$

$$V_{T\_Seeds} = 5.57 \times 10^{-2} m^3$$

This volume is the occupied by the seeds in the third (last) tray so we can rename it as V_{Tray3_Seeds} for further calculations.

It is known that during the drying process the seed undergoes through a shrinkage in its dimensions of about the 7%, by knowing this we can extend the volume for the middle and top tray keeping in mind the shrinkage percentage as:

$$V_{Tray1\_Seeds} = V_{Tray3\_Seeds} + (V_{Tray3\_Seeds} * 0.07)$$

$$V_{Tray1\_Seeds} = 5.57 \times 10^{-2} m^3 + (5.57 \times 10^{-2} m^3 * 0.07)$$

$$V_{Tray1\_Seeds} = 5.95 \times 10^{-2} m^3$$

And for the middle tray we can use an addition of the 35% as the average shrinkage at the stage as:

$$V_{Tray2\_Seeds} = V_{Tray3\_Seeds} + \left(V_{Tray3\_Seeds} * 0.035\right)$$

$$V_{Tray2\_Seeds} = 5.57 \times 10^{-2} m^3 + (5.57 \times 10^{-2} m^3 * 0.035)$$

$$V_{Tray2\_Seeds} = 5.76 \times 10^{-2} m^3$$

Now that we have the volume of seeds, we must calculate the total volume occupied and perform the difference to calculate the volume of empty space; we know that the whole volume of the box in the top tray is filled with coffee, and we know its dimensions, so we should calculate this volume as:

$$V_{Box} = 265mm * 657mm * 495mm$$

$$V_{Box} = 0.0862 m^3$$

So now is easy to calculate the empty space in the coffee box volume for tray 1, performing the difference of the occupied volume and the volume of the seeds we have that:

$$V_{Space} = V_{Box} - V_{Tray1\_Seeds}$$

$$V_{Space} = 0.0863 m^3 - 5.95 \times 10^{-2} m^3$$

$$V_{Space} = 0.0267 m^3$$

Finally, as we already calculated the empty volume and the occupied volume as well, then we are able to calculate the porosity for each tray using the Equation [17] as well as the shrinkage percentage:

$$\varepsilon = \frac{V_{Space}}{V_{Box}}$$

$$\varepsilon_1 = \frac{0.0267 m^3}{0.0862 m^3}$$

$$\varepsilon_1 = 0.3096$$

$$\varepsilon_2 = 0.3096 * 0.965$$

$$\varepsilon_2 = 0.2987$$

$$\varepsilon_3 = 0.3096 * 0.93$$

$$\varepsilon_3 = 0.2879$$

8.1.2 Metal sheet porosity calculation:

The metal sheet has, in addition to a flow resistance, a porosity that can be easily calculated and extended to all the metal sheets through which the air flows in the system.

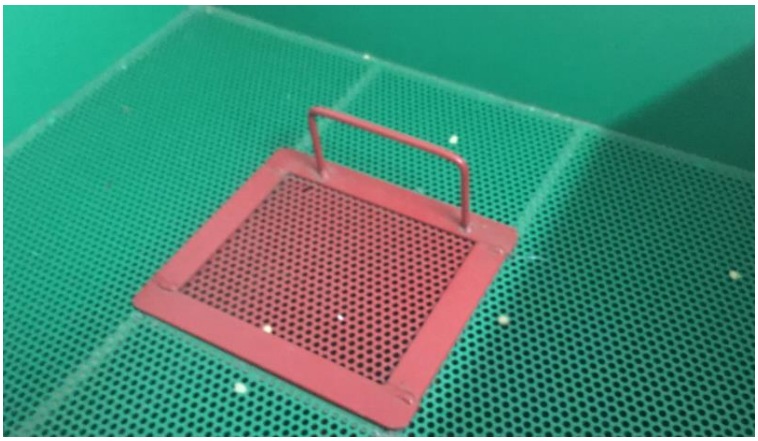

Figure 29. Metal sheet on dryer.

For the calculation of the porosity in this sheet we can use the same expression as expressed in the Equation 17 with, of course some slight changes which change its purpose, therefore we can refer it as Equation 18 porosity calculation for sheet metal:

$$\varepsilon_{SM} = \frac{V_{Holes}}{V_{Sheet}} \qquad (18)$$

The calculation of the volume holes is done by calculating the volume of one hole using the volume of a cylinder formula and multiplying the result for the number of holes. The sheet has around 6370 holes which have a diameter of 5mm

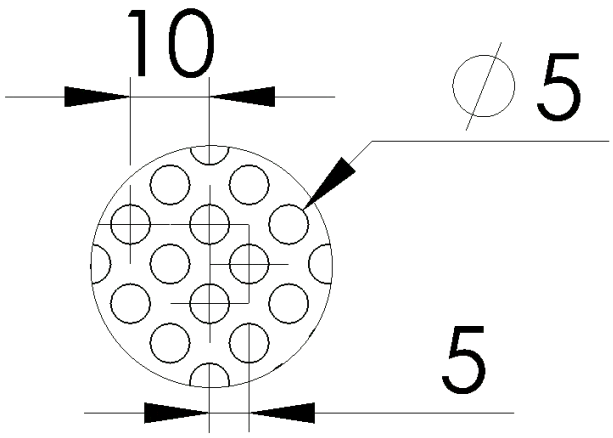

Figure 30. Holes distribution in the metal sheet. Drawn in solidworks by the author.

The volume of the holes can be further calculated as:

$$V_H = \pi * \frac{D^2}{4} * h * N_H$$

Were:

- $D = Diameter\ of\ hole\ [mm]$
- $h = Height\ of\ hole\ [mm]$
- $N_H = Number\ of\ holes$

Solving for the given data we have that:

$$V_H = \pi * \frac{(5mm)^2}{4} * 3mm * 6370$$

$$V_H = 375223.97mm^3$$

And the volume of the sheet metal is calculated as a normal parallelepiped volume:

$$V_{SM} = X * Y * Z$$

Where:

- $X = Length\ of\ the\ sheet\ metal\ [mm]$
- Y= $Width\ of\ the\ sheet\ metal\ [mm]$
- $Z = Height\ of\ the\ sheet\ metal\ [mm]$

Computing the values ewe obtain then that the volume of the sheet metal will be:

$$V_{SM} = 657mm * 495mm * 3mm$$

$$V_{SM} = 975645mm^3$$

And finally, as we have both volumes, we can use the Equation [18] for calculation of the porosity:

$$\varepsilon_{SM} = \frac{V_{Holes}}{V_{Sheet}}$$

$$\varepsilon_{SM} = \frac{375223.97mm^3}{975645mm^3}$$

$$\varepsilon_{SM} = 0.3846$$

This porosity will be the same for all 3 trays, because the geometry definition in all of them is the same.

8.2. Stage humidity and water removal calculation.

For calculating the total amount of water removed we must first establish the stages of drying for one batch as shown in the Figure 31, where the hatched areas represent the coffee loads in time, it was already explained how the coffee is dried: starting in the volume I, seven hours after is moved to the volume II, seven hours after is taken to the volume III and seven hours after the product has the required humidity.

As for the process it is known the inlet temperature of the air and the inlet and outlet humidity of the coffee, but we should then, in order to proper model the dryer, calculate the removed water and calculate the middle stages humidity and air temperature as well.

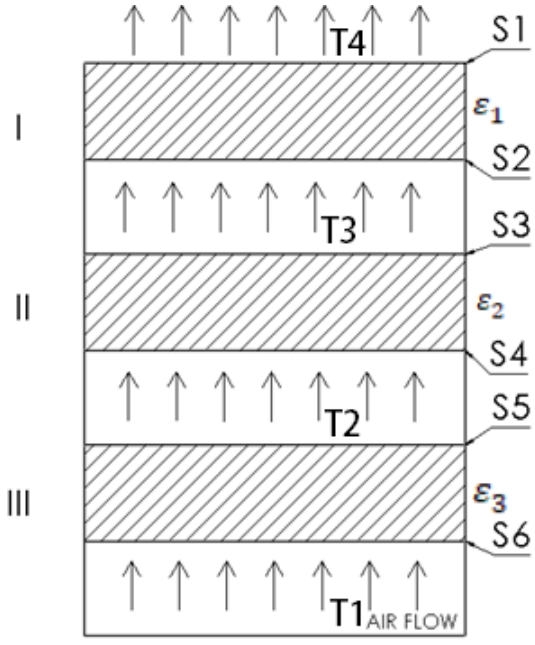

Figure 31. Drying stages. Drawn in solidworks by the author.

Now, having established the temperature stages, surfaces and porosities we can develop the box diagram which expresses the process phenomena for better understanding and description, the box diagram is related in the Figure 32.

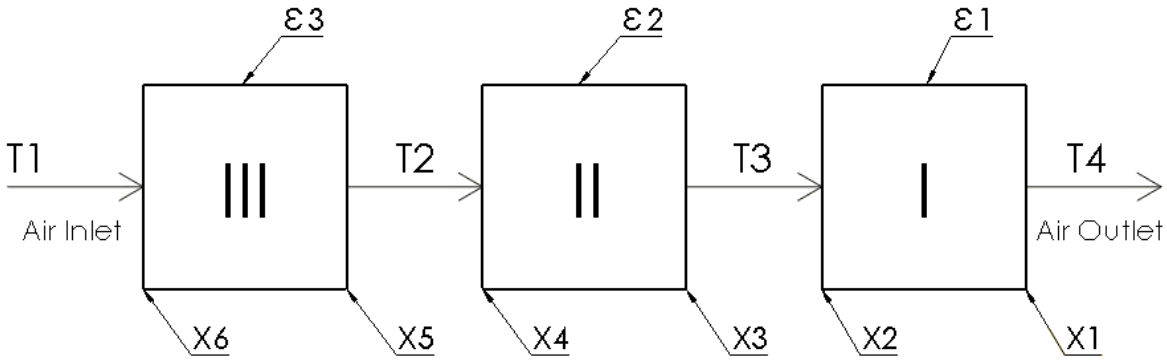

Figure 32. Box diagram of the process. Drawn in solidworks by the author.

Having defined the diagram, we could now analyze it:

- As for the temperatures we can establish that: $T1 > T2 > T3 > T4$

- As for the humidity, taking into account that $X2$ is actually the initial state of $X3$ and the same as for $X4$ to $X5$, we could say that: $X1 > X2 = X3 > X4 = X5 > X6$

- And for the porosity, as it was already calculated we have that: $\varepsilon_1 > \varepsilon_2 > \varepsilon_3$

Cenicafé performed several experiments for calculating the amount of water in all the stages, which can be calculated from the Equation 5 proposed in the MSU method for thin layer drying processes, which expresses the following statement.

$$\frac{\partial H}{\partial x} = -\frac{\rho_p}{G_a}\frac{\partial M}{\partial t}$$

Where:

- G_a: Air mass flow per unit area, $\left[\frac{kg}{hm^2}\right]$
- H: Ratio of air humidity, $\left[\frac{kg_{water}}{kg_{dry\ air}}\right]$
- M: Local moisture content of the grain, decimal bs.
- ρ_p: Density expressed on the basis of the dry weight of the grain, $\left[\frac{kg}{m^3}\right]$
- t: Time, $[h]$
- x: Coordinate within the deep layer of grain, $[m]$

It is known by personal experiences and according to CENICAFE that the mass ratio between wet and dry coffee is roughly 2:1, and we know that in the end of the process we will have 2.5@ =

31.25 kg of dry parchment coffee, therefore the inlet mass should be around 62.5 kg. It was found in literature that the averaged ratio is 1.968:1 which means that the inlet mass will be 61.5 kg, this is then the mass to be used in our calculation for the stage number 1.

To define the humidity in the stages we can use the Figure 18 and we can also compare the behaviour with the Figure 33, and then, by graphical way set the humidity in each stage (we know the time 7, 14 and 21 hours), and, with the humidity and the ratio mentioned above, we can then calculate the mass of wet coffee in each stage until reaching the desired humidity in the last stage.

Stage 1:	Stage 2:	Stage 3:
X= 53%	X= 30%	X= 30%
m= 61.5 kg	m= 54.4 kg	m= 54.4 kg
t=0 h	t=7 h	t=7 h

Stage 4:	Stage 5:	Stage 6:
X= 18%	X= 18%	X= 12%
m= 43.25 kg	m= 43.25 kg	m= 31.25 kg
t=14 h	t=14 h	t=21 h

Now, if we calculate the mass difference in all the stages, we can calculate an approximate total removed amount of water which should be:

$$\Delta m = -\big((m6 - m5) + (m4 - m3) + (m2 - m1)\big)$$

$$\Delta m = -\big((31.25 - 43.25) + (43.25 - 54.4) + (54.4 - 61.5)\big)kg$$

$$\Delta m = 30.25\ kg$$

So, as expected due to the wet-dry coffee ratio, the amount of removed water was the expected, which means that the calculated humidity for the different stages is correct. As following we could generate the humidity vs. time plot and also the humidity vs. kg of water removed.

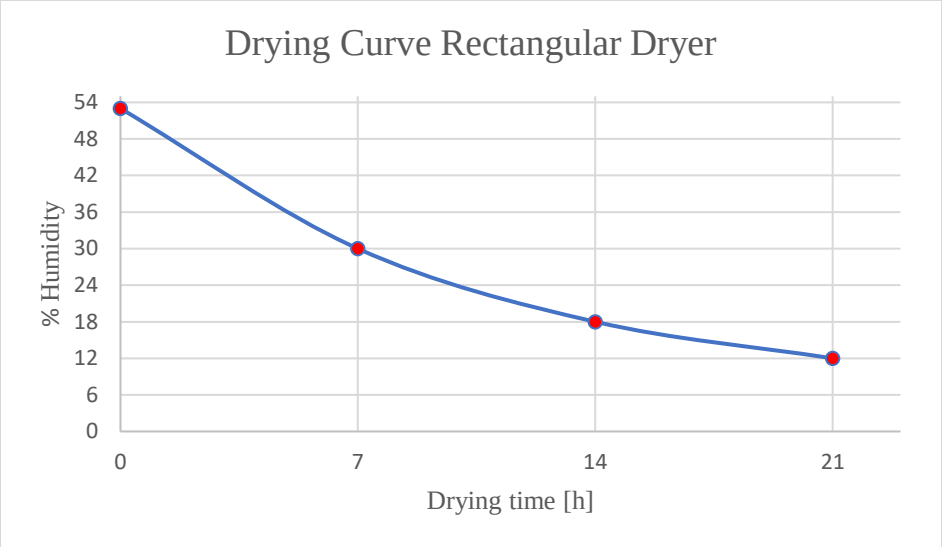

Figure 33. Obtained drying curve with the calculated stage humidity obtained from the book "Beneficio Ecológico del Café".

We can make some graphical verification comparing the Figure 33 with the Figure 34, which shows the drying curve for a thin coffee layer in a silo type coffee dryer exposing the sample to the same time as we did.

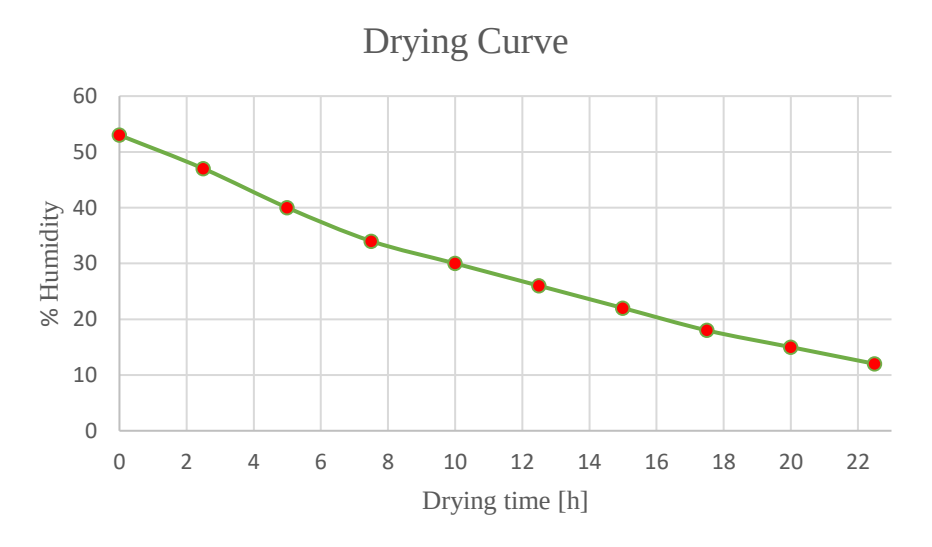

Figure 34. Drying curve for a thin layer in a silo type coffee dryer.

As it can be seen, the humidity content for the time is quite similar, as well as the drying curve. It is not completely the same because they used a different type of dryer but, even that fact the behavior is most likely the same, so now is double checked our calculation of the humidity in each stage of or dryer.

8.3 Temperature profile calculation.

According to the Figure 32, the only known temperature $T1 = 50°C$ and $T4 = 25°$; to be able to generate the temperature vs humidity we should calculate $T2$ and $T3$. Fortunately, the Thompson method displays an equation for this exact purpose referred as Equation 1 which reads as follows:

$$T_e = \frac{(0.24 + 0.45H)T + c_p T_g}{0.24 + 0.45H + c_p}$$

Where:

- c_p: Specific heat of the grain, $\left[\frac{kJ}{kgK}\right]$
- H: Ratio of air humidity, $\left[\frac{kg_{steam}}{kg_{dry\ air}}\right]$
- T: Drying air temperature, $[°C]$
- T_g: Grain temperature, $[°C]$
- T_e: Equilibrium temperature of drying air and grain, $[°C]$

All the values are known except for the c_p of the coffee, therefore Equation [11] can be used, which establishes that:

$$c_p = 1.3556 + 5.7859M$$

Where:

- c_p: Specific heat, $\left[\frac{kJ}{kgK}\right]$
- M: Moisture content, decimal.

According to Serna et al. the temperature of grain T_g can be calculated as:

$$T_g = \frac{T * M * 1.14}{h}$$

Where:

- H: Ratio of air humidity, $\left[\frac{kg_{steam}}{kg_{dry\ air}}\right]$
- T: Drying air temperature, $[°C]$
- T_g: Grain temperature, $[°C]$
- h: Height of layer $[m]$

Solving for the tray 3 then:

$$T_g = \frac{50°C * 0.18 * 1.145}{0.265}$$

$$T_g = 38.88°C$$

$$c_p = 1.3556 + 5.7859M$$

$$c_p = 1.3556 + 5.7859(0.18)$$

$$c_p = 2.397\ \frac{kJ}{kgK}$$

$$T_2 = \frac{(0.24 + 0.45H)T + c_p T_g}{0.24 + 0.45H + c_p}$$

$$T_2 = \frac{(0.24 + 0.45 * 0.18)50 + (2.397 * 38.88)}{0.24 + (0.45 * 0.18) + 2.397}$$

$$T_2 = 40.19°C$$

Solving for the tray 2:

From the the first T_g the up following grain temperatures in each layer if the layer has the same height can be calculated as:

$$T_{g\_new} = T_{g1} - 9°C$$

Góngora et. al developed the relationship which establish this ratio, then:

$$T_g = 38.88 - 9$$

$$T_g \approx 29.88°C$$

$$c_p = 1.3556 + 5.7859M$$

$$c_p = 1.3556 + 5.7859(0.30)$$

$$c_p = 3.09\ \frac{kJ}{kgK}$$

$$T_3 = \frac{(0.24 + 0.45H)T + c_p T_g}{0.24 + 0.45H + c_p}$$

$$T_3 = \frac{(0.24 + 0.45 * 0.3)40.19 + (3.09 * 29.88)}{0.24 + (0.45 * 0.3) + 3.09}$$

$$T_3 = 30.99°C$$

For the tray 1 we already know that the measured outlet temperature is around $25°C$ but just to check the functionality of the used equations above we can re check the outlet temperature:

$$T_g = 29.88 - 9$$

$$T_g = 20.88°C$$

$$c_p = 1.3556 + 5.7859M$$

$$c_p = 1.3556 + 5.7859(0.53)$$

$$c_p = 4.42\ \frac{kJ}{kgK}$$

$$T_4 = \frac{(0.24 + 0.45H)T + c_p T_g}{0.24 + 0.45H + c_p}$$

$$T_4 = \frac{(0.24 + 0.45 * 0.53)30.99 + (4.42 * 20.88)}{0.24 + (0.45 * 0.53) + 4.42}$$

$$T_4 = 21.86°C$$

So, as it is seen the $T_4 = 21.86°C$ makes sense with the calculated physically$T_{4_exp} \approx 25°C$, we must remember that in the physical performed measurements a lot of factors can alter an accurate result. Reason why we will use the T_4 calculated analytically $T_4 = 21.86°C$.

The Figure 35 was generated then to show the temperature profile across the drying process, the profiles show a logical behaviour, this plot then double checks the calculated data above. Plus, the information contained in the Figure 35 can be used after the actual dryer is re-designed to see whether if the drying air temperature will be improved or not, if yes, then it can be translated in efficiency and furtherly translated as well in economical profit.

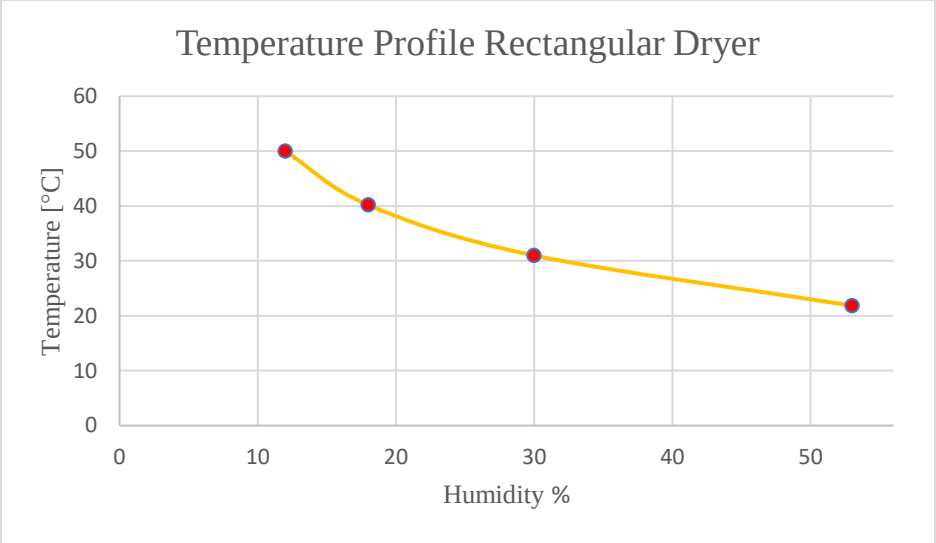

Figure 35. Temperature profile for the 93.75 kg coffee dryer.

8.4. Pressure drop ΔP calculation.

To calculate the pressure drop, it must be taken into account that it has losses in two parts, mainly: porous beds, for which the porosity, height, etc. data are available. And the perforated plates that hold the coffee.

8.4.1 Losses in the porous bed.

For calculating the losses in the porous media, we could use the Equation 19 which reads as follows:

$$e_z = \lambda' \frac{1-\varepsilon}{\varepsilon^3} \frac{h}{D_p} {u_0}^2 \qquad (19)$$

Where:

- e_z: Friction losses, $\left[\frac{m^2}{s^2}\right]$

- λ': Friction coefficient, $[-]$

- ε: Porosity, $[-]$

- h: Height of the bed, $[m]$

- D_p: Diameter of particle, $[m]$

- u_0: Initial velocity, $\left[\frac{m}{s}\right]$

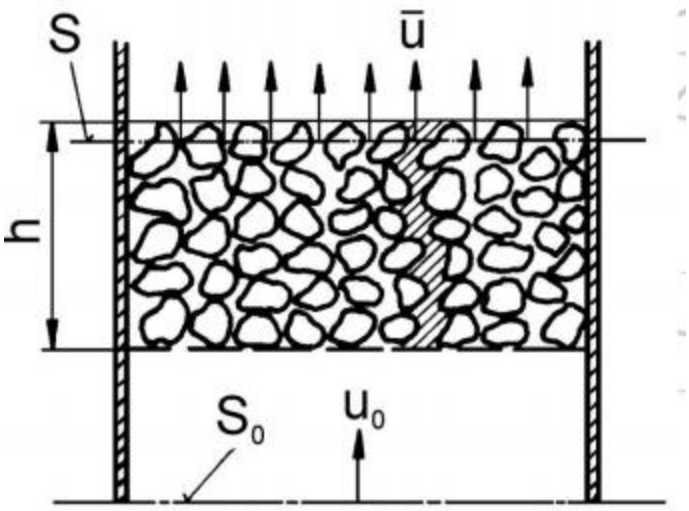

Figure 36. Disposition of a general porous bed. Taken from http://users.fs.cvut.cz/tomas.jirout/

For determining λ' in the Equation 19 we should use some of the lambda calculation equations presented in the Figure 37, which include some constants depending on the regime flow where the phenomena is developed, and it takes into account e particle shape as well. The Reynolds number must be estimated using the Equation 20

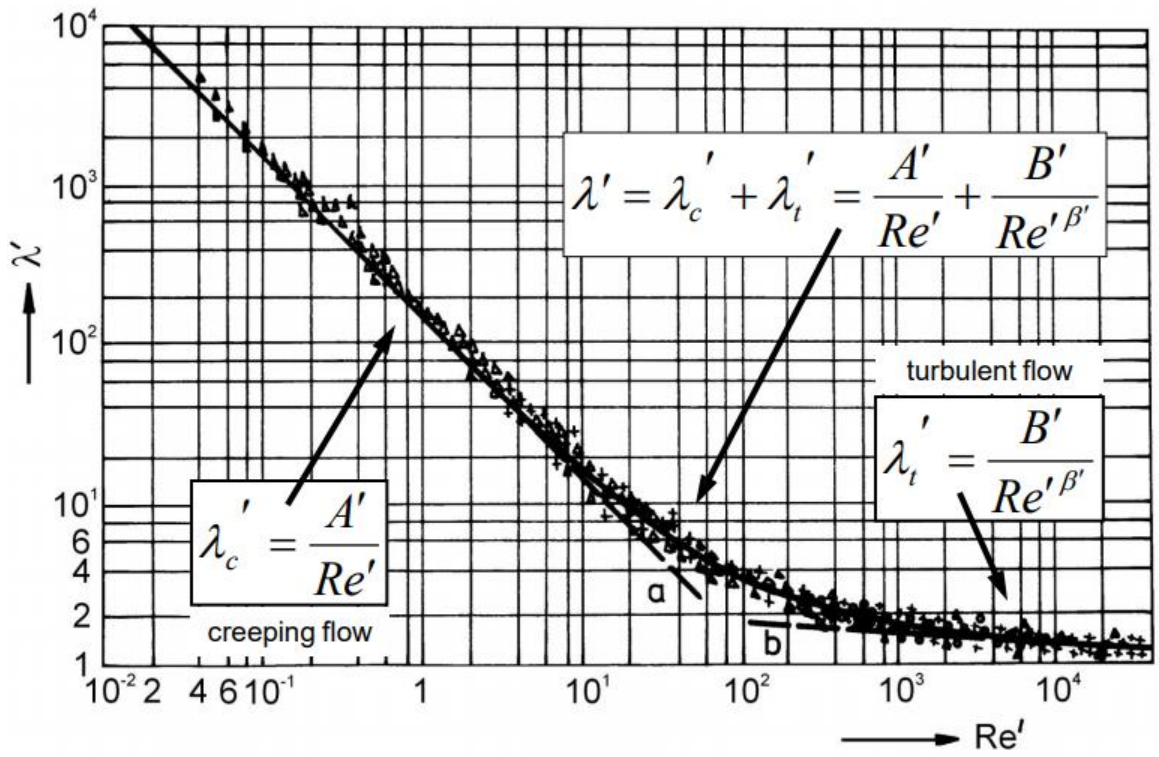

Figure 37. Dependence of friction factor λ' for single phase flow in monodisperse bed with spherical particles on modified Reynolds number R (for spherical particles A'=160; B'=3.1; β=0.1). Taken from http://users.fs.cvut.cz/tomas.jirout/

And for the calculation of Reynolds number in a porous bed we can compute the following required values for so:

$$Re = \frac{u_0 D_p \rho_{air}}{(1-\varepsilon)\mu_{air}} \qquad (20)$$

For the tray number 3:

- Velocity of the air:

$$\dot{V} = 9.8 \frac{m^3}{min}$$

$$u_0 = \frac{\dot{V}}{S_0}$$

$$u_0 = \frac{9.8 \frac{m^3}{min}}{0.125\ m^2}$$

$$u_0 = 78.4 \frac{m}{min}$$

$$u_0 = 1.3 \frac{m}{s}$$

- Reynolds calculation:

$$Re = \frac{1.3 \frac{m}{s} * 0.012m * 1.092 \frac{kg}{m^3}}{(1-0.2879)\ 1.963 \times 10^{-5} \frac{kg}{ms}}$$

$$Re = 1218.67$$

If we look for the Reynolds number result in the Figure 37, we can deduce that we are working, in this first part in laminar regime. It is important to remember that the density ρ_{air} and the dynamic viscosity of the air μ_{air} change depending on the temperature of the same, in the tray 3 the temperature of air is $50°C$. Properties of the air taken from: ÇENGEL, Yunus A. y John M. CIMBALA, "Mecánica de fluidos: Fundamentos y aplicaciones", 1ª edición, McGraw-Hill, 2006. Tabla A-9.

- Friction coefficient λ' calculation:

$$\lambda' = \frac{A'}{Re}$$

$$\lambda' = \frac{160}{(1218.67)}$$

$$\lambda' = 0.1313$$

- Friction loss e_z calculation:

$$e_{z3} = 0.1313 * \frac{(1 - 0.2879)}{(0.2879)^3} * \frac{0.265}{0.012} * (1.3)^2$$

$$e_{z3} = 146.23 \frac{m^2}{s^2}$$

For the tray number 2:

- Velocity of the air:

For calculating the velocity of the air about to enter to the second porous bed, we must find the mean velocity which can be calculated by using the Equation 21.

$$\bar{u} = \frac{V_p}{V} u_0 \qquad (21)$$

Where:

- V:Volume occupied, $[m^3]$

- V_p: Volume pores, $[m^3]$

But if we take a close look at the Equation 21 the relationship which the volume ratio want to express is actually the porosity, but we should use the porosity of the third bed because this is the one from which the air is coming from. We can then re arrange terms according to the mentioned above and formulate the Equation 22.

$$\bar{u} = \varepsilon_3 u_0 \qquad (22)$$

Solving for our data;

$$\bar{u}_2 = 0.2879 * 1.3 \frac{m}{s}$$

$$\bar{u}_2 = 0.3743 \frac{m}{s}$$

- Reynolds calculation:

$$Re = \frac{0.3743\frac{m}{s} * 0.012m * 1.127\frac{kg}{m^3}}{(1-0.2987)\ 1.918 \times 10^{-5}\frac{kg}{ms}}$$

$$Re = 376.33$$

If look up for our just obtained value of Reynolds number in the tray number 2 we can see that we are still in laminar regime, therefore we can now proceed and calculate the friction coefficient.

- Friction coefficient λ' calculation:

$$\lambda' = \frac{160}{(376.33)}$$

$$\lambda' = 0.4252$$

- Friction loss e_z calculation:

$$e_{z2} = 0.4252 * \frac{(1-0.2987)}{(0.2987)^3} * \frac{0.265}{0.012} * (0.3743)^2$$

$$e_{z2} = 34.61\frac{m^2}{s^2}$$

<u>For the tray number 1:</u>

- Velocity of the air:

$$\bar{u}_1 = \varepsilon_2 \bar{u}_2$$

$$\bar{u}_1 = 0.2987 * 0.3743\frac{m}{s}$$

$$\bar{u}_1 = 0.112\frac{m}{s}$$

Again, we should use the porosity of the second bed, because this is the one from which the air is coming from, that is how the velocity is mainly affected.

- Reynolds calculation:

$$Re = \frac{0.112\frac{m}{s} * 0.012m * 1.164\frac{kg}{m^3}}{(1-0.3096)\ 1.872 \times 10^{-5}\frac{kg}{ms}}$$

$$Re = 121.044$$

Remember that for the calculation of Reynolds number we must take into account the temperature of the air, because the density and dynamic viscosity will change according to the temperature of air.

- Friction coefficient λ' calculation:

$$\lambda' = \frac{160}{(121.044)}$$

$$\lambda' = 1.3218$$

- Friction loss e_z calculation:

$$e_{z1} = 1.3218 * \frac{(1 - 0.3096)}{(0.3096)^3} * \frac{0.265}{0.012} * (0.112)^2$$

$$e_{z1} = 8.52 \frac{m^2}{s^2}$$

We already calculated the losses in all the porous beds present in the apparatus, now to be able to estimate the total friction loss e_z we must just add all the local e_{z1}, e_{z2} and e_{z3} :

$$e_z = e_{z1} + e_{z2} + e_{z3}$$

$$e_z = 146.23 + 34.61 + 8.52$$

$$e_z = 189.36 \frac{m^2}{s^2}$$

8.4.2 Friction losses in perforated plate.

For the pressure drop in the perforated plates we used an online calculator which solves the required calculations for a flow through a perforated plate. In short words, as we already know the velocities in each stage of drying, we could then search on tables for the hydraulic resistance coefficient or use the calculator which will automatically find the resistance coefficient for the plate depending on the velocity of air flow, temperature and dependent on temperature properties. The equation for the friction losses in a perforated plate reads as follows:

$$e_z = \xi \frac{u^2}{2} \qquad (23)$$

Where:

- ξ: Resistance coefficient, $[-]$

- u: Velocity of fluid before the plate, $\left[\frac{m}{s}\right]$

For the plate in tray 3:

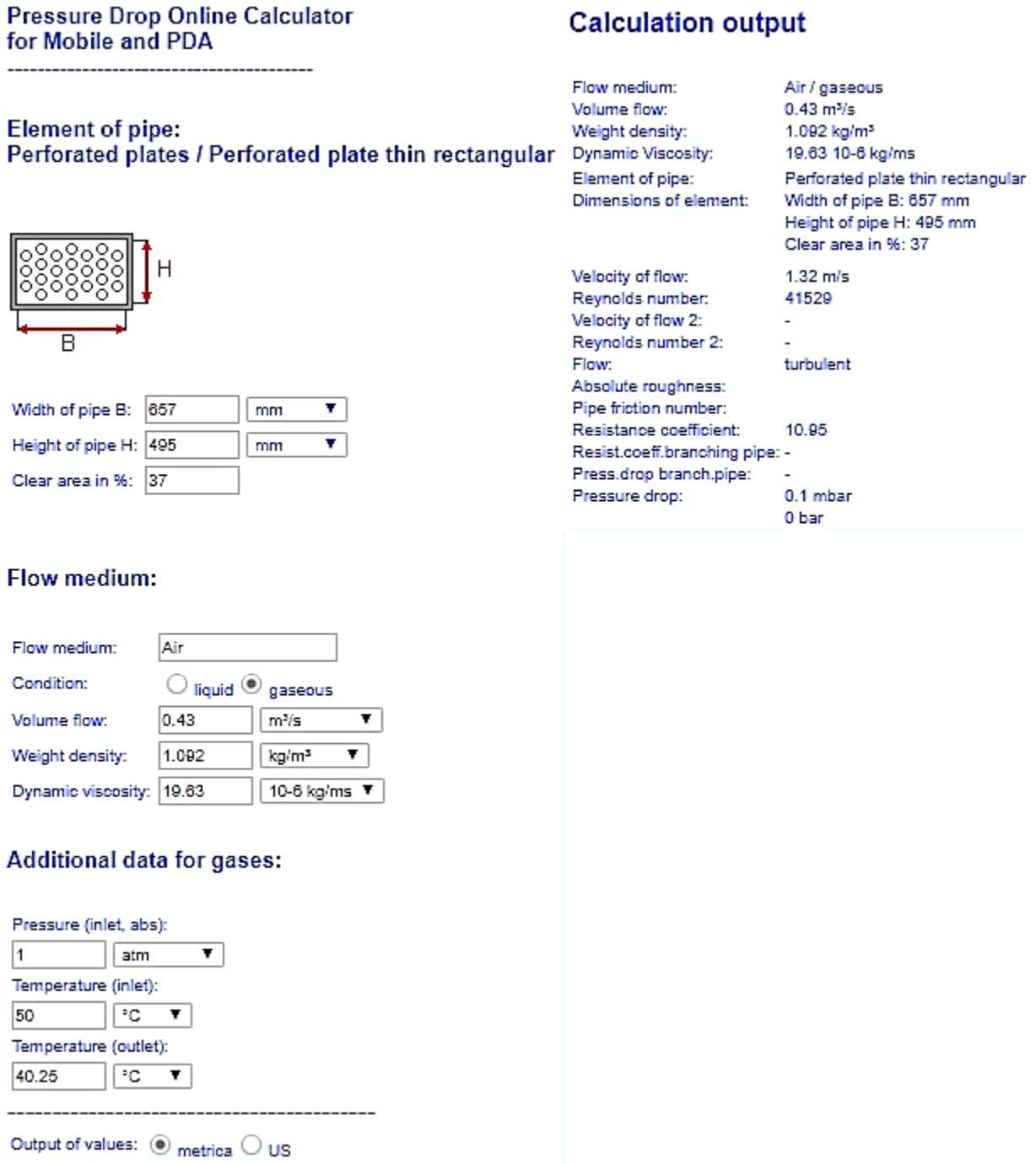

Figure 38. Results of pressure drop calculation for perforated plate in tray 3. http://www.pressure-drop.com/Online-Calculator/

As we can see, in the results given by the calculator we have the hydraulic resistance coefficient and also the pressure drop, we will save the ξ_3 coefficient as for calculating the friction losses and being able to calculate the pressure drop by ourselves.

For the plate in tray 2:

Pressure Drop Online Calculator for Mobile and PDA

Element of pipe:
Perforated plates / Perforated plate thin rectangular

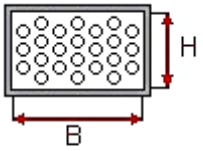

Width of pipe B:	657	mm
Height of pipe H:	495	mm
Clear area in %:	37	

Flow medium:

Flow medium:	Air	
Condition:	○ liquid ◉ gaseous	
Volume flow:	0.12	m³/s
Weight density:	1.127	kg/m³
Dynamic viscosity:	19.18	10-6 kg/ms

Additional data for gases:

Pressure (inlet, abs):
1 atm
Temperature (inlet):
40.25 °C
Temperature (outlet):
31.035 °C

Output of values: ◉ metrica ○ US

Calculation output

Flow medium:	Air / gaseous
Volume flow:	0.12 m³/s
Weight density:	1.127 kg/m³
Dynamic Viscosity:	19.18 10-6 kg/ms
Element of pipe:	Perforated plate thin rectangular
Dimensions of element:	Width of pipe B: 657 mm Height of pipe H: 495 mm Clear area in %: 37
Velocity of flow:	0.37 m/s
Reynolds number:	12241
Velocity of flow 2:	-
Reynolds number 2:	-
Flow:	turbulent
Absolute roughness:	
Pipe friction number:	
Resistance coefficient:	10.95
Resist.coeff.branching pipe:	-
Press.drop branch.pipe:	-
Pressure drop:	0.01 mbar 0 bar

Figure 39. Results of pressure drop calculation for perforated plate in tray 2. http://www.pressure-drop.com/Online-Calculator/

We will save the ξ_2 coefficient as for calculating the friction losses and being able to calculate the pressure drop by ourselves.

For the plate in tray 1:

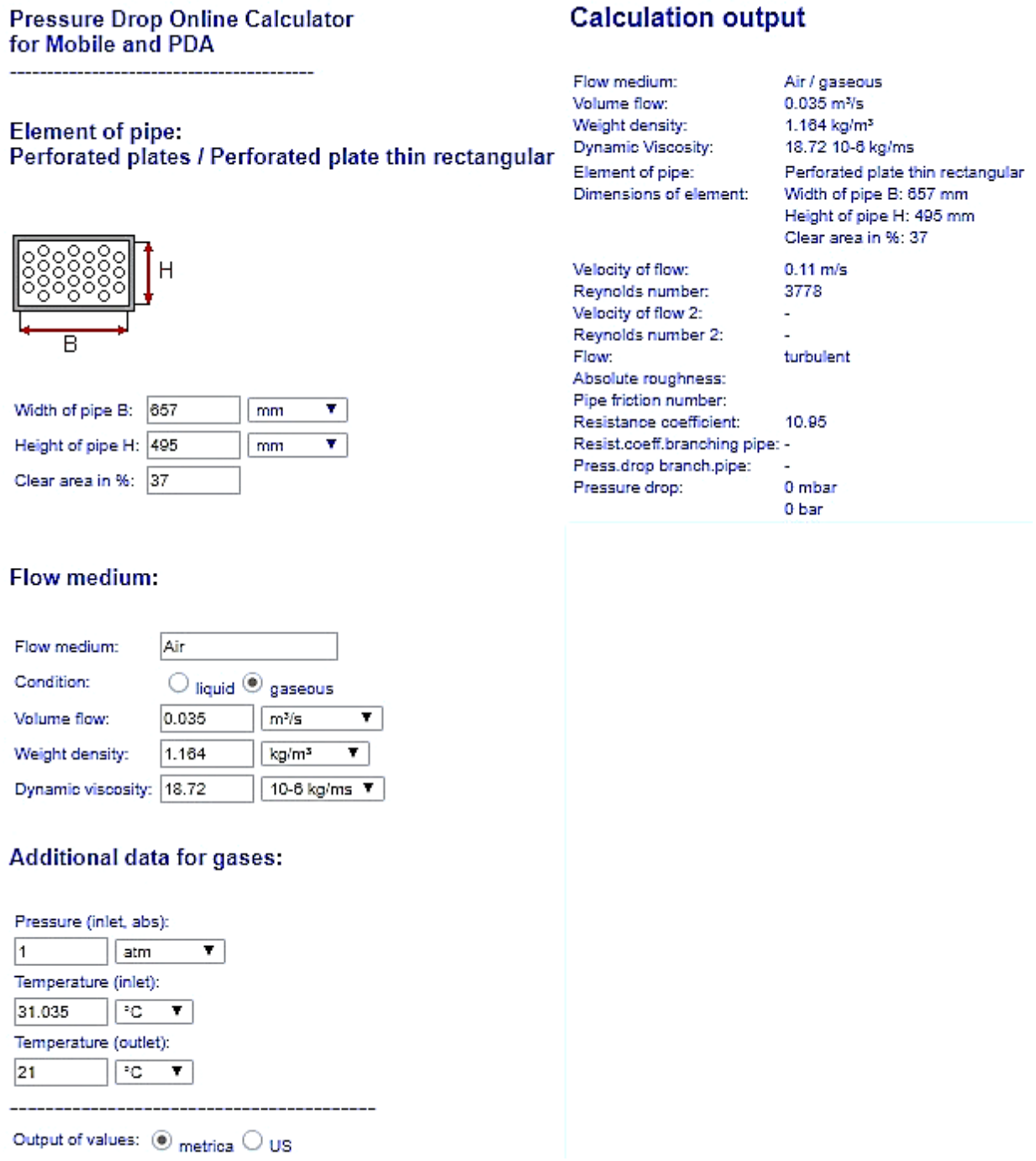

Figure 40. Results of pressure drop calculation for perforated plate in tray 1. http://www.pressure-drop.com/Online-Calculator/

We will save the ξ_1 coefficient as for calculating the friction losses and being able to calculate the pressure drop by ourselves.

Now, we already have all the hydraulic resistance coefficients, and we also know the velocity of the air in each stage of the dryer. We also know that the friction loss can be calculated as:

$$e_z = e_{zt1} + e_{zt2} + e_{zt3}$$

So, since we have all the information required for calculating the different friction losses, we compute them in the Equation [23] as follows:

$$e_{zt1} = \xi_1 \frac{{u_1}^2}{2}$$

$$e_{zt1} = 10.95 * \frac{0.112^2}{2}$$

$$e_{zt1} = 0.0687 \ \frac{m^2}{s^2}$$

$$e_{zt2} = \xi_2 \frac{{u_2}^2}{2}$$

$$e_{zt2} = 10.95 * \frac{0.3743^2}{2}$$

$$e_{zt2} = 0.767 \ \frac{m^2}{s^2}$$

$$e_{zt3} = \xi_3 \frac{{u_3}^2}{2}$$

$$e_{zt3} = 10.95 * \frac{1.3^2}{2}$$

$$e_{zt3} = 9.25 \ \frac{m^2}{s^2}$$

$$e_z = e_{zt1} + e_{zt2} + e_{zt3}$$

$$e_z = 0.0687 + 0.767 + 9.252$$

$$e_z = 10.09 \ \frac{m^2}{s^2}$$

8.4.3 Reynolds calculation in the air segments

For calculating the Reynolds number in the air segments, we have to relate the flow to its orthogonal cross section area. For the air 1 and 2 segments is quite easy to calculate because the geometry does not change and we have all data for the air at these points, but for the air 3 in the bottom segment the geometry will represent a problem, that is why first of all we will split into boxes this geometry for calculation.

The Reynolds number for a rectangular section can be calculated from the hydraulic diameter of the geometry which can be calculated taking into account the perimeter and the area of the section:

$$A = wh$$

$$P = 2w + 2h$$

$$D_{eq} = \frac{4A}{P}$$

Where:

- w: Width of the section $[m]$
- h: Height of the section $[m]$
- P :Perimeter of the section $[m]$
- A: Area of the section $[m^2]$
- D_{eq}: Hydraulic diameter $[m]$

And then we can calculate Reynolds for each section as:

$$Re = \frac{\rho D_{eq} u}{\mu}$$

Air 3:

– Box 1: Air Inlet

For calculating the Reynolds in this point, we will use the cross section area shown in the Figure 41 flowing horizontally to the equipment we have that

$$A = 0.146m * 0.156m = 0.023m^2$$

$$P = 2 * 0.146m + 2 * 0.156m = 0.604m$$

$$D_{eq} = \frac{4 * 0.023}{0.604} = 0.1523m$$

Now, we must use the μ and ρ properties at 50°C for Reynold calculation

$$Re_{Box1} = \frac{1.092 \frac{kg}{m^3} * 0.1523m * 1.3 \frac{m}{s}}{1.963 \times 10^{-5} \frac{kg}{ms}}$$

$$Re_{Box1} = 11014.013 \rightarrow Turbulent$$

– Box 2: Air U

$$A = 0.207m * 0.117m = 0.0242m^2$$

$$P = 2 * 0.207m + 2 * 0.117m = 0.648m$$

$$D_{eq} = \frac{4 * 0.0242}{0.648} = 0.1494m$$

Now,

$$Re_{Box2} = \frac{1.092\frac{kg}{m^3} * 0.1494m * 1.3\frac{m}{s}}{1.963 \times 10^{-5}\frac{kg}{ms}}$$

$$Re_{Box2} = 10804.29 \rightarrow Turbulent$$

– Box 3: Upgoing Air

$$A = 0.494m * 0.654m = 0.323m^2$$

$$P = 2 * 0.494m + 2 * 0.654m = 2.296m$$

$$D_{eq} = \frac{4 * 0.343}{2.296} = 0.5976m$$

Now,

$$Re_{Box3} = \frac{1.092\frac{kg}{m^3} * 0.597m * 1.3\frac{m}{s}}{1.963 \times 10^{-5}\frac{kg}{ms}}$$

$$Re_{Box3} = 43173.77 \rightarrow Turbulent$$

<u>Air 2:</u>

$$Re_2 = \frac{1.127\frac{kg}{m^3} * 0.597m * 0.3743\frac{m}{s}}{1.918 \times 10^{-5}\frac{kg}{ms}}$$

$$Re_2 = 13130.143 \rightarrow Turbulent$$

Air 1:

$$Re_3 = \frac{1.164\frac{kg}{m^3} * 0.597m * 0.112\frac{m}{s}}{1.872 \times 10^{-5}\frac{kg}{ms}}$$

$$Re_3 = 4157.57 \rightarrow Turbulent$$

Now that we have all the Reynolds numbers for the air segments, we can calculate the pressure drop generated by the flow in pipe as:

$$\Delta P = \lambda \frac{L}{D}\frac{u^2}{2}\rho$$

But for the Lambda calculation we need Reynolds number, and since we are in turbulent regime, we can determine lambda as:

$$\lambda = 0.316Re^{-0.25}$$

So, we could say that:

$$\lambda_{Box1} = 0.03085,\ \Delta P_{Box1} = 0.02243Pa$$

$$\lambda_{Box2} = 0.03099, \Delta P_{Box2} = 0.02297Pa$$

$$\lambda_{Box3} = 0.02192, \Delta P_{Box3} = 0.0045Pa$$

$$\lambda_2 = 0.02952, \Delta P_2 = 0.00084Pa$$

$$\lambda_1 = 0.03935, \Delta P_{Box2} = 0.00010Pa$$

$$\Delta P_{Air\ Total} = 0.051Pa$$

8.4.4 Computation for drop calculation

For the calculation of the pressure drop we can use the Bernoulli equation which reads as follows:

$$\frac{{u_1}^2}{2} + \frac{P_1}{\rho_1} + gz_1 = \frac{{u_2}^2}{2} + \frac{P_2}{\rho_2} + gz_2 + e_z \qquad (24)$$

If we analyze the Equation 24, we can define the term $gz_1 = 0$ if we use the base as reference level for our system, the densities are also different in both stages but for easing the calculations, since the they do not differ that much from each other we can then establish a new average density which will look like this:

$$\bar{\rho} = \frac{\rho_1 + \rho_2}{2}$$

The new averaged density will be then equal to:

$$\bar{\rho} = \frac{1.092 + 1.164}{2}$$

$$\bar{\rho} = 1.128\ \frac{kg}{m^3}$$

The friction losses for our equipment will be equal to the total sum of the friction losses due to the porous beds and also the friction losses due to the perforated plates, then we could say that:

$$e_z = 189.36 + 10.09$$

$$e_z = 199.45\ \frac{m^2}{s^2}$$

Notice that the losses through the perforated plate is really low, that is why, in the calculation outputs (Figures 38, 39 and 340) the pressure drop is absolutely negligible. Even though we included these friction losses to be establish the results for our own methods.

After some rearrangement we could express the pressure drop as:

$$P_1 - P_2 = \left(\frac{{u_2}^2}{2} + gz_2 + e_z - \frac{{u_1}^2}{2}\right)\bar{\rho}$$

Computing the values, we have that:

$$P_1 - P_2 = \left(\frac{(0.112)^2}{2} + 9.81 * 1.23 + 199.45 - \frac{(1.3)^2}{2}\right)1.128$$

$$\Delta P = 237.64\ Pa + 0.051 = 237.7Pa = 2.38 \times 10^{-3}\ bar$$

9. Simulation

We will perform a CFD Simulation to determine the pressure drop, velocity profiles, vectors of pressure, contours, etc. when we perform the simulation, we will obtain important data for our further comparison and redesign of the equipment. Plus, we will obtain some graphical description of an approximation of the real behaviour of the apparatus, and this will allow us to see where the actual equipment present most of the problems and try to solve them in the new design which, at the same time is the reason and "soul" of this project.

The simulation will be carried out in the ANSYS Fluent software, all the performed actions will be explained furthermore as continues:

9.1 Model design

The first step of the simulation will be to generate the model of the geometry which will be simulated, but first of all we did the whole actual model for understanding of the problem and the functioning of the equipment. The model was designed in the SolidWorks software, due to its facility to maneuver and modelling characteristics, on the other hand, when saving the geometry in STEP file can be easily imported to ANSYS.

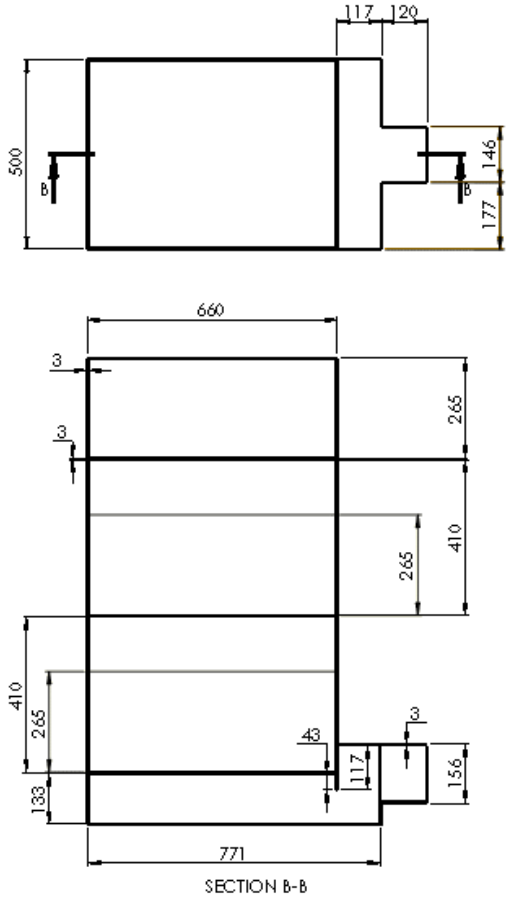

Figure 41. 93.75 kg Coffee dryer general dimensions. Drawn in Solidworks by the author.

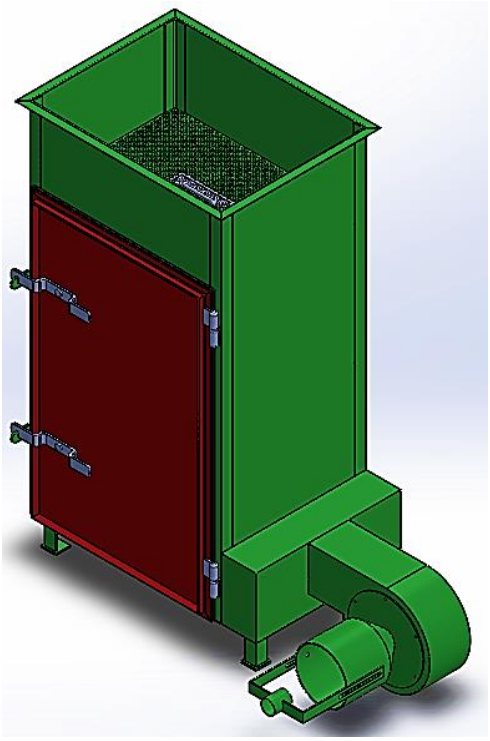

Figure 42. 93.75 kg Coffee dryer model isometric view. Drawn in Solidworks by the author.

As it can be seen in the Figure 42 and the Figure 43 the model was done trying to keep most of the details constructed in order to approximate the results as much as we can to the real behaviour.

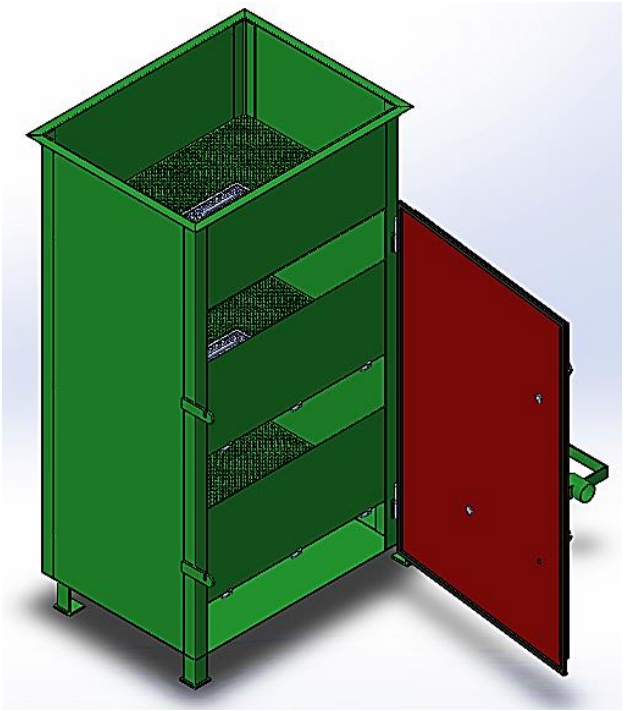

Figure 43. 93.75 kg Coffee dryer inside characteristics. Drawn in Solidworks by the author.

The number of perforations was kept as the real one, the trays, air inlet and general dimensions were kept as the real ones, the only thing which was not taken into account in this model was the gas burner and the fan, but they are not that important since we have already the air temperature and flow into the equipment.

After generating this geometry is possible then to either create the negative geometry (Figure 44) of the same which will actually represent the fluid in the equipment or simply draw it because all the dimensions are known for us. We should create boxes for all of the zones, in the end we will have a multibody solid, in which each box will represent air, coffee or tray.

You might ask yourself why are we including the coffee and trays in the boxes representation since they are solid materials, but in the simulation stage we can give to those boxes an specific permeability factor which will include the porosity of the material and the inertial and viscous resistances, so actually the software will recreate this solids from the porosity point of view (the opposite) and therefore it can be simulated as a fluid.

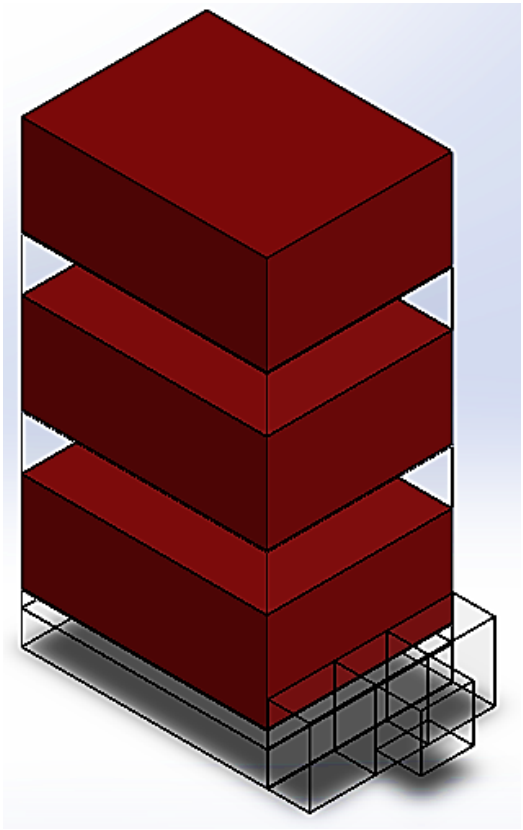

Figure 44. 93.75 kg Coffee dryer negative geometry (fluid geometry). Drawn in Solidworks by the author.

The Figure 44 displays the negative geometry of the dryer. The red boxes represent the coffee, the black boxes which might be more visible in the Figure 45 represent the perforated plates, and, finally the invisible boxes represent the air. As it can be seen, the air is further divided in plenty of

boxes, especially in the bottom side, this is done because the geometry in the bottom is a bit more complex, so, to ease the mesh generation and the node connections in this geometry is easier to split it into boxes and then just try to make the mesh more homogeneous with sizing and mesh generation methods.

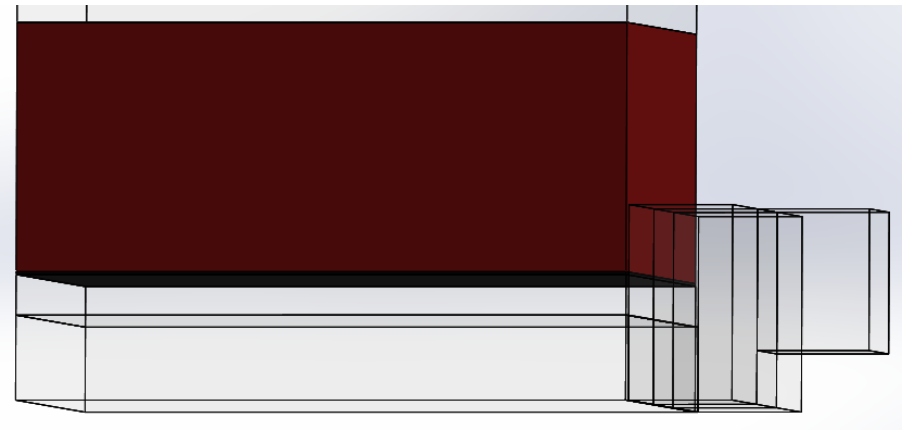

Figure 45. Bottom side boxes distribution. Drawn in Solidworks by the author.

For having a more complete approach to the problem, we also generated a model with the fluid geometry generated by each system, to be clearer, in the bottom side all the air was generated as one body as shown in the Figure 46, then it is possible to calculate the pressure drop in this specific segment by creating a new body from it. This calculation can get quite extensive and complicated to calculate by hand.

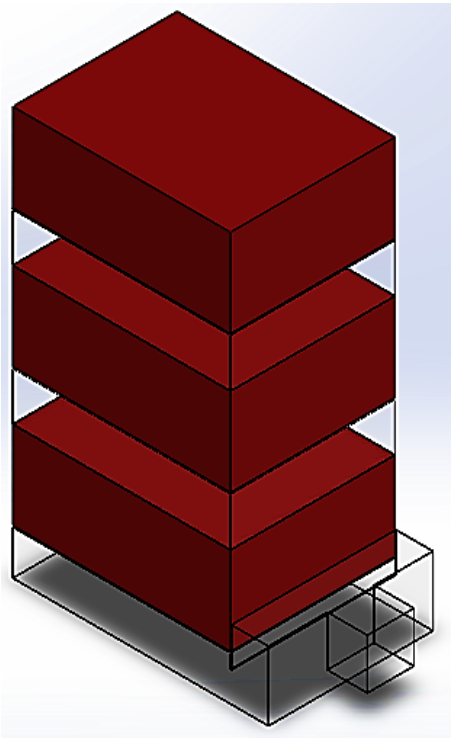

Figure 46. 93.75 kg Coffee dryer negative geometry with bottom side air merged. Drawn in Solidworks by the author.

9.2 Mesh generation

For the mesh generation we will generate a single .msh file in the ANSYS Workbench and then save it for further manipulation in the Fluent component.

The first step then will be to import the geometry which was saved as a STEP file (Figure 47), then we should, for ease the whole calculation rename all of the geometries (boxes) so it will be more understandable in the mesh generation step because there we must re-check the contacts held between each body.

We can define the geometry as "fluid" by selecting all the generated bodies and picking in the left hand side tab called "detail of bodies" (Figure 48) the correct option: fluid.

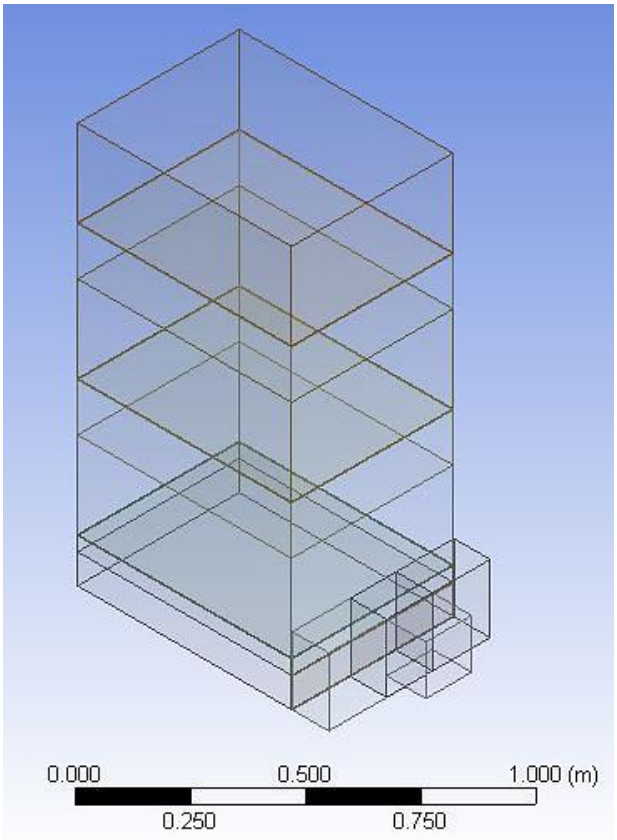

Figure 47. STEP file imported into the ANSYS Design Modeler add. Done in ANSYS by the author.

The definition of the geometry or bodies as a fluid can be also done after, when we set up the simulation parameters, but it is some advantage to do it now just to keep an ordered and organized solution scheme.

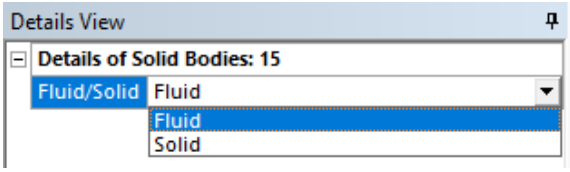

Figure 48. Fluid/Solid Selection for the geometry's bodies. Done in ANSYS by the author.

When we finish renaming the boxes depending on their nature e.g. Coffee 1, Tray 3, Air 2, etc. and when we select the adequate type of state of them, we can continue then performing the mesh generation, to do so we have to be sure that our model is ready (just check the down left hand corner) close the Design Modeler.

Now we will be back in the workbench, we will see a green mark just right next to the geometry, which will indicate that the geometry was well defined, and it is ready for use. Next step then will be the mesh creation, then we will double click on mesh and the add "Meshing" will open and will display the geometry which was defined in the past step.

The mesh generation should be taken seriously because our accuracy in the results will depend on it, our advantage is that the geometry of our dryer is mostly rectangular, so the mesh can be set up as with quadrilateral type and it will be good enough.

Nevertheless, the first thing that we should take an eye on is the contact regions in the connections menu, because our model has very thin geometries such as the trays, air lid, etc.

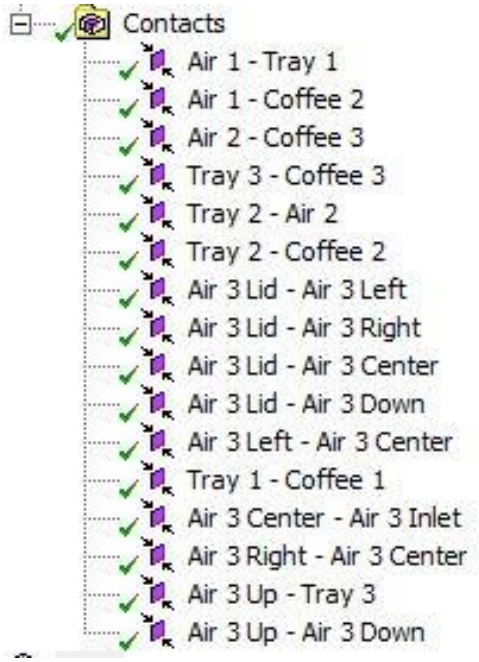

Figure 49. Fluid/Solid Selection for the geometry's bodies. Done in ANSYS by the author.

The software then ignores this space which should be kept, and we have to check the automatically created connections and then manually delete those which do not exist, taking into account that we know which bodies have contact between each other. Then we should have 16 contact regions between the solids and we can rename these contacts to understand which bodies are interacting at the moment.

When we have already set the correct connections, we should proceed then to define the mesh properties. First, we will define in "Defaults", "Physics Preference" CFD, this due to the kind of problem we want to solve (Computational Fluid Dynamics) since we want to analyze the air flow through the equipment we should as well select the solver preference as Fluent; then in the "Sizing"

menu we will select a fine mesh from the relevance center with a high smoothing and slow transition; by doing this selection the calculation might take more time but the approximation will be better.

After doing this we will generate the mesh and then analyze how many elements and nodes we have. The required quantity for such a geometry shall be around half a million elements, but with the basic mesh generation that we performed we obtained roughly 54000 elements (Figure 50), reason why we should insert some meshing method.

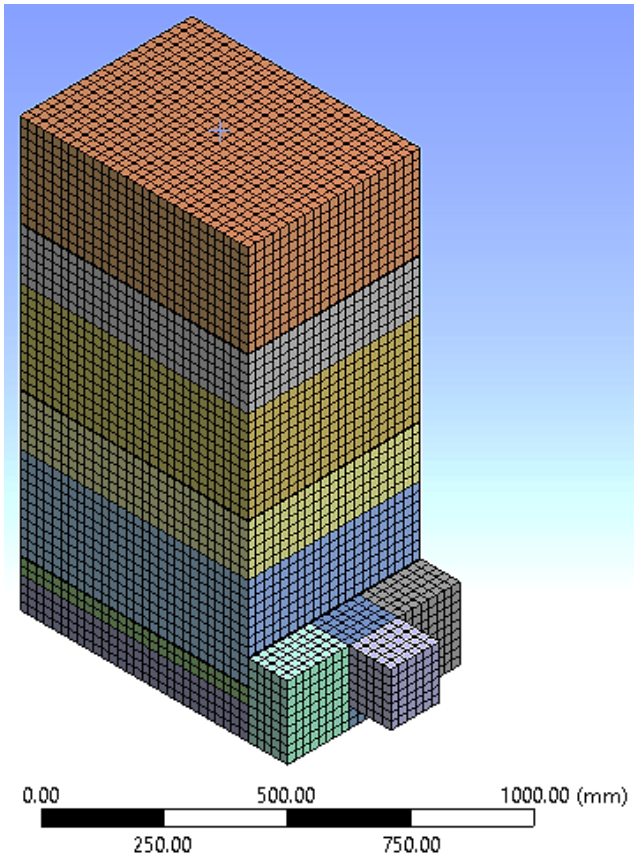

Figure 50. First generated mesh. Done in ANSYS by the author.

Further in the mesh generation we inserted the sizing options to make the size of the element smaller. In the scoping method we select the whole geometry (all the boxes), afterwards we use an 8 mm element size and a hard behaviour. This was established after performing a lot of tries and finally, with this value we obtained a good number of elements, and plus the nodes match from body to body and, as we already explained this is a good phenomenon because the simulation will be more accurate and wont drift when it changes the surface under analysis.

Scope	
Scoping Method	Geometry Selection
Geometry	15 Bodies
Definition	
Suppressed	No
Type	Element Size
Element Size	8. mm
Behavior	Hard

Figure 51. Used parameters in the sizing option. Done in ANSYS by the author.

After generating the mesh with the desired parameters, we obtained the following result as for the general view of the mesh.

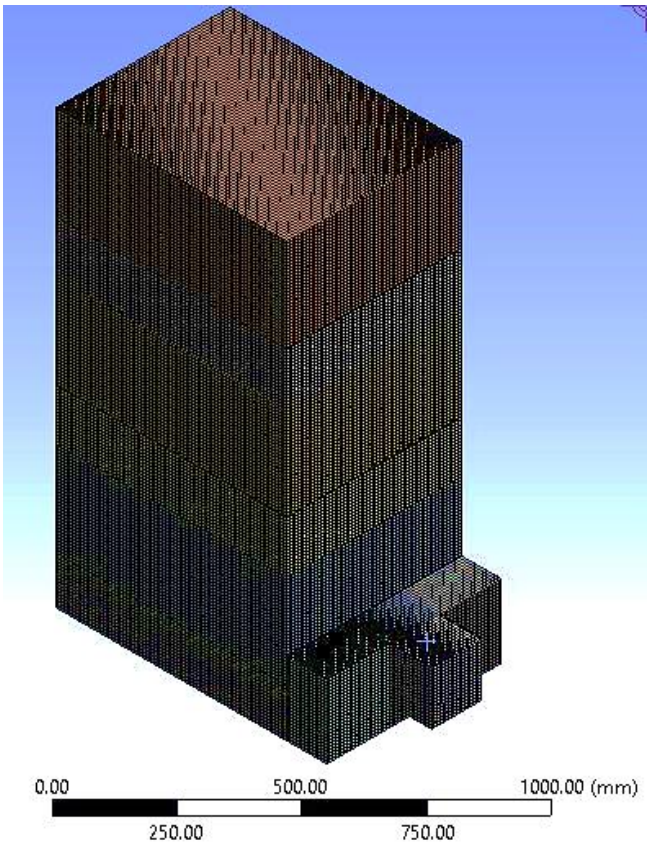

Figure 52. Obtained mesh with the desired parameters. Done in ANSYS by the author.

With this mesh we obtained the following statistics:

- Nodes: 881108
- Elements: 801651

As it is seen the number of elements exceeded the required (500000), but even though we have already a good quantity of elements we should not rely only on it, we should take a look at the skewness and orthogonal quality which will determine the mesh quality.

The orthogonal quality is computed for cells using the vector from the cell centroid to each of its faces, the corresponding face area vector, and the vector from the cell centroid to the centroids of each of the adjacent cells. The worst cells will have an orthogonal quality closer to 0, with the best cells closer to 1. The minimum orthogonal quality for all types of cells should be more than 0.01, with an average value that is significantly higher.

- Orthogonal Quality: Min (0.99998); Max (1); Average (1).

Skewness is defined as the difference between the shape of the cell and the shape of an equilateral cell of equivalent volume. Highly skewed cells can decrease accuracy and destabilize the solution. For example, optimal quadrilateral meshes will have vertex angles close to 90 degrees which is our case. A general rule is that the maximum skewness in most flows should be kept below 0.95, with an average value that is significantly lower. A maximum value above 0.95 may lead to convergence difficulties and may require changing the solver controls.

- Skewness: Min (1.3057e-010); Max (3.2038e-003); Average (7.0003e-004).

As we can see then our mesh complies with the required conditions for a good performance in the simulation. We can re check the location of the elements from body to body and it is also well placed as seen in the Figure 53, which displays a zoom to the bottom side geometry and the mesh looks good in the contact bodies.

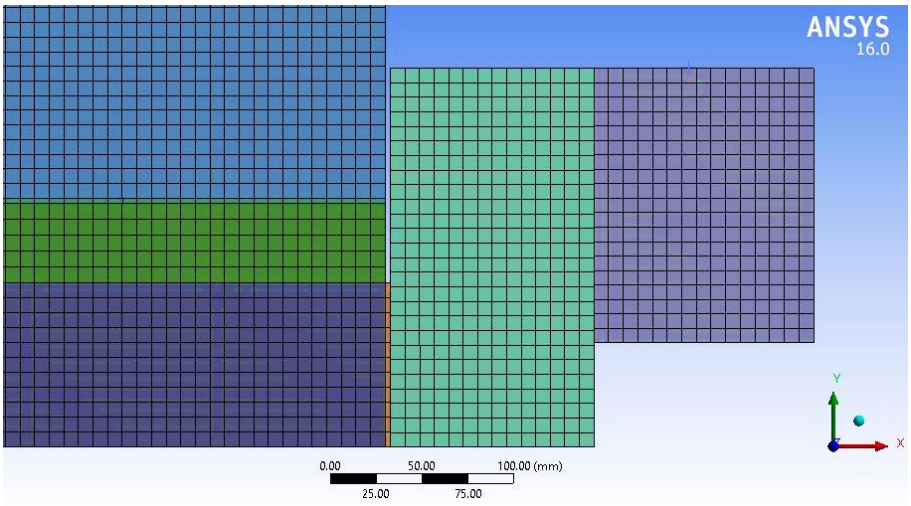

Figure 53. Bottom side geometry zoom for meshing display. Done in ANSYS by the author.

We could also perform a section to observe the internal mesh and element distribution as shown in the Figure 54 to ensure that we created an optimal meshing operation.

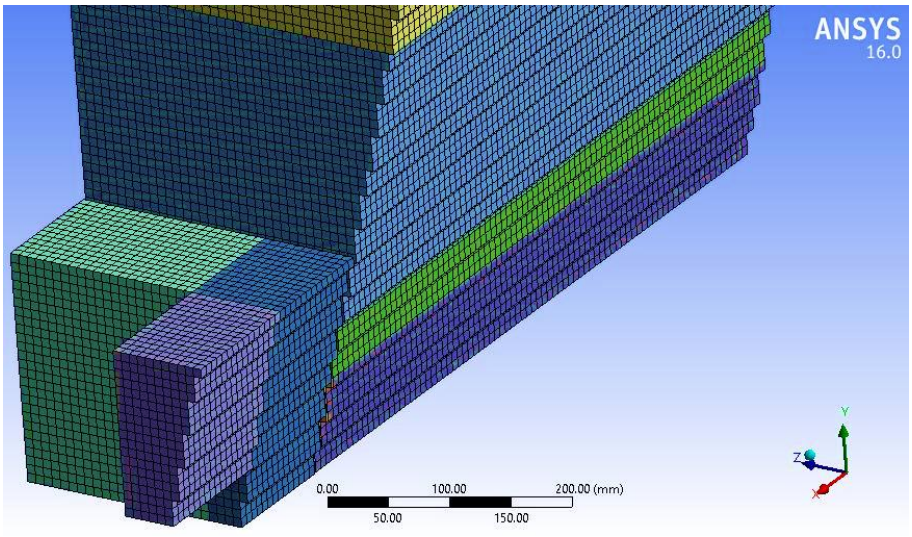

Figure 54. Section for internal elements display. Done in ANSYS by the author.

Finally, we could then name the inlet, outlet and wall faces; this will be pretty useful when we set the initial conditions in the setup of the analysis:

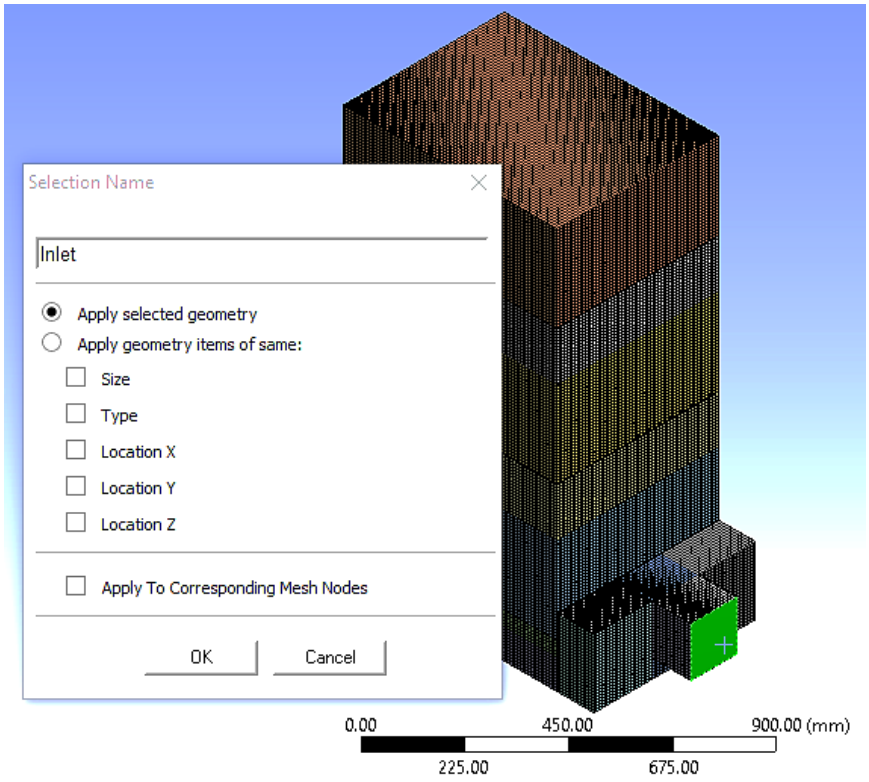

Figure 55. Definition of inlet face. Done in ANSYS by the author.

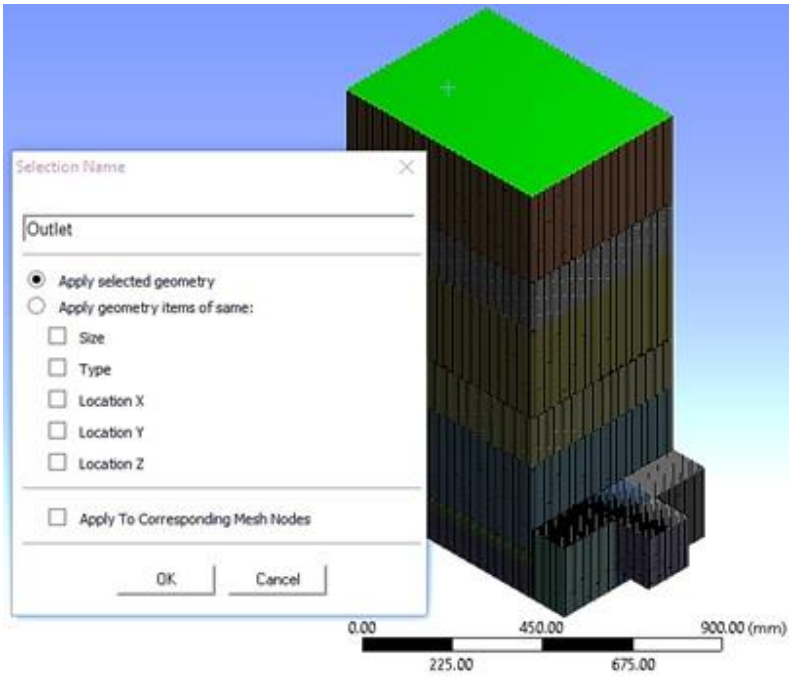

Figure 56. Definition of outlet face. Done in ANSYS by the author.

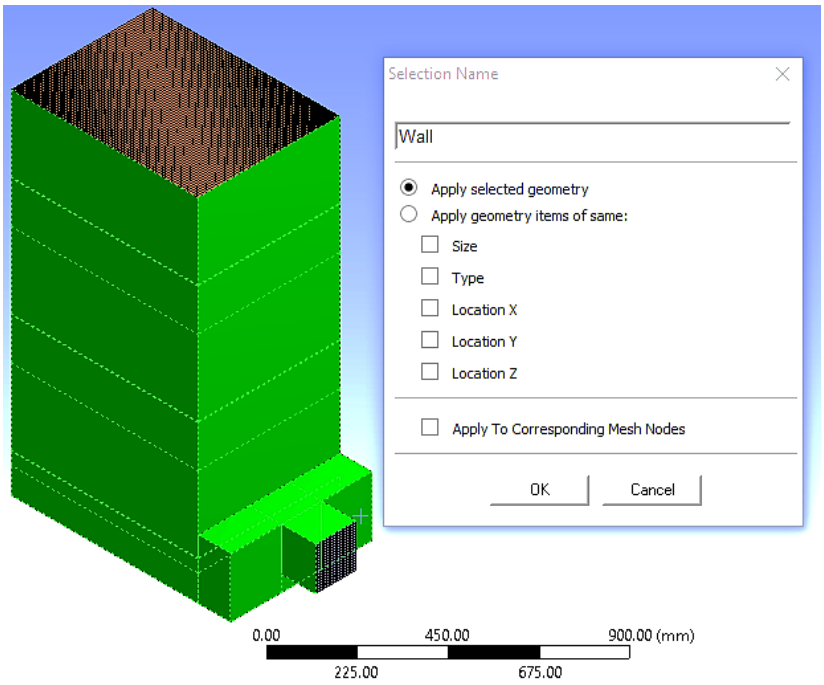

Figure 57. Definition of wall faces. Done in ANSYS by the author.

Then, by finishing the last named section our mesh is finished, we have to remember that we will perform the solution using the Fluent add in, we can do it directly in the workbench but sometimes it can get a bit risky because the platform tend to present general problems related with file management; that is why we will save the mesh file as a .msh file and then we will read it from the Fluent software directly to avoid any type of problem that might come up.

9.3 Setup

Let us remind that the analysis will be performed directly in the Fluent add on, by executing the study in this way we will avoid file management problems.

First of all, we must of course open the Fluent environment and we will select the "double precision" command for a tighter calculation. After the environment is fully displayed, we will then click in the "file" menu, select "read mesh" and we will browse for our .msh file which was previously saved somewhere from the Meshing component in the workbench.

The software will read and perform a fast reconnaissance of the mesh and the geometry we selected to work on, after the reading and building the mesh process will finish (Figure 58), we must "check" the mesh to ensure that all elements and components were well constructed and to avoid strange interferences as well.

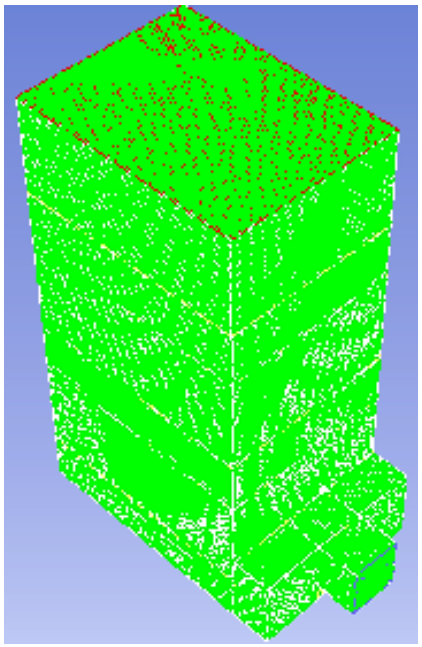

Figure 58. Created mesh. Done in ANSYS by the author.

The mesh is not presented quite clear, but this is due to the number of elements present and the small space which we have to display it, but the mesh was built without problem and well checked.

As well, the mesh is shown in a green color interface which was selected from the Mesh Display Configuration menu to be able to distinguish the inlet (blue) and outlet (red) faces. We will then finish the general setup by selecting the options displayed on the Figure 59, which will describe the type of solver, formulation of the velocity and the type of study, either time dependent or not.

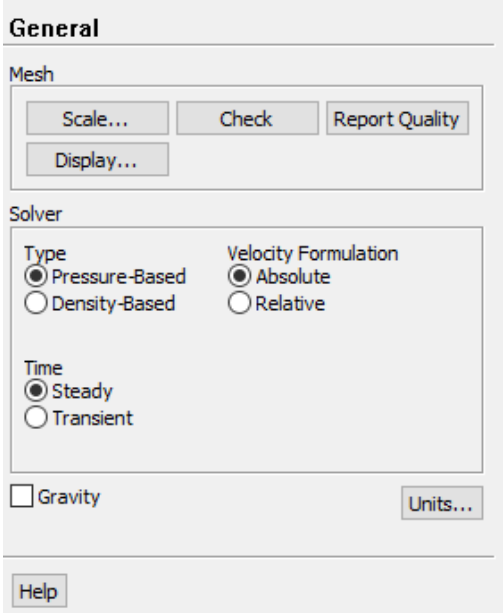

Figure 59. General set up conditions. Done in ANSYS by the author.

Afterwards we will open the "models" menu and edit the viscous model by selecting the k-epsilon model since we would like to enhance a turbulent model solution (Figure 60). The rest of options then will be shown as "off", and we will let them be as that since we are interested just in the selected model (Figure 61).

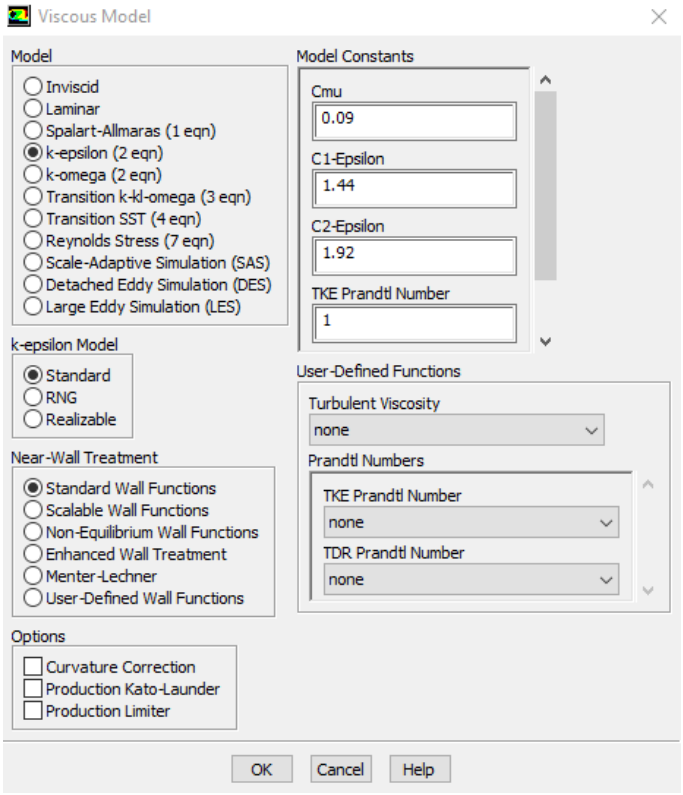

Figure 60. k-epsilon model selection. Done in ANSYS by the author.

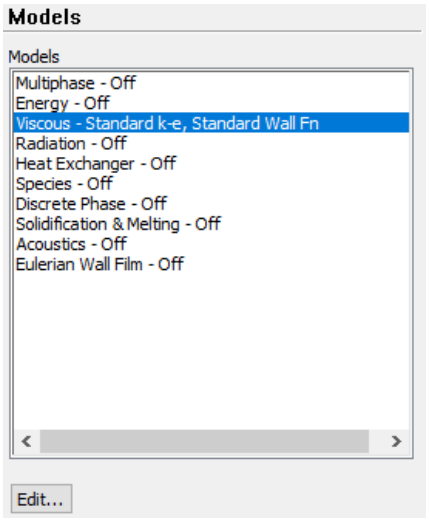

Figure 61. Resulting model setup. Done in ANSYS by the author.

As for materials we are interested just in air fluid, even though the software suggests aluminum as for solid compounds we should not take it into account for nothing. Again, as it was explained before, even if we know that the trays and coffee are solid materials it is quite complex to define for instance the properties of the coffee or the tray which holds a layer of paint, etc. but we can define them as air with certain porosity and it will be the same since we are considering the free air across the solid bodies which, it properties rely in the porosity characteristics.

The next step is really important because we will define the characteristics of the bodies, here we must be quite delicate because all the calculation will depend on the values, which we will fill in.

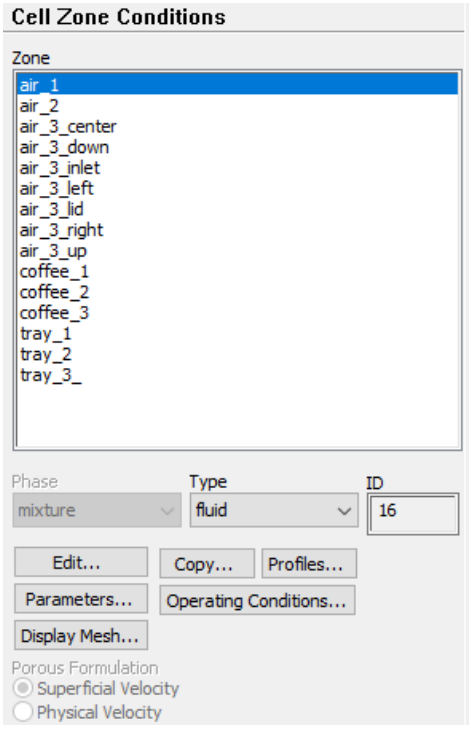

Figure 62. Cell Zone Conditions interface. Done in ANSYS by the author.

The Cell Zone Conditions display all the bodies present in the entire geometry, which as a reminder are 15 bodies (Coffee 1, Tray1, Air 1, Coffee 2, Tray 2, Air 2, Coffee 3, Tray 3, Air 3 Up, Air 3 Down, Air 3 Lid, Air 3 Left, Air 3 Center, Air 3 Right and Air 3 Inlet),as shown in the Figure 62, and here we will define the characteristics of those which have some special condition, such as the porosity for instance.

We will edit such elements, click the porous zone box, head to the porous zone tab and fill in the requirements as shown in the Figure 63.

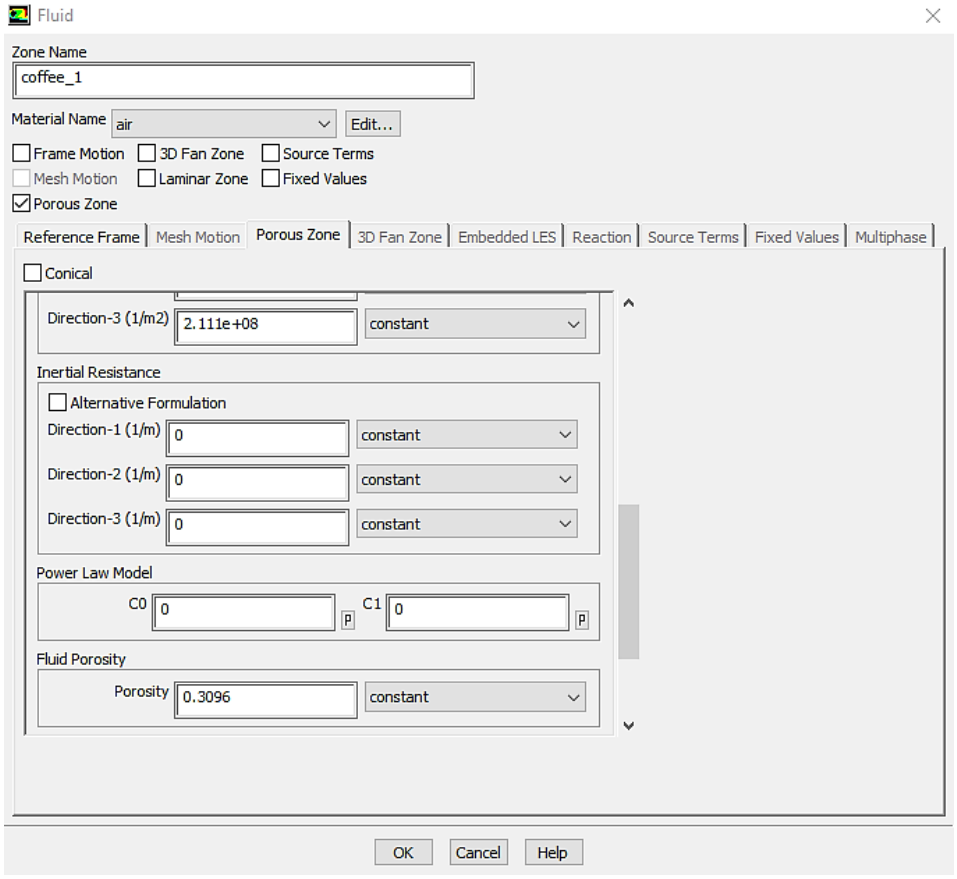

Figure 63. Interface for Cell Zone Conditions data. Done in ANSYS by the author.

While setting up the conditions of the cell zones, we see that the software is asking for some Inertial Resistance and Viscous Resistance, both of these resistances are quite important to be taken into account because they describe both resistances which, depending on the porous bed porosity value will restrict the flow by the inertia and viscosity.

To be able to calculate these values we will use the Equation 25 which will allow us to calculate the viscous resistance and the Equation 26 for calculating the inertial resistances:

$$R_V = \frac{150}{{d_p}^2} * \frac{(1-\varepsilon)^2}{\varepsilon^3} \qquad (25)$$

$$R_I = \frac{3.5}{d_p} * \frac{(1-\varepsilon)}{\varepsilon^3} \qquad (26)$$

Where:

- R_V: Viscous resistance $\left[\frac{1}{m^2}\right]$
- R_I: Inertial resistance $\left[\frac{1}{m}\right]$
- d_p: Particle diameter $[m]$

And performing the calculation for all the coffee porous beds we have that the viscous resistance output is:

$$R_{V\_Coffee\_1} = \frac{150}{(0.0128)^2} * \frac{(1-0.3096)^2}{(0.3096)^3} = 1.47 \times 10^7\ m^{-2}$$

$$R_{V\_Coffee\_2} = \frac{150}{(0.0124)^2} * \frac{(1-0.2987)^2}{(0.2987)^3} = 1.8 \times 10^7\ m^{-2}$$

$$R_{V\_Coffee\_3} = \frac{150}{(0.012)^2} * \frac{(1-0.2879)^2}{(0.2879)^3} = 2.21 \times 10^7\ m^{-2}$$

And for the inertial resistance we have the following results:

$$R_{I\_Coffee\_1} = \frac{3.5}{(0.0128)} * \frac{(1-0.3096)}{(0.3096)^3} = 6361.45\ m^{-1}$$

$$R_{I\_Coffee\_2} = \frac{3.5}{(0.0124)} * \frac{(1-0.2987)}{(0.2987)^3} = 7427.53\ m^{-1}$$

$$R_{I\_Coffee\_3} = \frac{3.5}{(0.012)} * \frac{(1-0.2879)}{(0.2879)^3} = 8703.68\ m^{-1}$$

Now that we have calculated these values, we should include them in the cell zone conditions for the coffee bodies with their porosity as well and as for the perforated plate we will use the calculated porosity as well.

When finishing this setup, we will move on now to the boundary conditions menu, here we will seek to establish the input data which is known already. Let us then search for the inlet face and we will set the "type" as "velocity inlet" and in the dialog box which will pop up we will set the value; this will be our first boundary condition since we know this value (1.3 m/s). After we will find the outlet face and the "type" will be "pressure outlet", in the upcoming dialog box we will fill the Gauge pressure as 0 Pa because it is open to the atmosphere.

After setting the boundary conditions we can take a look at the mesh interfaces, which holds the information related to the linkage between the nodes across the bodies of the whole geometry (Figure 64). In the interfaces dialog box, we can see all the bodies we named and if we take a deep look at this feature, we have it correctly settled since the software already recognized the relationship between the already mentioned bodies.

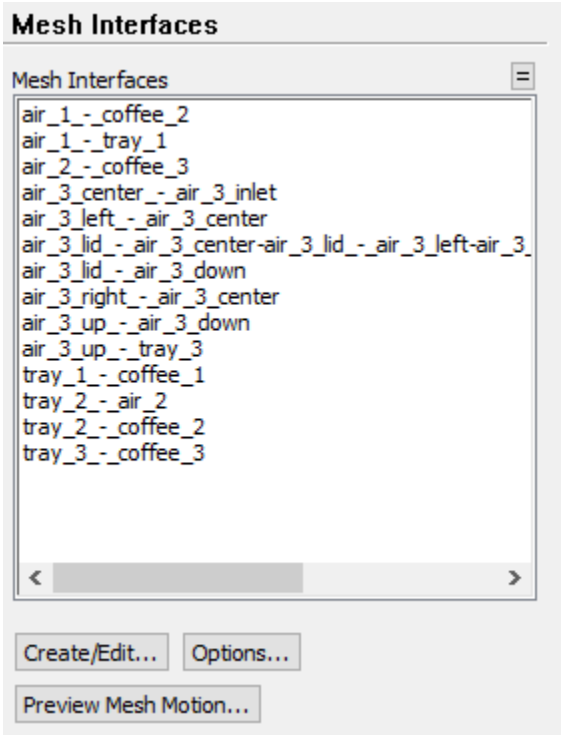

Figure 64. Mesh interfaces between the geometry bodies. Done in ANSYS by the author.

When finishing this last step, our setup will be ready for further purposes.

9.4 Solution

Now it is time then to perform our calculation, this segment consists basically in setting the activities related with the study analysis. First, we should take look at the "solution methods" and "solution control" tabs to verify that the adequate spatial discretization, pressure-velocity coupling and under-relaxation factors are well defined by the software. After, we will click the "monitors" tab and then we will "edit" the "Residuals, Statistics and Force Monitors" and in the "Equations" area we will then un-check all the convergence boxes; this will be done because we do not want to depend on the convergence but on the number of iterations, by this we can approach a more precise result.

We will after in the "Solution Initialization" run the Hybrid Initialization, it will perform 10 iterations and we will receive a message in the display window that the hybrid initialization is done (Table 1)

And we will receive the following data as for the Hybrid Initialization execution:

Checking case topology...

-This case has both inlets & outlets

Iteration	Scalar - 0
1	1.000000e+00
2	2.861420e-06
3	2.405645e-07
4	2.440013e-08
5	2.718533e-09
6	3.156469e-10
7	2.120392e-11
8	2.488563e-12
9	2.570853e-13
10	3.013676e-14

Table 1. Hybrid Initialization iteration results. Done in ANSYS by the author.

hybrid initialization is done.

When we perform correctly the hybrid initialization, we can now start the calculation, but after we will set the autosave option in the "Calculation Activities" tab each 250 iterations just in case something will happen, we do not want to lose our work.

After doing this in the "Run Calculation" tab we will check our case and take a look at the software recommendations, we can apply those changes or not, then we set the number of iterations to 2000 and click "Calculate" and wait.

9.5 Results

When the calculation is completed (after 2000 iterations) we can start to compute the desired results.

First of all, we will obtain the scaled residuals plot, which displays the behaviour of the study and its velocities, continuity, k and epsilon tendencies to stabilize in certain number of iterations, the plot is presented for analysis in the Figure 65.

We must remind again that we did not ran the calculation seeking for some convergence range, but we set a number of iterations and the software is "forced" to iterate as many times as we want even if some results already stabilized. This is for ensuring an accurate and precise result in all of the variables present in the case.

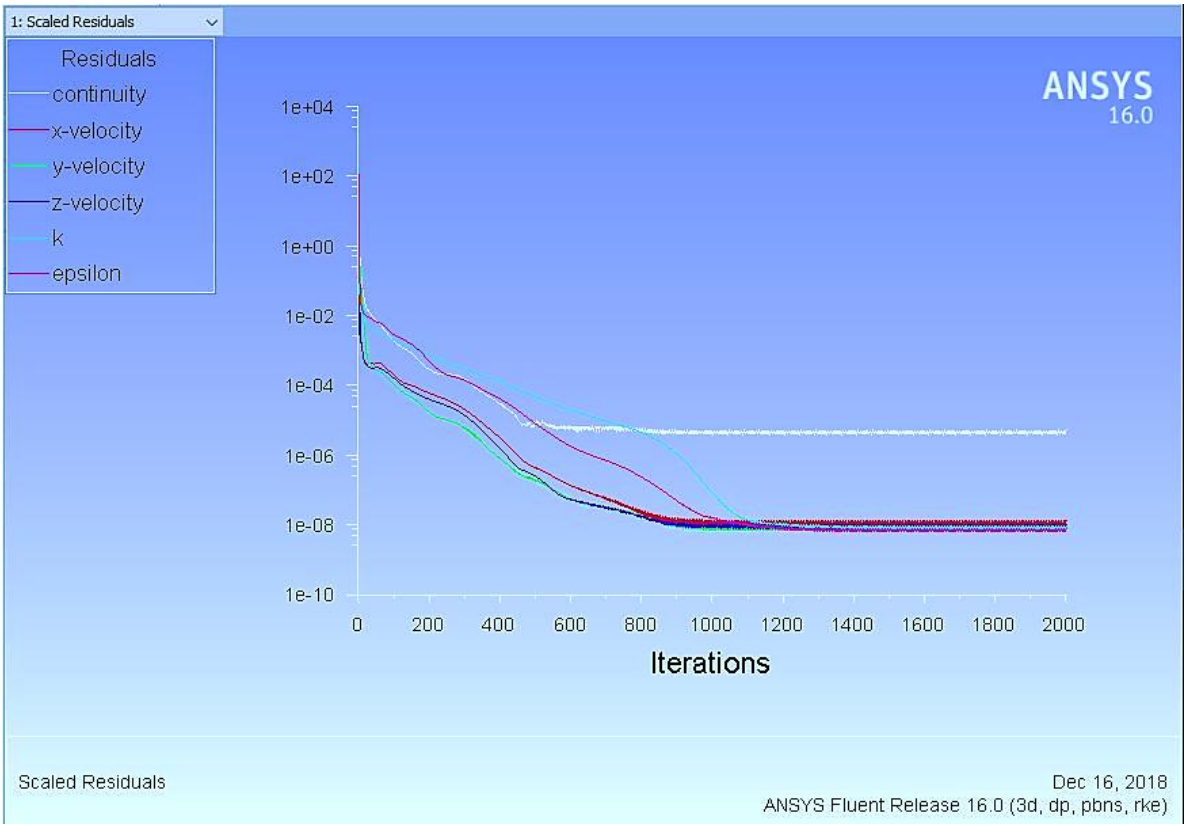

Figure 65. Scaled Residuals plot. Done in ANSYS by the author.

As it can be seen in the Figure 65 some residuals such as the continuity stabilized around the iteration number 500 while the rest of items reached the same around the iteration 1200. This is why we decided not to set a convergence but a number of iterations, which was enough because as it can be seen, all of the residuals have a stable behaviour at the iteration number 2000, therefore we could say that the results which will come after this calculation will be trustable and certain.

Going on, we can now click on the "graphics" tab in the Results menu, here we can display a graphical approach for our matter of interest. We must make a statement that the Fluent do not count with a friendly graphical environment, therefore we will generate the plots in the CFD Post add, which will display clearer and sharper graphs. But as we already have some plots, we can take a look at them to see how the apparatus is working.

We can then generate the auxiliary plots for the pressure, velocity and turbulence which are the most relevant elements which we would like to analyze and discuss for further re design of the coffee dryer.

In the dialog box which appears while clicking in Results/Graphics we will select for instance vectors of velocity, select all the surfaces and display the resultant graph which is shown in the Figure 66.

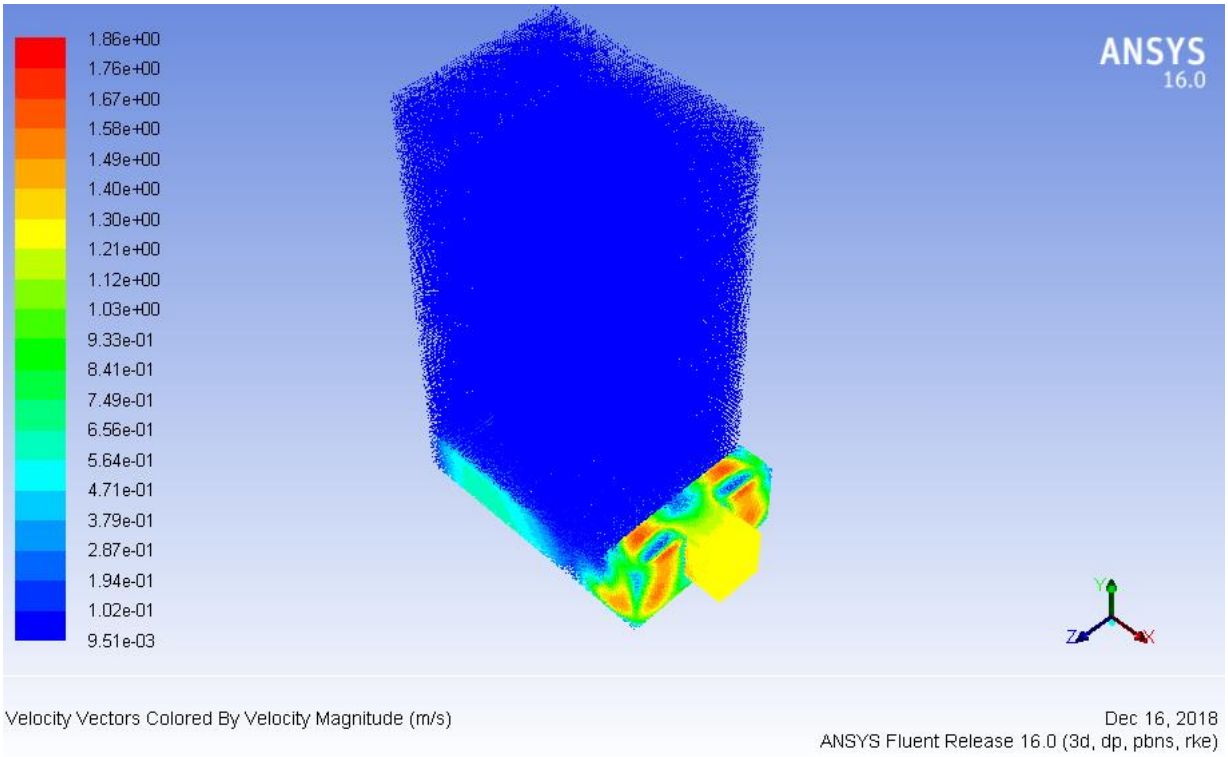

Figure 66. Velocity vectors graphic. Done in ANSYS by the author.

As we can see in the Figure 66, the obtained results appear to be correct, since we can denote some velocity behaviour according to the expected due to the geometry of the dryer, it can be seen as well that the apparatus present some conflict zone in the bottom geometry since it has a complex geometry. But as it was said the plots will be generated in the CFD Post which is quite good for displaying graphically any type of desired information. By now, we will move on to the "Reports" tab to verify, for instance our pressure drop calculation.

We will generate an area weighted average report in the surface integral box for the total pressure computing the inlet and outlet pressure and we obtain the following result:

Area-Weighted Average	
Total Pressure	(Pascal)
Inlet	257.59286
Outlet	1.2811924
Difference	256.31167

Table 2. Pressure drop results.

If we compare the obtained result with the fluent and the one obtained by hand we can see that they are pretty similar since we obtained a value of $\Delta P = 237.64\ Pa$, it is still a bit far from the calculated with fluent but we must take into account that in our handmade calculation we did not considered the pressure drop due to the air flow through the bottom side geometry and the one in the air 2 and 3 bodies because they can be considered as small, and if we check the results we have roughly $18.67\ Pa$ difference which is a small value, we can say then that our calculations are quite similar, which will let us assume that the analysis is well performed.

Now that we can say that our calculation is correct, we should move then to the graphical CFD Post environment to be able to see and perform the correspondent study of the functioning of the equipment, and by doing this we could see then which are the spots to improve in the design of our new dryer.

9.6 Post Analysis

As it was said before, we will display the main graphs of the performance of the actual equipment to be able to detect the poor design places in the same, first of all we would like to explain how to generate these plots and after we will see the most important results.

After opening the CFD Post add on and the we will head to the "file" tab, "load results" and we will select our .dat file which was obtained from Fluent; once the model opens (Figure 67), we should insert now a location, plane in the XY direction (Figure 68) to be able to see the vertical behaviour of the flow in this plane and create.

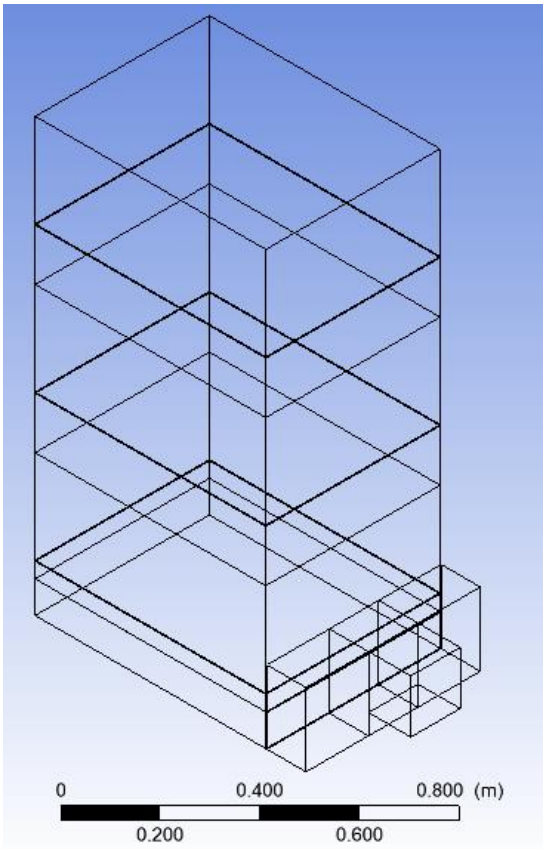

Figure 67. Result model from the Fluent loaded in the CFD Post. Done in ANSYS by the author.

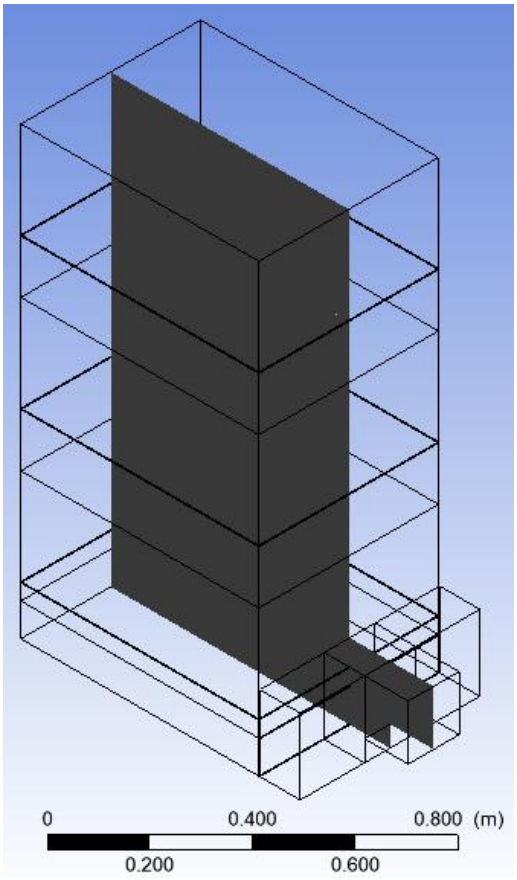

Figure 68. Created plane in the XY plane which will display the results across this section for further study. Done in ANSYS by the author.

Now that the plane is created, we can start to generate graphs; we must state that the plain is created in this orientation because as it is seen in the Figure 68 it contains all the side geometry, including the air inlet and all the bottom side geometry which is one of the most interesting for us.

Plots:

The first graph which we would like to display is the pressure graph to compare it with the already obtained in the Fluent.

We will then insert a contour in all the domains since we want to see the behaviour across the whole apparatus, the location will be the plane (we named it "plane 1"), pressure will be selected as variable and a global range. All this configuration is shown in the Figure 69. We can see that the pressure is already displayed as Min: 0 [Pa] and Max 257.603 [Pa], which was the already calculated value but at least we can re check that there was non mistake performed during the loading of results. After we will set the number of contours with a considerable value such as one hundred (100), so the graph will be displayed with a soft transition across the whole plane and by displaying such a figure it will be easier to understand the transition between bodies.

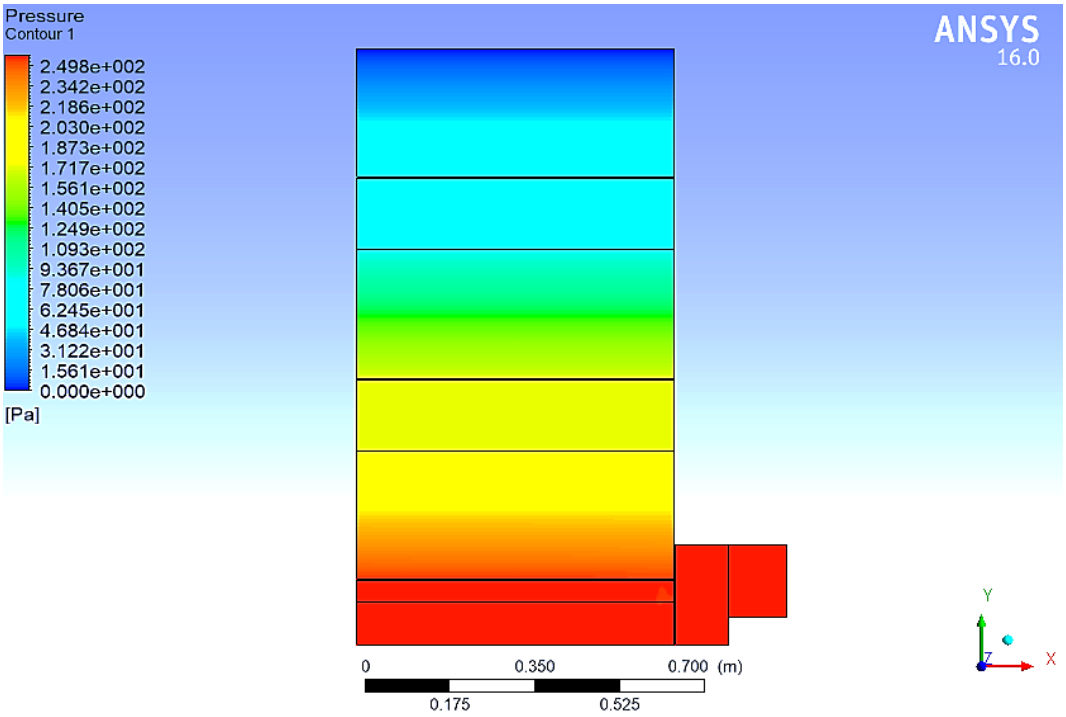

Figure 69. Pressure contour graph. Done in ANSYS by the author.

As it can be seen in the Figure 69 the pressure drop occurs in an uniform way but, in the complex bottom geometry, which include the air inlet, air 3 bodies and it enters a bit into the coffee 3 the pressure maintains a most likely uniform behaviour, which represent good news because as we did not considered the pressure drop in the bottom air geometry this graph is confirming that the same is quite low, reason why we can be sure that by not taking it into account in our calculations was not a big problem. On the other hand, the pressure change between the coffee layers, 3, 2 and 1 is quite big, being the 3 one higher (as expected), and the drop in the upper layer of the dryer was not that representative (as expected). We can also see that the drop in the trays is non perceptible, which matches as well with our calculations. So, we could say that the pressure drop was calculated and double checked properly.

Continuing our graphical analysis, it would be good as following step display the plots of the velocity profile across the entire dryer. With the velocity variable we will display a bunch of elements which will supply the study with different information.

The first element to display will be the velocity vector tendency, this plot will provide us with a graphical interpretation of the vector distribution as it comes with the velocity profile and we could for instance follow the most accelerated or non homogeneous elements and, while taking a look at their trajectories we could then detect critical points of malfunction in the dryer.

For displaying such graph we could then locate the “insert” menu, deploy it and insert the “vector” option; as it opens a configuration box we will select: All domains, plane 1 as location, vertex as sampling, reduction factor (to display clearer the path of each element), velocity as variable and then we will just “apply” these selections and we will obtain the graph showed in the Figure 64.

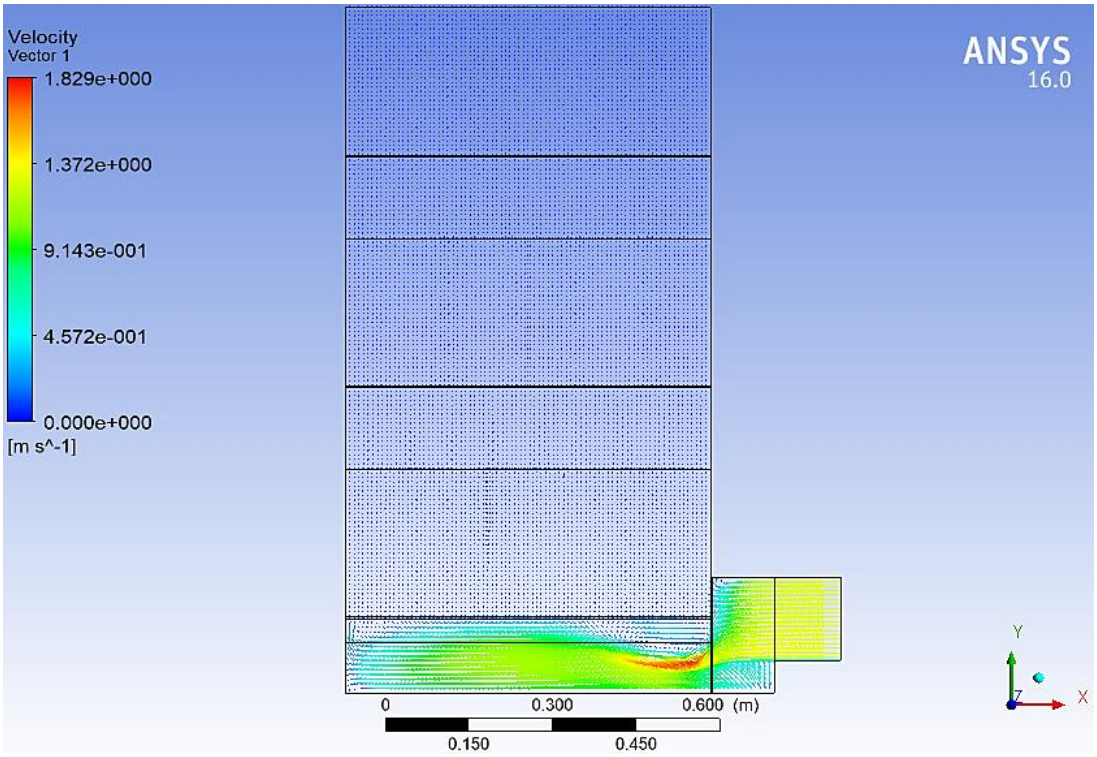

Figure 70. Velocity vector graphical behaviour. Done in ANSYS by the author.

As it was expected from the complex bottom side geometry the velocity follows a quite rough behaviour in the first stages of the dryer (Air 3). If we take into consideration the main purpose of the dryer, a more behaviour for the velocity would be better. The air by basic knowledge should be even across the apparatus, and in the drying stage it is even, but it has already lost a lot of velocity which, at this point could be translated into a better drying due to a higher velocity.

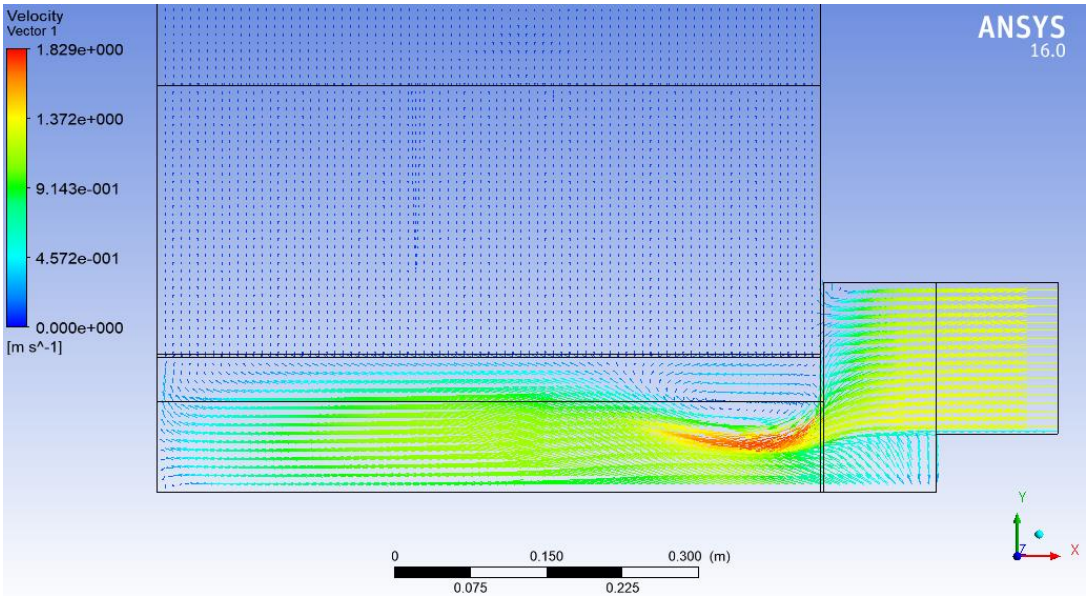

Figure 71. Zoom into the velocity vector graphical behaviour in the bottom side geometry. Done in ANSYS by the author.

As it can be seen in the Figure 71, the air distribution is very poor, it is unknown why the main design hold this geometry, the air is crashing against the wall, then it is generating a high velocity zone which has no meaning at all and as it was said before, the main problem with this setup, even if the dryer works, is that the velocity is lost because of nonsenses, if this problem would be fixed then the velocity will be on the opposite, used to perform a quick drying, with the same fan power, the same heating, but less drying time, therefore the same amount of energy spent on the fan and heater can be used for drying more amount of coffee, which equals to efficiency.

Once that we already know the velocity vector distribution, we would like to perform a better description of the velocity problem, reason why we would like to present the stream line behaviour in our model. The streamline is the path that a particle of zero mass would take through the fluid domain.

The path is calculated using a Runge-Kutta method of vector variable integration with variable timestep control. As usual, we will head for the "insert" flag and select "Streamline" and in the further parameter configuration we will select: 3D Streamline, All Domains, Start from Inlet, equally spaced, we will use 500 points for a more even distribution and coverage, we will select velocity as variable and forward as direction and then we will apply these selections.

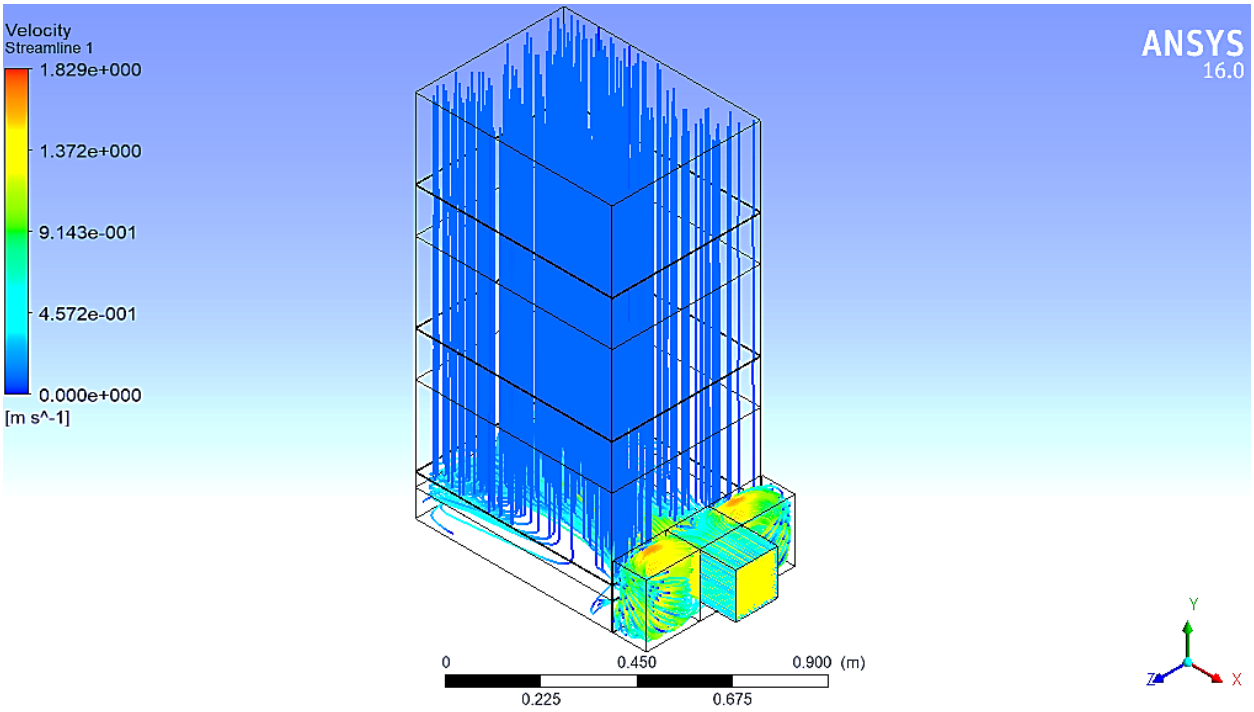

Figure 72. Velocity Streamline display with 500 points. Done in ANSYS by the author.

As expected, the velocity performance is really low, the downside geometry results just corroborated our previously said statements, most of the velocity is lost just in the beginning of the process, and it is lost due to wrong design causes.

Another question arises: how is the air velocity streamlines? Which, can further be adapted or considered as air distribution, how does it look like from the top of the equipment? view which

ultimately will let us know how the flow is mainly directed through the porous bed of coffee and through the apparatus and this of course can be directly related with the drying efficiency.

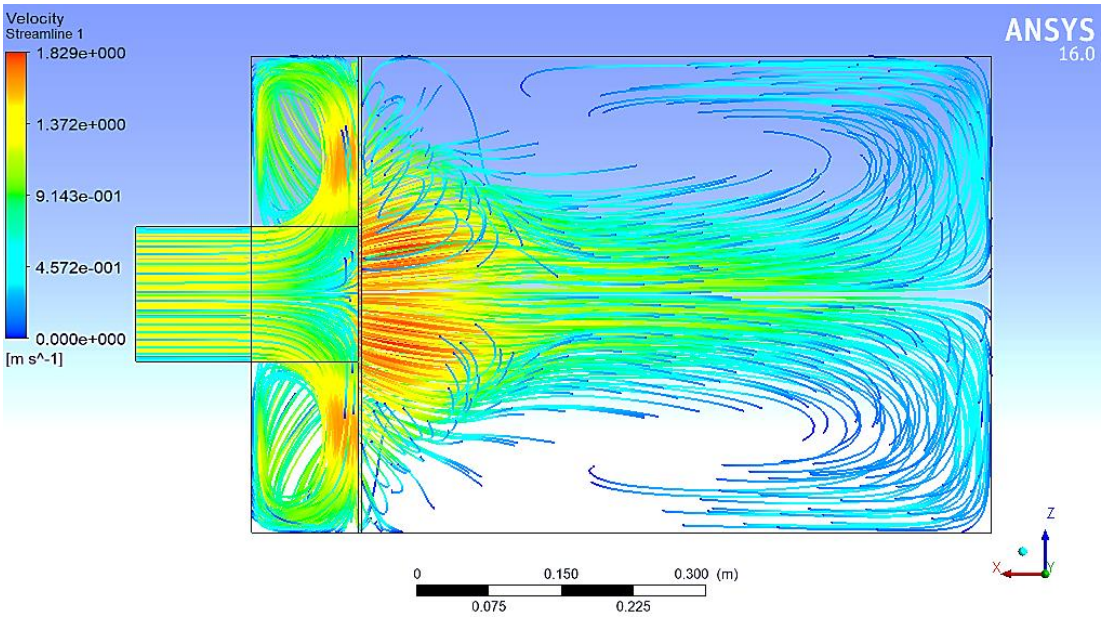

Figure 73. Velocity Streamline display with 500 points top view. Done in ANSYS by the author.

The Figure 73 displays one of the most telling images in this document, it can be seen that most of the dryer is working without presence of air, this failure is not admissible at all, and it is fully relying to geometry deficient design. All that area which holds non streamline can be considered ideally as blank spots, where, by chance the air is not flowing, and again, this is due mostly because of the design plus the velocity losses in the air entrance. This information is so shocking that the same plot was generated using 1000 points to re check the information obtained above:

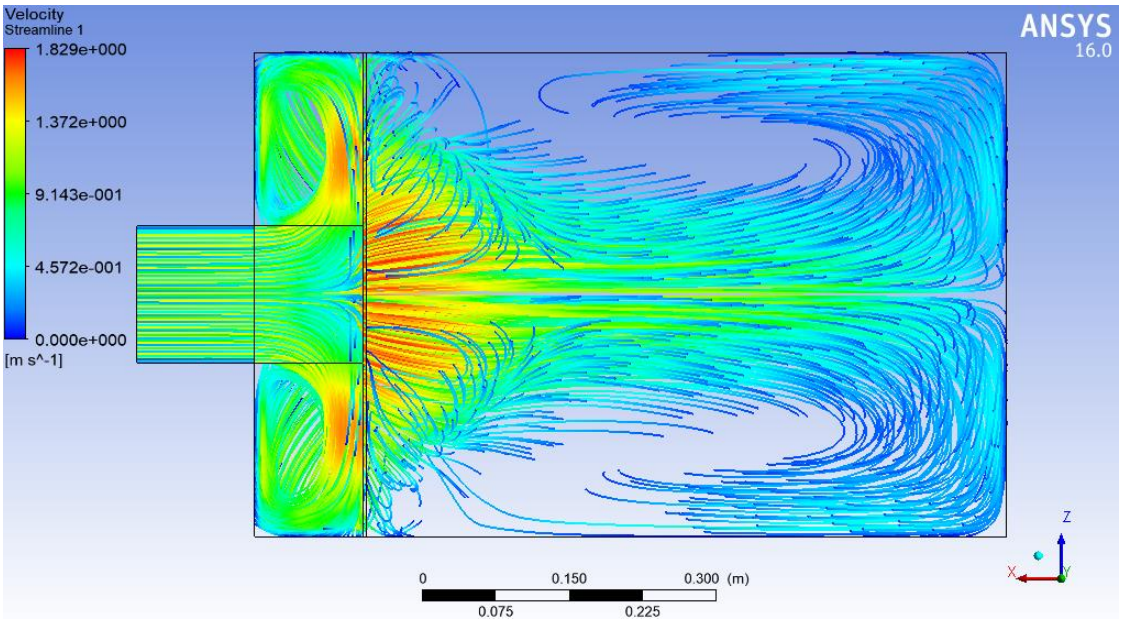

Figure 74. Velocity Streamline display with 1000 points top view. Done in ANSYS by the author.

The Figure 74 contains the same erratic streamline behaviour, even if we increased the amount of points to the double, and some sort of improvement can be seen, those blank spaces still quite big and the velocity stills, of course having a poor performance, now we have even more reasons to perform the re design of the dryer, and, from the engineering point of view supply a solution with the necessary changes for obtaining the best product and quality of the same.

One of the best suggestions to solve this problem is to take into consideration a circular geometry of the dryer and also to change the location of the inlet, maybe in the bottom would be a good place to supply the air. A diffusor would be a good idea as well taking into consideration that by doing so the drying air could be homogeneously distributed and the velocity will be even in all the starting line.

10. Re-Design

Now that we had already stablished the main problems and we know as well where to focus our attention as for the re designing we can start then the development. It is important to remind that our approach for the improvement of the performance of the equipment relies mostly in the geometry we have a good start point.

10.1 Geometry considerations

While performing the CFD Simulation to the rectangular dryer we could see that the air distribution was very poor due to two main reasons:

- The rectangular shaped geometry of the equipment.

- The strange geometry that follows the air inlet.

As these problems do not represent a big challenge, we decided to firstly design the new dryer changing the outer geometry for a circular shaped body and the inlet of air will be placed in the bottom of the apparatus.

The volume for maintaining the same output of coffee will be then:

$$V = 0.08619\ m^3$$

And, as we already know the target volume, we can find a first temporal diameter to see how it will fit our conditions, so, maintaining the height of the layer we have that:

$$V = \pi \frac{d^2}{4} h$$

$$0.08619 m^3 = \pi * \frac{d^2}{4} * 0.265 m$$

$$d = 0.6435\ m$$

The obtain diameter is quite good since it is a "small" value taking into consideration that the coffee growers have to manipulate the apparatus at this point, but we could also reduce the layer height a little bit and by doing so not only the manipulation will be easier but also as the layer will be thinner the drying at the same will be better. Let us try for example a height of $200\ mm$.

$$0.08619m^3 = \pi * \frac{d^2}{4} * 0.200m$$

$$d = 0.7407\ m$$

It seems to be a good result since the diameter still maneuverable and again, while reducing the coffee height the drying in a thin layer will be better.

As for the rest of the apparatus, the air gap between the trays will be reduced in the same proportion as the height was reduced $65\ mm$ and the whole structure will look like the one described in the Figure 75.

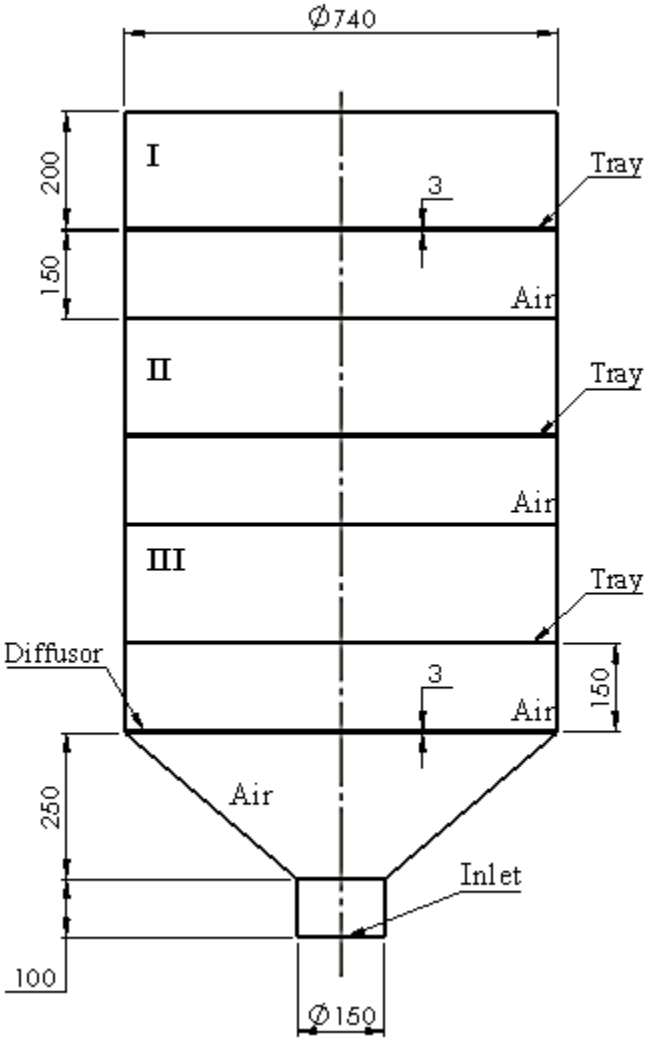

Figure 75. New dryer distribution with the general dimensions. Drawn in Solidworkd by the author.

The main changes despite the geometry is the air inlet and the location of a diffusor to make the air flow even across the whole apparatus and to disperse in all the locations.

10.2 Porosity calculations

The porosity as it is known is a ratio between the empty volume of a body and the solid volume of the same, as reads the equation 17

$$\varepsilon = \frac{V_{Space}}{V_{Total}}$$

10.2.1 Coffee Porosity

For the coffee porosity we have a very big advantage, because as we kept a constant volume for obtaining the same output of dried coffee, which means that the amount of seeds will be still the same, and, since the porosity is, in this case is dependent just on the volume of empty spaces of the whole bed and the volume of coffee we could say then that the porosity of the coffee layers are the same as those calculated for the rectangular dryer which have the following values.

$$\varepsilon_1 = 0.3096$$

$$\varepsilon_2 = 0.2987$$

$$\varepsilon_3 = 0.2879$$

10.2.2 Metal sheet porosity calculation

Now, the volume of the metal sheet will definitely change since we are now working with a circular shaped dryer, let us remind that the metal sheet has the following measures:

$$D = 740mm$$

$$h = 3mm$$

Then, calculating the value of the volume of the whole geometry we have that:

$$V_{Total\ Plate} = \pi * \frac{D^2}{4} * h$$

$$V_{Total\ Plate} = \pi * \frac{(749mm)^2}{4} * 3mm$$

$$V_{Total\ Plate} = 1290252mm^3$$

But now we should subtract from this volume the value of the empty geometries, to be able to calculate it in an easier way we created the 3D geometry in Solidworks (Figure 76), performed the

cuts and then the software automatically calculated the volume of the perforated plate which had the following value:

$$V_{Perforated\ plate} = 790259.76mm^3$$

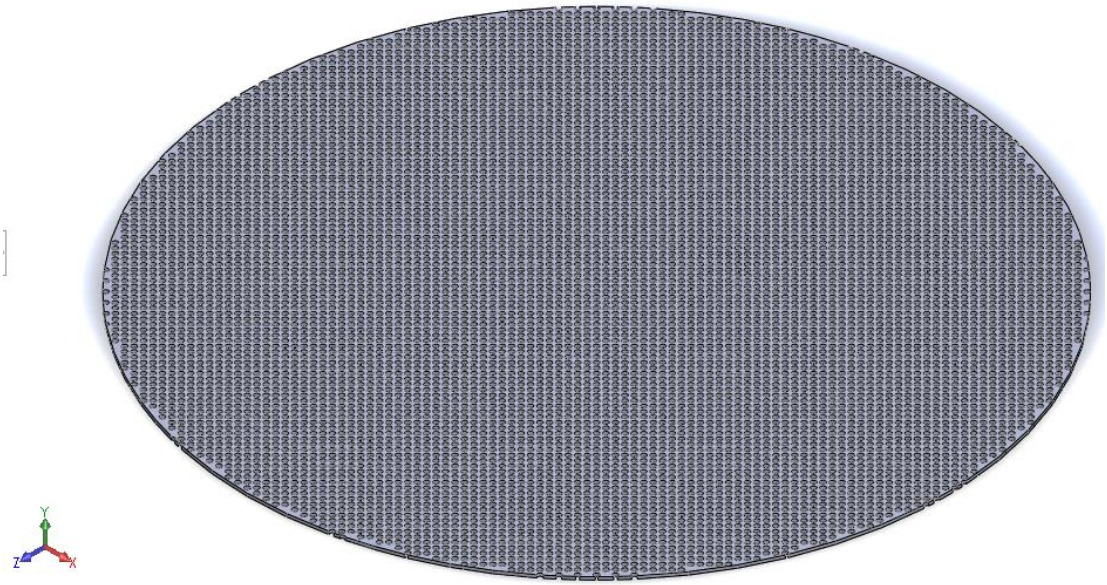

Figure 76. Circular shaped perforated plate drawn in Solidworks by the author.

Then we can easily calculate the porosity of the plate following the sated in the equation [18] which reads as follows:

$$\varepsilon_{SM} = \frac{V_{Holes}}{V_{Sheet}}$$

We could say that the V_{Holes} can be calculated as:

$$V_{Holes} = V_{Total\ Plate} - V_{Perforated\ plate}$$

$$V_{Holes} = 1290252mm^3 - 790259.76mm^3$$

$$V_{Holes} = 499992.34mm^3$$

And finally, we could consider the porosity of the whole perforated plate as:

$$\varepsilon_{Plate} = \frac{V_{Holes}}{V_{Perforated\ plate}}$$

$$\varepsilon_{Plate} = \frac{499992.34mm^3}{1290252mm^3}$$

$$\varepsilon_{Plate} = 0.3875$$

10.3 Temperature profile and stage humidity calculation

Now we will recalculate the temperature profiles across the apparatus since these temperatures are dependent on the height of the layer. We will use the same procedure as we did in the rectangular dryer, the problem is that we do not know the stage humidity for this specific case because the if the stage temperature will be higher, then the stage humidity will change and the drying time will change as well, so we will use the same stage humidity for a first approach and after we will iterate until we find the correct humidity.

$$T_e = \frac{(0.24 + 0.45H)T + c_p T_g}{0.24 + 0.45H + c_p}$$

Where:

- c_p: Specific heat of the grain, $\left[\frac{kJ}{kgK}\right]$
- H: Ratio of air humidity, $\left[\frac{kg_{steam}}{kg_{dry\ air}}\right]$
- T: Drying air temperature, $[°C]$
- T_g: Grain temperature, $[°C]$
- T_e: Equilibrium temperature of drying air and grain, $[°C]$

For calculating the c_p of the coffee:

$$c_p = 1.3556 + 5.7859M$$

Where:

- c_p: Specific heat, $\left[\frac{kJ}{kgK}\right]$
- M: Moisture content, decimal.

According to Serna et al. the temperature of grain T_g can be calculated as:

$$T_g = \frac{T * M * 0.95}{h}$$

Where:

- H: Ratio of air humidity, $\left[\frac{kg_{steam}}{kg_{dry\ air}}\right]$
- T: Drying air temperature, $[°C]$
- T_g: Grain temperature, $[°C]$
- h: Height of layer $[m]$

Solving for the tray 3 then:

$$T_g = \frac{50°C * 0.18 * 0.95}{0.2}$$

$$T_g = 42.75°C$$

$$c_p = 1.3556 + 5.7859M$$

$$c_p = 1.3556 + 5.7859(0.18)$$

$$c_p = 2.397\ \frac{kJ}{kgK}$$

$$T_2 = \frac{(0.24 + 0.45H)T + c_p T_g}{0.24 + 0.45H + c_p}$$

$$T_2 = \frac{(0.24 + 0.45 * 0.18)50 + (2.397 * 42.75)}{0.24 + (0.45 * 0.18) + 2.397}$$

$$T_2 = 43.6°C$$

Solving for the tray 2:

From the the first T_g the up following grain temperatures in each layer if the layer has the same height can be calculated as:

$$T_{g\_new} = T_{g1} - 9°C$$

Góngora et. al developed the relationship which establish this ratio, then:

$$T_g = 42.75 - 9$$

$$T_g \approx 33.75°C$$

$$c_p = 1.3556 + 5.7859M$$

$$c_p = 1.3556 + 5.7859(0.30)$$

$$c_p = 3.09\ \frac{kJ}{kgK}$$

$$T_3 = \frac{(0.24 + 0.45H)T + c_p T_g}{0.24 + 0.45H + c_p}$$

$$T_3 = \frac{(0.24 + 0.45 * 0.3)43.6 + (3.09 * 33.75)}{0.24 + (0.45 * 0.3) + 3.09}$$

$$T_3 = 34.82°C$$

Solving for the tray 1:

For the rectangular dryer the output temperature was around $21°C$ so now we could check the increase of the same as we have seen in the past two stages.

$$T_g = 33.75 - 9$$

$$T_g = 24.75°C$$

$$c_p = 1.3556 + 5.7859M$$

$$c_p = 1.3556 + 5.7859(0.53)$$

$$c_p = 4.42 \ \frac{kJ}{kgK}$$

$$T_4 = \frac{(0.24 + 0.45H)T + c_p T_g}{0.24 + 0.45H + c_p}$$

$$T_4 = \frac{(0.24 + 0.45 * 0.53)34.82 + (4.42 * 24.75)}{0.24 + (0.45 * 0.53) + 4.42}$$

$$T_4 = 25.73°C$$

We see that even while keeping the same humidity the temperatures are slightly higher than in the previous case, now we should recalculate the stage humidity with these new temperatures and after iterate the whole process until we reach some convergence values.

Using the equation 5 and 6 which respectively express the balance for the humidity ratio of the air:

$$\frac{\partial H}{\partial x} = -\frac{\rho_p}{G_a}\frac{\partial M}{\partial t}$$

And the thin-film drying equation of the product or grain moisture balance:

$$\frac{\partial M}{\partial t} = f(M, M_e, M_o, T, \dots t)$$

We can, with the new temperatures re calculate the stage humidity and drying time at all stages obtaining the following new results (take into consideration that the values of temperature must be re checked by some iterative procedure, see the calculations in the appendix A):

Stage 1:	Stage 2:	Stage 3:
X= 53%	X= 27%	X= 27%
m= 61.5 kg	m= 46.6 kg	m= 46.6 kg
t=0 h	t=6.16 h	t=6.16 h

Stage 4:	Stage 5:	Stage 6:
X= 15%	X= 15%	X= 12%
m= 39.75 kg	m= 39.75 kg	m= 31.19 kg
t=11.35 h	t=11.35 h	t=15.35 h

It is seen that even though the temperature values are not the final, the change in the geometry helped us to reduce the drying time in $3.58h$ which is a pretty good result for the moment. Now we will perform the iterations for temperature calculations and recalculate everything until convergence is obtained.

As final results we obtained the following data:

Dryer/Stage	Stage 1	Stage 2	Stage 3	Stage 4	Stage 5	Stage 6
Rectangular Dryer	X=53% m=61.5kg t= 0h T=21.86°C	X= 30% m=54.4kg t=7h T=30.99°C	X= 30% m=54.4kg t=7h T=30.99°C	X= 18% m=43.25kg t=14h T=40.19°C	X= 18% m=43.25kg t=14h T=40.19°C	X= 12% m=30.25kg t=21h T=50°C
Circular Dryer	X=53% m=61.5kg t= 0h T=26.3°C	X= 28.6% m=46.18kg t=6.1h T=35.1°C	X= 28.6% m=46.18kg t=6.1h T=35.1°C	X= 15.8% m=37.6kg t=12.8h T=43.8°C	X= 15.8% m=37.6kg t=12.8h T=43.8°C	X= 12% m=30.25kg t=17.42h T=50°C

Table 3. Stage humidity and temperature results.

As it can be seen in the Table 3, the influence of the geometry changes substantially the performance of the dryer. First of all, the drying time is around 3.58 hours less, which represent a huge advantage for the coffee grower because this mean that he will be able to dry the same amount of coffee with less energy. At the same time, he will be able to dry more quantity because the waiting time for the next load will be lower of course. Another remarkable element to highlight is

that the exit air in the circular shaped dryer is roughly 4.5°C higher than the rectangular one, and, if somebody will plan to reuse this stream for recirculating or some another use, those 4.5°C will definitely represent another energy saving.

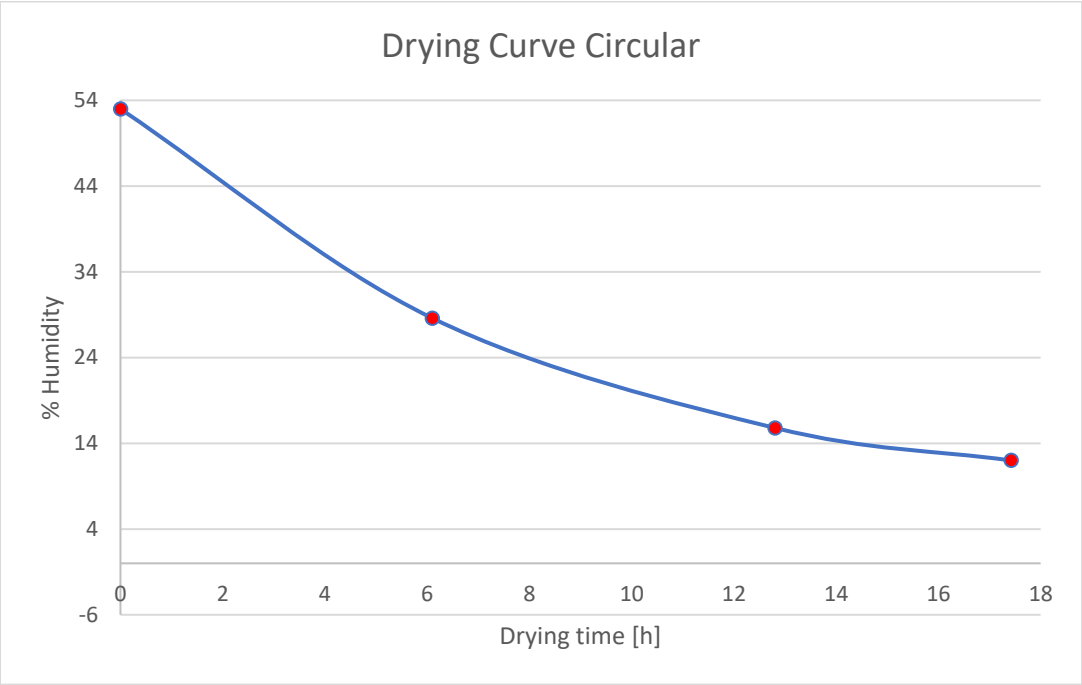

Figure 77. Drying curve of the circular dryer.

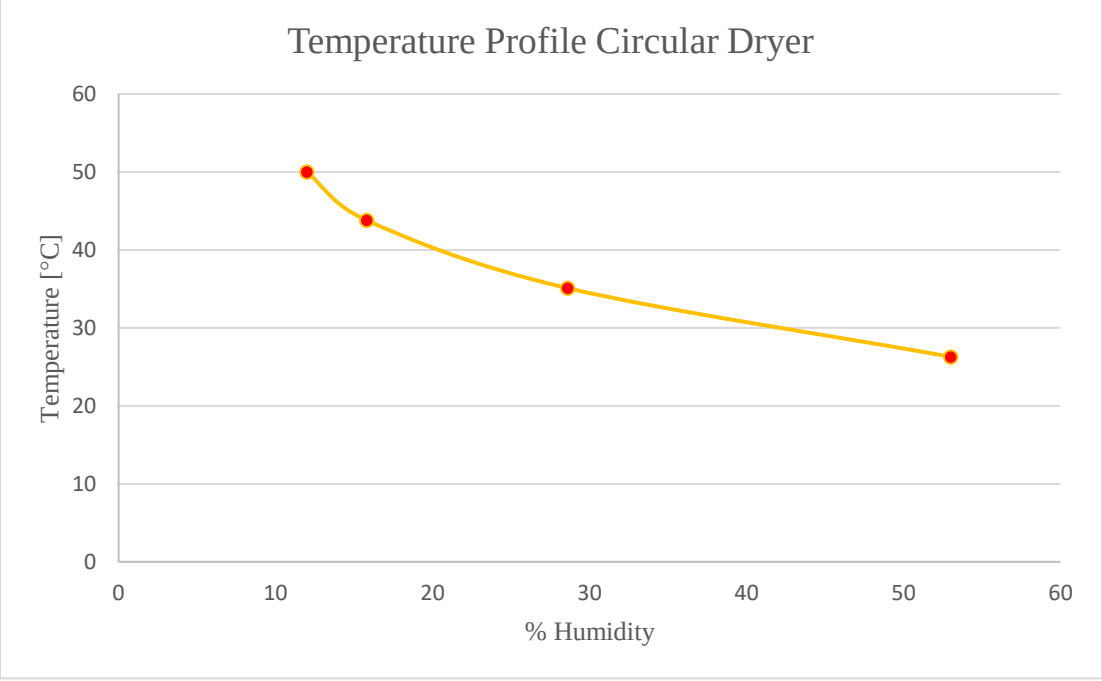

Figure 78. Temperature profile curve of the circular dryer.

As it can be seen in the Figures 77 and 78 the behaviour between both dryers is quite similar, nevertheless the fact of obtaining a higher output temperature and reducing the drying time represent really big achievements for our project.

10.4 Pressure drop ΔP calculation

10.4.1 Losses in the porous bed.

For calculating the losses in the porous media, we could use the same procedure as we used in the previous dryer by following the the Equation 19 which reads as follows:

$$e_z = \lambda' \frac{1-\varepsilon}{\varepsilon^3} \frac{h}{D_p} {u_0}^2$$

For determining λ' in the Equation 19 we should use some of the lambda calculation equations presented in the Figure 37.

And for the calculation of Reynolds number in a porous bed we can solve the Equation [20]:

$$Re = \frac{u_0 D_p \rho_{air}}{(1-\varepsilon)\mu_{air}} \qquad (20)$$

<u>For the tray number 3:</u>

- Velocity of the air:

$$u_0 = 1.3 \frac{m}{s}$$

- Reynolds calculation:

$$Re = \frac{1.3 \frac{m}{s} * 0.012m * 1.092 \frac{kg}{m^3}}{(1-0.2879)\ 1.963 \times 10^{-5} \frac{kg}{ms}}$$

$$Re = 1218.67$$

Since the Reynolds number do not depends on some changed variable, we will obtain the same value as in the past case.

- Friction coefficient λ' calculation:

$$\lambda' = \frac{A'}{Re}$$

$$\lambda' = \frac{160}{(1218.67)}$$

$$\lambda' = 0.1313$$

- Friction loss e_z calculation:

$$e_{z3} = 0.1313 * \frac{(1 - 0.2879)}{(0.2879)^3} * \frac{0.200}{0.012} * (1.3)^2$$

$$e_{z3} = 110.36 \frac{m^2}{s^2}$$

For the tray number 2:

- Velocity of the air:

We execute the same procedure described in the previous pressure drop calculation of the mean velocity as did for the rectangular shaped dryer:

$$\bar{u} = \frac{V_p}{V} u_0 \qquad (21)$$

Where:

- V:Volume occupied, $[m^3]$

- V_p: Volume pores, $[m^3]$

But again, taking a deep look into the Equation 21 the relationship which the volume ratio want to express is actually the porosity of the "obstacle" layer, which in this case is the porosity of the third bed. Rearranging terms we can formulate the following equation:

$$\bar{u} = \varepsilon_3 u_0 \qquad (22)$$

Solving for our data;

$$\bar{u}_2 = 0.2879 * 1.3 \frac{m}{s}$$

$$\bar{u}_2 = 0.3743 \frac{m}{s}$$

- Reynolds calculation:

$$Re = \frac{0.3743\frac{m}{s} * 0.012m * 1.127\frac{kg}{m^3}}{(1-0.2987)\ 1.918 \times 10^{-5}\frac{kg}{ms}}$$

$$Re = 376.33$$

Again, since the Reynolds number do not depend on any variated value it will remain the same and we can deduce from it that we are still in laminar regime, therefore we can now proceed and calculate the friction coefficient.

- Friction coefficient λ' calculation:

$$\lambda' = \frac{160}{(376.33)}$$

$$\lambda' = 0.4252$$

- Friction loss e_z calculation:

$$e_{z2} = 0.4252 * \frac{(1-0.2987)}{(0.2987)^3} * \frac{0.200}{0.012} * (0.3743)^2$$

$$e_{z2} = 26.13\frac{m^2}{s^2}$$

<u>For the tray number 1:</u>

- Velocity of the air:

$$\bar{u}_1 = \varepsilon_2 \bar{u}_2$$

$$\bar{u}_1 = 0.2987 * 0.3743\frac{m}{s}$$

$$\bar{u}_1 = 0.112\frac{m}{s}$$

Remember that it should be used the porosity of the second bed, because this is the one from which the air is coming from.

- Reynolds calculation:

$$Re = \frac{0.112\frac{m}{s} * 0.012m * 1.164\frac{kg}{m^3}}{(1-0.3096)\ 1.872 \times 10^{-5}\frac{kg}{ms}}$$

$$Re = 121.044$$

- Friction coefficient λ' calculation:

$$\lambda' = \frac{160}{(121.044)}$$

$$\lambda' = 1.3218$$

- Friction loss e_z calculation:

$$e_{z1} = 1.3218 * \frac{(1 - 0.3096)}{(0.3096)^3} * \frac{0.200}{0.012} * (0.112)^2$$

$$e_{z1} = 6.43 \frac{m^2}{s^2}$$

We already calculated the losses in all the porous beds present in the apparatus, now to be able to estimate the total friction loss e_z we must just add all the local e_{z1}, e_{z2} and e_{z3} :

$$e_z = e_{z1} + e_{z2} + e_{z3}$$

$$e_z = 110.36 + 26.13 + 6.43$$

$$e_z = 142.92 \frac{m^2}{s^2}$$

10.4.2 Friction losses in perforated plate.

For the pressure drop in the perforated plates we used the same online calculator but of course we selected the circular shaped perforated plate, let us remind that this calculator solves the required equations for a flow through a perforated plate (just as we need). Summarizing, as we already know the velocities in each stage of drying, temperature of the gas and general properties, we could search on tables for the hydraulic resistance coefficient and apply the Equation 23 or use the calculator which will automatically find the resistance coefficient for the plate depending on the velocity of air flow, temperature, dependent on temperature properties and pressure drop. The Equation 23 reads as follows:

$$e_z = \xi \frac{u^2}{2} \qquad (23)$$

Where:

- ξ: Resistance coefficient, $[-]$

- u: Velocity of fluid before the plate, $\left[\frac{m}{s}\right]$

For the plate in tray 3:

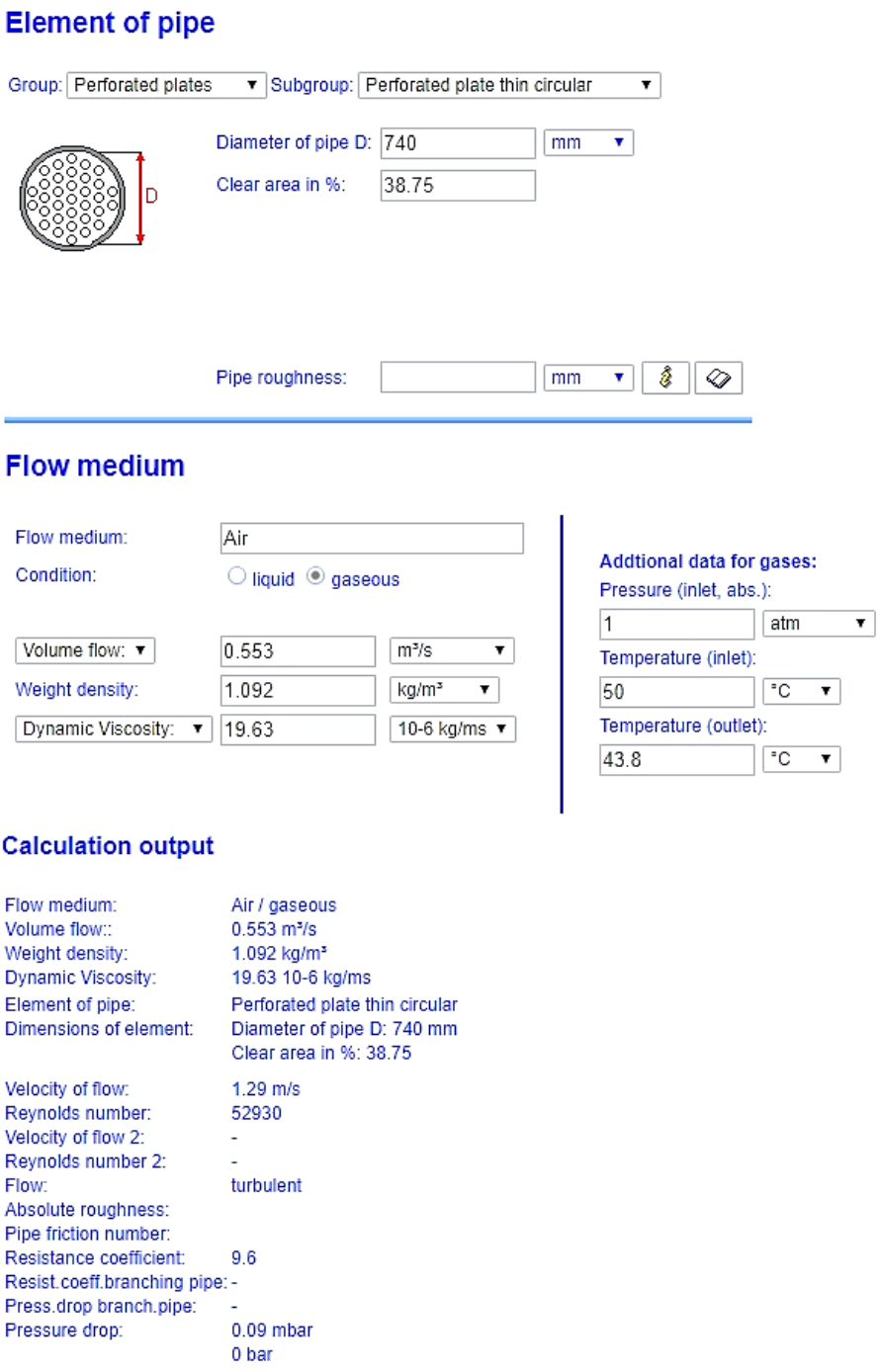

Figure 79. Results of pressure drop calculation for perforated plate in tray 3. http://www.pressure-drop.com/Online-Calculator/

The results of the pressure drop calculator are quite interesting because we can see that for instance the pressure drop is less than the one obtained in the rectangular dryer, as well have been given the hydraulic resistance coefficient, we will save the ξ_3 coefficient as for calculating the friction losses and being able to calculate the pressure drop by ourselves.

For the plate in tray 2:

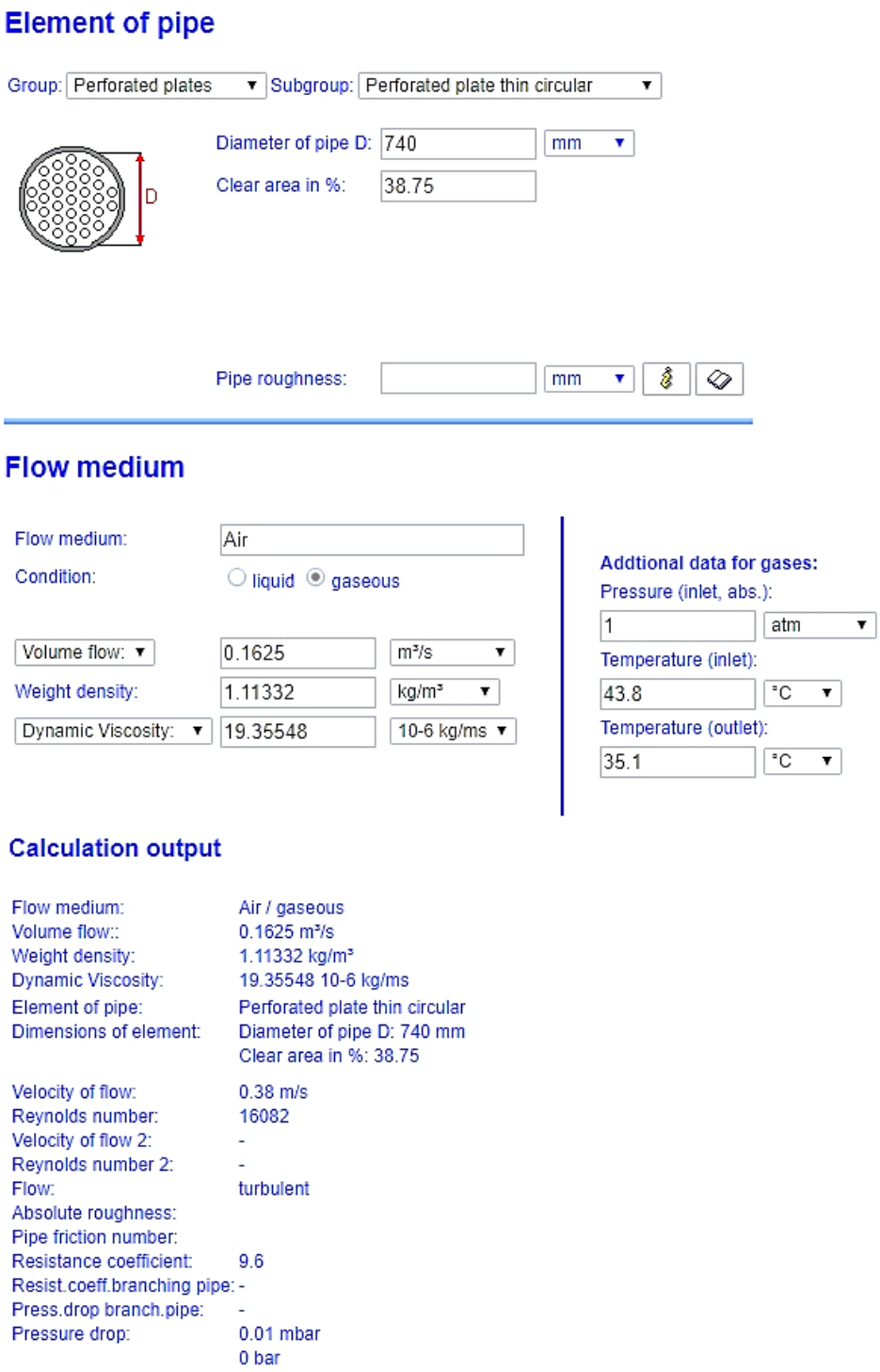

Figure 80. Results of pressure drop calculation for perforated plate in tray 2. http://www.pressure-drop.com/Online-Calculator/

We will save the ξ_2 coefficient as for calculating the friction losses and being able to calculate the pressure drop by ourselves.

For the plate in tray 1:

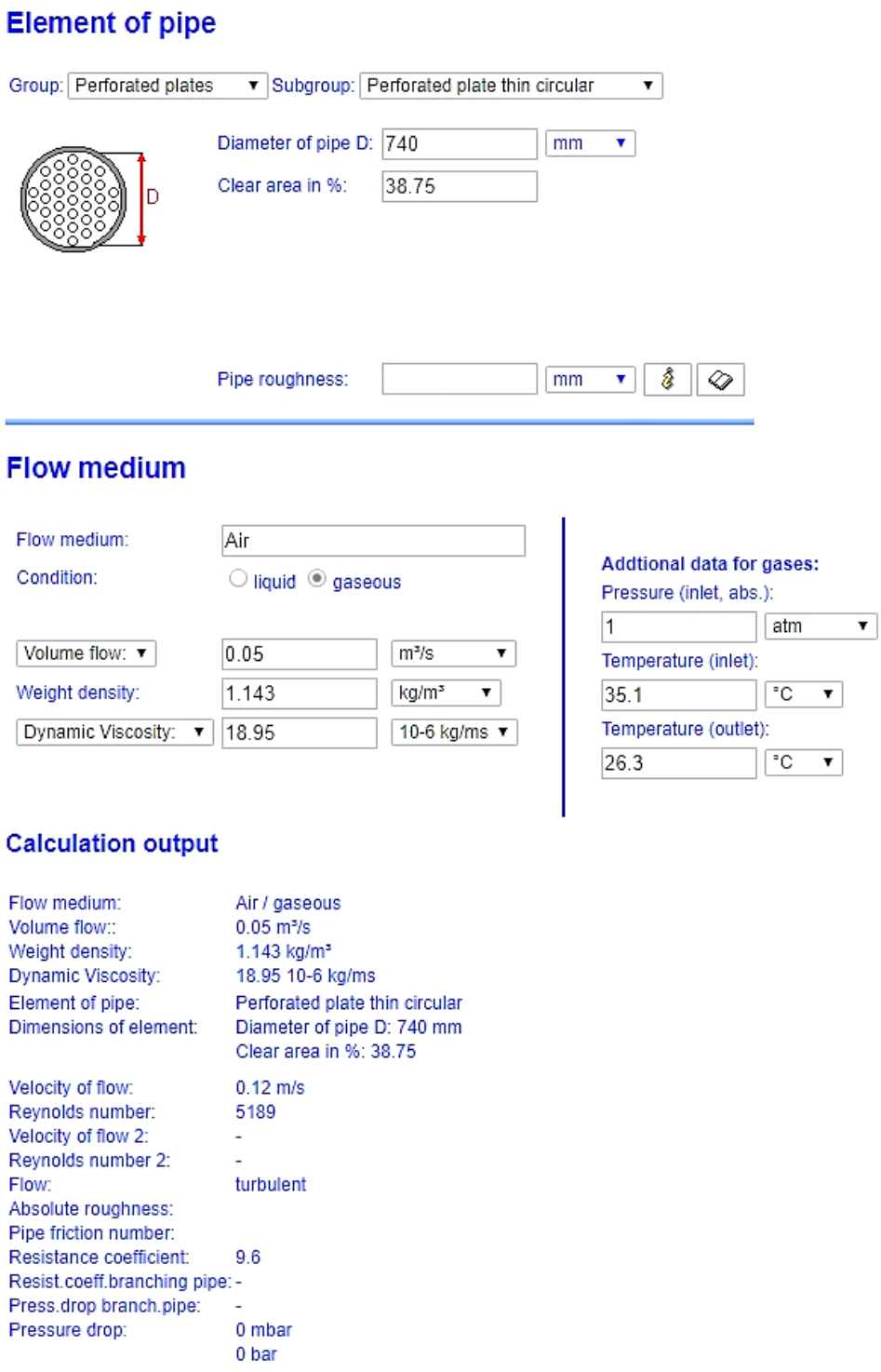

Figure 81. Results of pressure drop calculation for perforated plate in tray 1. http://www.pressure-drop.com/Online-Calculator/

We will save the ξ_1 coefficient as for calculating the friction losses and being able to calculate the pressure drop by ourselves.

Now, we already have all the hydraulic resistance coefficients, and we also know the velocity of the air in each stage of the dryer. We also know that the friction loss can be calculated as:

$$e_z = e_{zt1} + e_{zt2} + e_{zt3}$$

So, since we have all the information required for calculating the different friction losses, we compute them in the Equation [23] as follows:

$$e_{zt1} = \xi_1 \frac{{u_1}^2}{2}$$

$$e_{zt1} = 9.6 * \frac{0.112^2}{2}$$

$$e_{zt1} = 0.0602 \ \frac{m^2}{s^2}$$

$$e_{zt2} = \xi_2 \frac{{u_2}^2}{2}$$

$$e_{zt2} = 9.6 * \frac{0.3743^2}{2}$$

$$e_{zt2} = 0.6725 \ \frac{m^2}{s^2}$$

$$e_{zt3} = \xi_3 \frac{{u_3}^2}{2}$$

$$e_{zt3} = 9.6 * \frac{1.3^2}{2}$$

$$e_{zt3} = 8.112 \ \frac{m^2}{s^2}$$

$$e_z = e_{zt1} + e_{zt2} + e_{zt3}$$

$$e_z = 0.0602 + 0.6725 + 9.112$$

$$e_z = 9.8447 \ \frac{m^2}{s^2}$$

10.4.3 Computation for drop calculation

For the calculation of the pressure drop we can use the Bernoulli equation which reads as follows:

$$\frac{{u_1}^2}{2} + \frac{P_1}{\rho_1} + gz_1 = \frac{{u_2}^2}{2} + \frac{P_2}{\rho_2} + gz_2 + e_z$$

Equation [24]

Maintaining the same assumptions as in the previous pressure drop calculation, we can jump directly to the density calculation which will be as follows:

$$\bar{\rho} = \frac{\rho_1 + \rho_2}{2}$$

The new averaged density will be then equal to:

$$\bar{\rho} = \frac{1.092 + 1.184}{2}$$

$$\bar{\rho} = 1.138\ \frac{kg}{m^3}$$

The friction losses for our equipment will be equal to the total sum of the friction losses due to the porous beds and also the friction losses due to the perforated plates, then we could say that:

$$e_z = 142.92 + 9.85$$

$$e_z = 152.77\ \frac{m^2}{s^2}$$

After some rearrangement we could express the pressure drop as:

$$P_1 - P_2 = \left(\frac{{u_2}^2}{2} + gz_2 + e_z - \frac{{u_1}^2}{2}\right)\bar{\rho}$$

Computing the values, we have that:

$$P_1 - P_2 = \left(\frac{(0.112)^2}{2} + 9.81 * 1.41 + 152.77 - \frac{(1.3)^2}{2}\right)1.138$$

$$\Delta P = 188.64\ Pa = 1.88 \times 10^{-3}\ bar$$

11. Circular dryer simulation

Now that the general functioning of the new dryer has been calculated and we know on behalf that the performance regarding the drying time and the humidity removal is better, it is time then to perform a CFD simulation with the new geometry and elements which compose the new coffee

dryer. For such purposes three different types of dryer are proposed so we can ensure that the general performance of the dryer is the best. The three dryers vary mainly in the air distribution, we aim to make it even and as most equal as it can be across the whole apparatus. Having said this, we can introduce each type as the following:

- ***Diffuser in the bottom:*** The dryer will hold a diffusor in the bottom part to ensure that the velocity profile will be lowered and then on, homogeneous across the entire equipment (grey plate surrounded with blue in Figure 82).

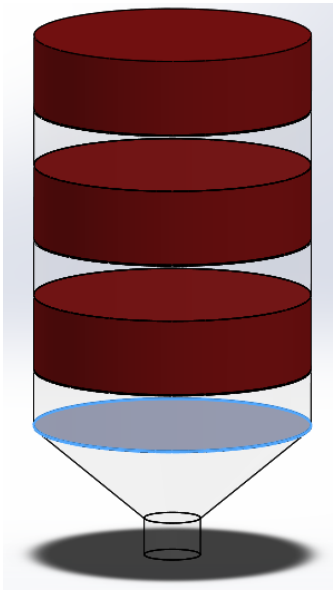

Figure 82. Bottom diffuser option. Drawn in Solidworks by the author.

- ***Diffuser and conical nozzle:*** to the first variant a conical shaped nozzle will be added in the bottom geometry, just at the air inlet to help distribute the air to the most peripherical regions of the dryer (orange surrounded geometry in Figure 83).

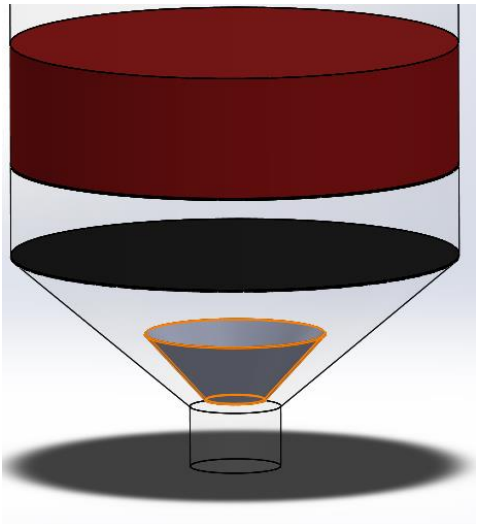

Figure 83. Bottom diffuser plus conical nozzle option. Drawn in Solidworks by the author.

– ***Ring Diffuser:*** Instead of using a single porosity diffuser as in the first option, a three ringed diffuser where each ring has a different porosity is proposed. By doing so the air distribution will be easily influenced and again the aim is to hit the peripherical places of the dryer (black geometries shown in Figure 84).

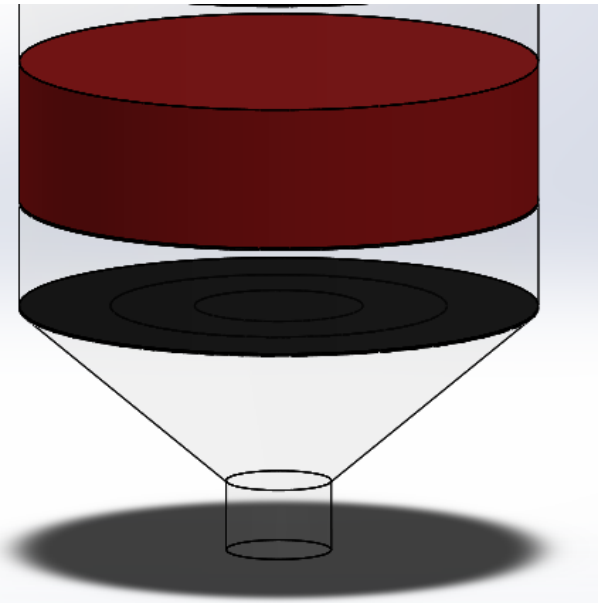

Figure 84. Ring diffuser. Drawn in Solidworks by the author.

After having defined the geometry a CFD simulation shall be done for a better understanding of the dryer functioning. Previous to run the CFD simulation, of course is necessary to mesh the geometries, in the table shown below we can see the mesh statistics for the three types of dryers:

Study	Number of elements	Number of nodes	Orthogonal quality			Skewness		
			Min	Avg	Max	Min	Avg	Max
Diffuser in the bottom	1894049	2023310	0.3544	0.9538	0.9999	5.1e-4	0.1291	0.841
Diffuser and conical nozzle	2141240	1621238	0.2674	0.9446	0.9999	1.05e -7	0.1258	0.794
Ring diffuser	1894564	2024886	0.3544	0.9538	0.9999	5.1e-4	0.1291	0.841

Table 4. Different circular dryer feature mesh statistics.

As for the mesh we can see that the three variants fulfill the requirements of skewness, orthogonal quality and number of elements, we can now run the simulation under the known process parameters (air velocity, flow, temperature, etc.) and a very important plot that should be taken into account is the convergence of the residuals.

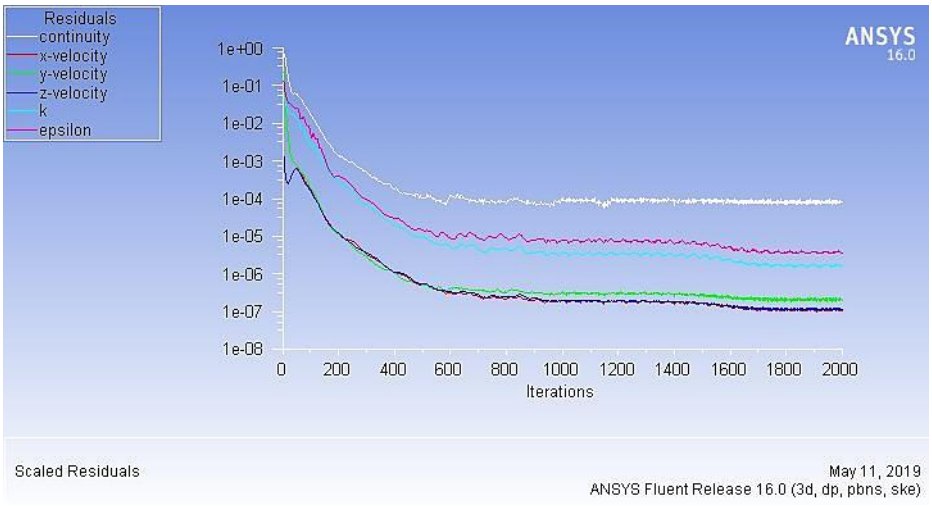

Figure 85. Scaled residuals plot bottom diffuser. Obtained from ANSYS by the author.

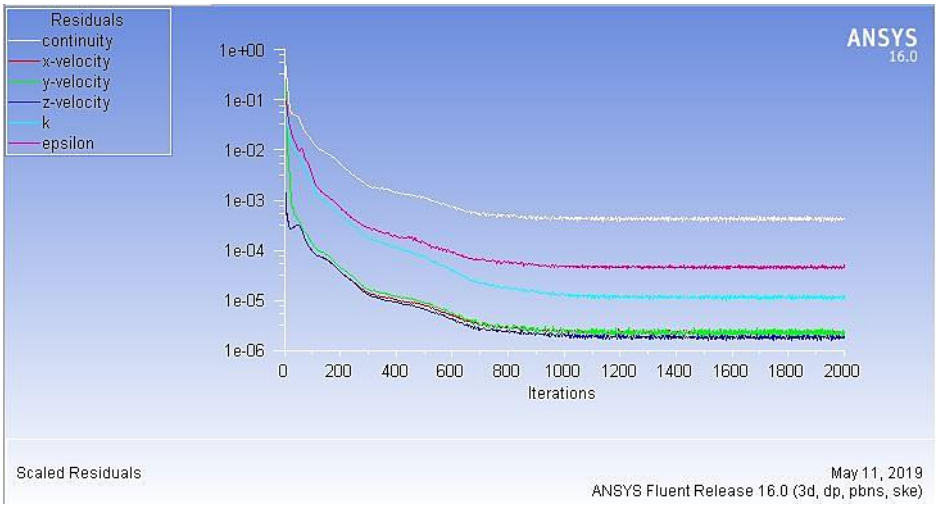

Figure 86. Scaled residuals plot bottom diffuser and conical nozzle. Obtained from ANSYS by the author.

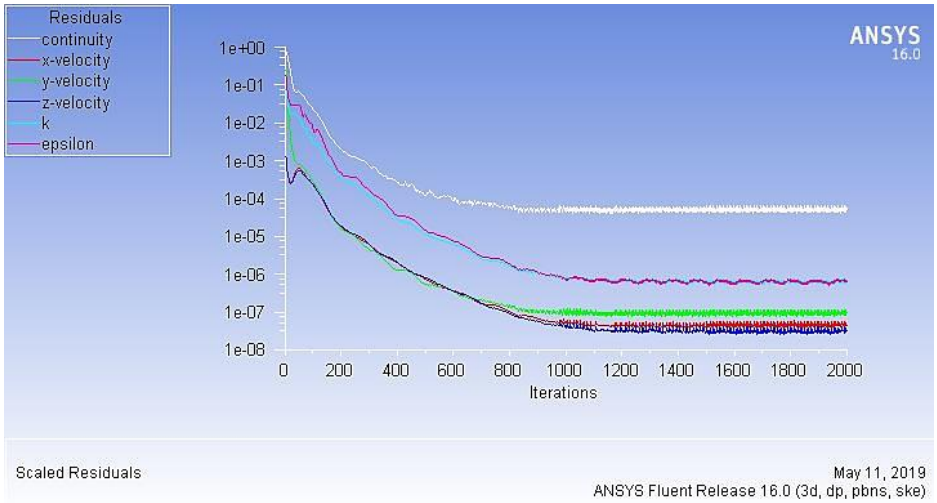

Figure 87. Scaled residuals plot ring diffusor. Obtained from ANSYS by the author.

As it can bee seen in the Figures 85, 86 and 87; the convergence was achieved in the three different cases, the convergence is important to be acquire because it means that a uniform solution behaviour has been found, therefore the general functioning can be predicted and forward trusted.

It was not settled any convergency value, because it was decided, for ensuring a long convergence time a value of 2000 iterations, it can be seen in the three graphs that by the iteration number 1000 the convergence is already achieved, therefore we have a homogeneous system solution along the next 1000 iterations, this will improve the accuracy of the results.

11.1 Post-analysis

Now that we have got some results it is time to analyze them one by one. We will analyze the velocity vectors and the streamlines of airflow across the three different geometries, then we can decide which dryer adjusts to our needs by having the most uniform airflow distribution and velocities.

11.1.1 Bottom diffuser dryer

As it was explained before, this dryer holds a sieve diffusor in the bottom part of its geometry (see Figure 82), by doing so it is expected that the airflow will be dispersed uniformly across the geometry and the velocities profile across the cross sectional area equalized, by achieving this we could expect a evener drying.

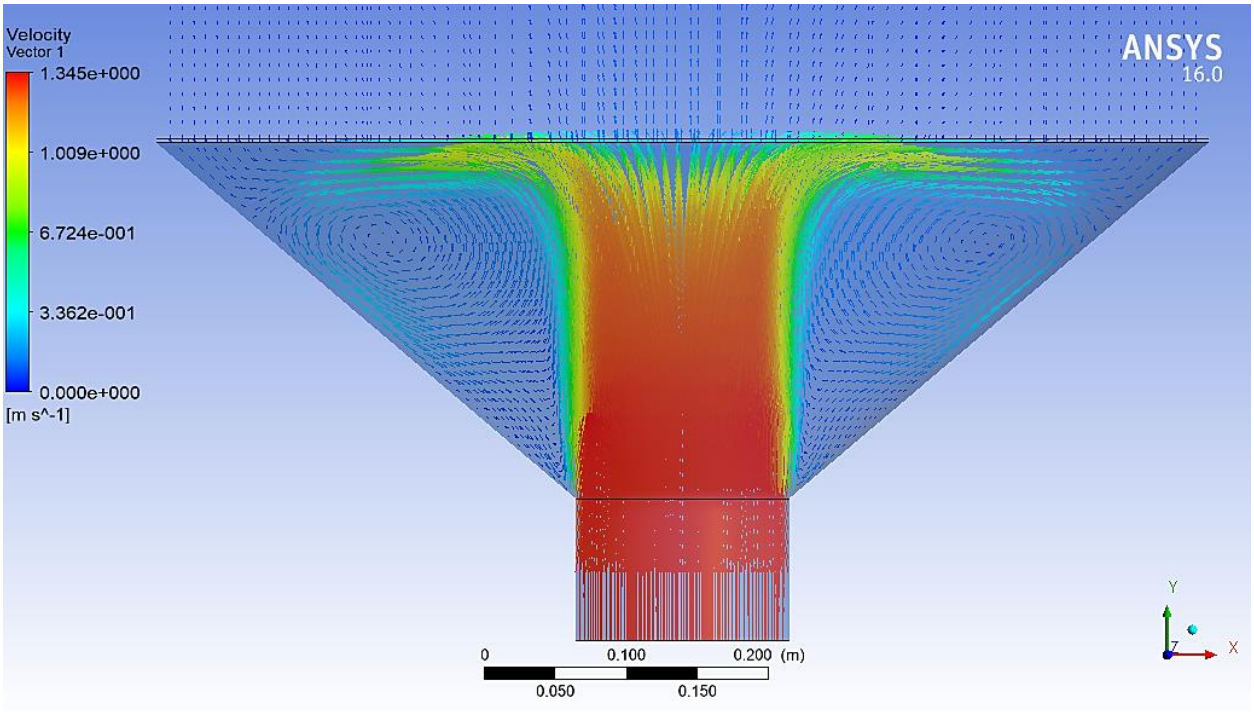

Figure 88. Velocity vector plot. Obtained from ANSYS by the author.

We can now make the first comparison with the square dryer; the air velocity is not lowered by a strange geometry (see Figure 71). This is good because the air velocity will improve the drying of course, as it was seen, the velocity has a very important impact in the thin layer drying, so, if we are able to have a higher velocity in the dryer and then make it more uniform as we can also see in the Figure 88 we are already in a good way.

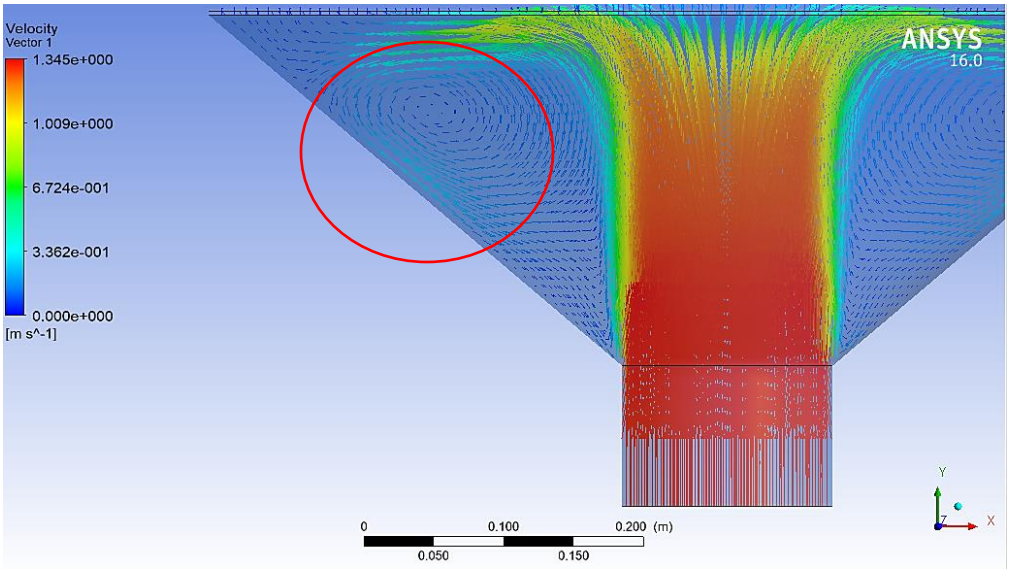

Figure 89. Velocity vector vortex. Obtained from ANSYS by the author.

It can be seen as well that the behaviour is completely symmetrical, at the same time in the Figure 89 we can see some vortexes generated circled in red, these vortexes are good because they will somehow, by the nature of the phenomena ensure a better air distribution. It is also seen that even in the corners of the dryer we have vectors present, this is also a remarkable achievement because the airflow will be even. Let us now see the streamlines and confirm the hypothesis stablished.

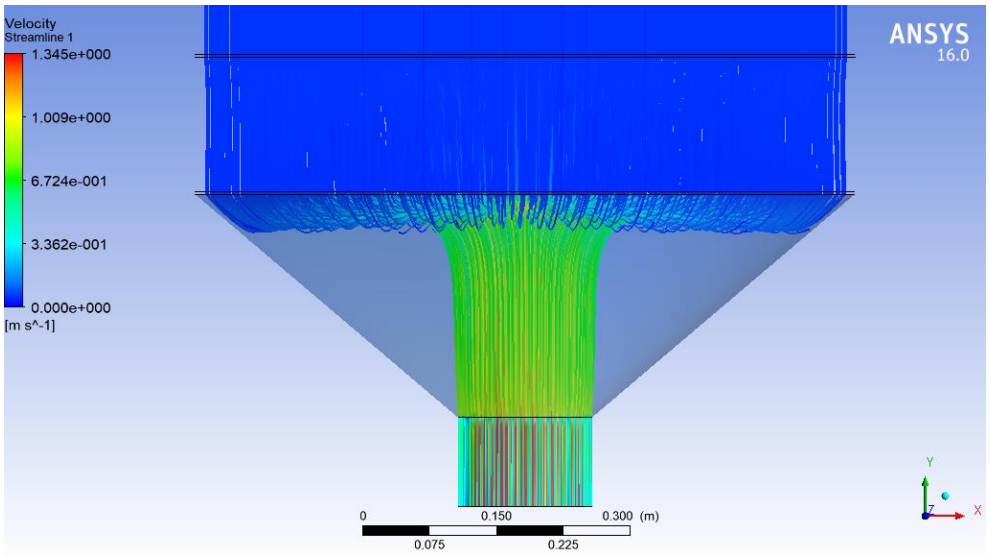

Figure 90. Velocity streamlines front-bottom view. Obtained from ANSYS by the author.

The Figure 90 displays the velocity streamlines for the actual model, it is seen that there is a relationship between the streamlines and the velocity vectors, a good thing is that the streamlines are present across all the geometry, even the corners. There is a action that can be taken to split the main airflow (in green) and try to spread it across the conical bottom shape, that is why the conical nozzle solution was proposed, but before performing the analysis on it let us take a look at the top view to see the air distribution across the cross section area.

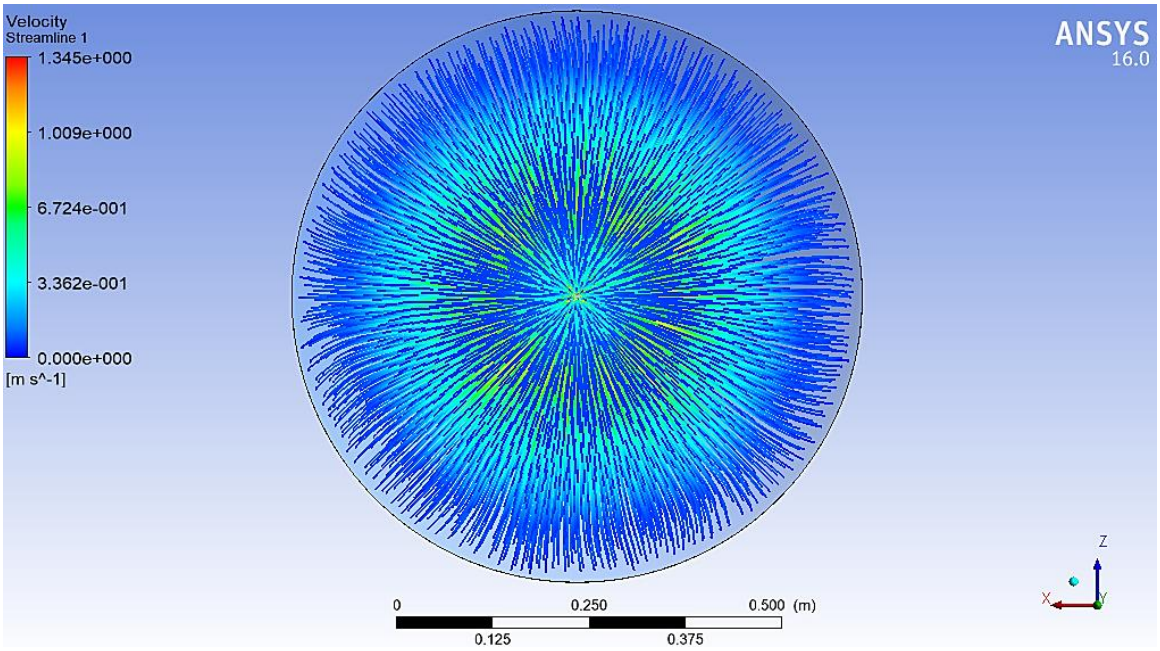

Figure 91. Velocity streamlines top view. Obtained from ANSYS by the author.

Well the Figure 91 is quite telling, we can see that the distribution of air improved notoriously compared with the square shaped dryer (Figure 74), it is seen that there are not blind spots, and we reached the peripherical zones with air, this will of course improve the drying hugely.

This dryer option represents a quite good option, the manufacturing is not that complicated, the air is well distributed, and it counts with the benefit that out of the three options, this one is the easiest to produce, which will have also a impact in the manufacturing cost, nevertheless we must have at least the other studies to compare the results and to have a solid base to defend or discard this option.

11.1.2 Bottom diffuser dryer and conical nozzle

So now we will try to break the main air current, to do so a conical shaped nozzle was proposed to be present in the conical segment of the dryer, just above the air inlet (Figure 83). By doing so it is expected to have a more homogeneous air distribution, but at the same time we can have the risk of velocity lowering and by so the drying would not be as efficient as needed.

At the same time, we can create reciprocate vortexes which are not good because they will create blind spots and perturbate a fine and steady air distribution.

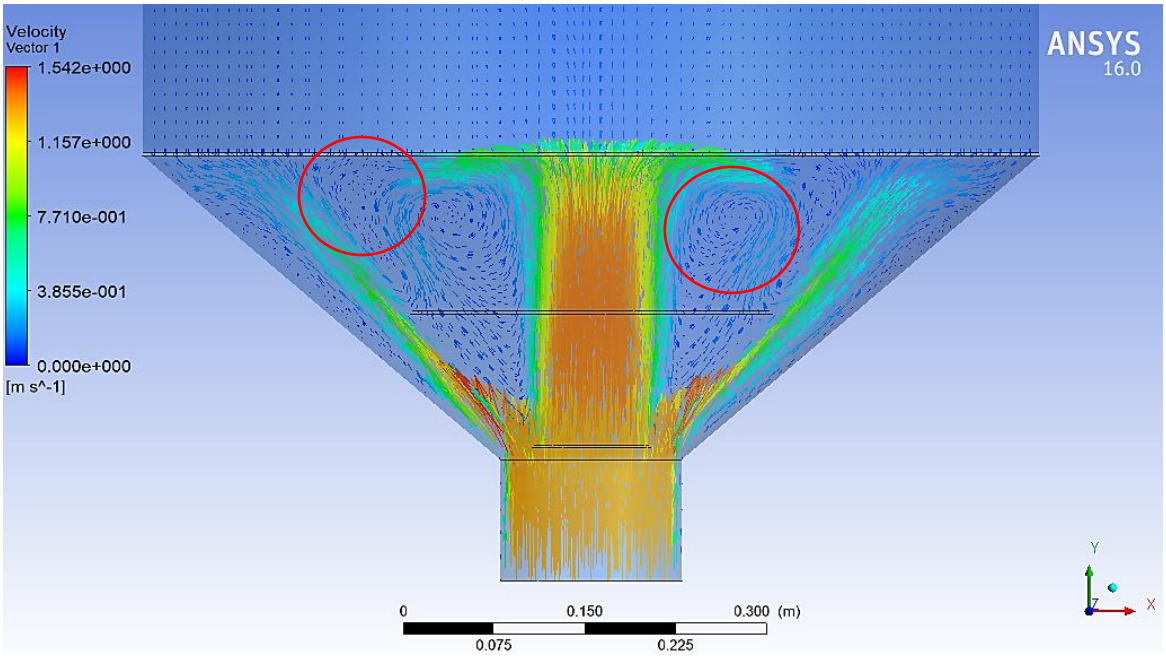

Figure 92. Velocity vector plot conical nozzle. Obtained from ANSYS by the author.

Well, as expected, the main airflow was split satisfactorily; it is seen that the conical shape distributes the air, and it looks good so far, but also, as it was predicted, some reciprocate vortexes can be seen in the figure. Let us take a look at those circled in red; they are locked between to main streams, therefore, in these places we could expect a blind spot, plus the angled wall of the dryer is facing a lack or air.

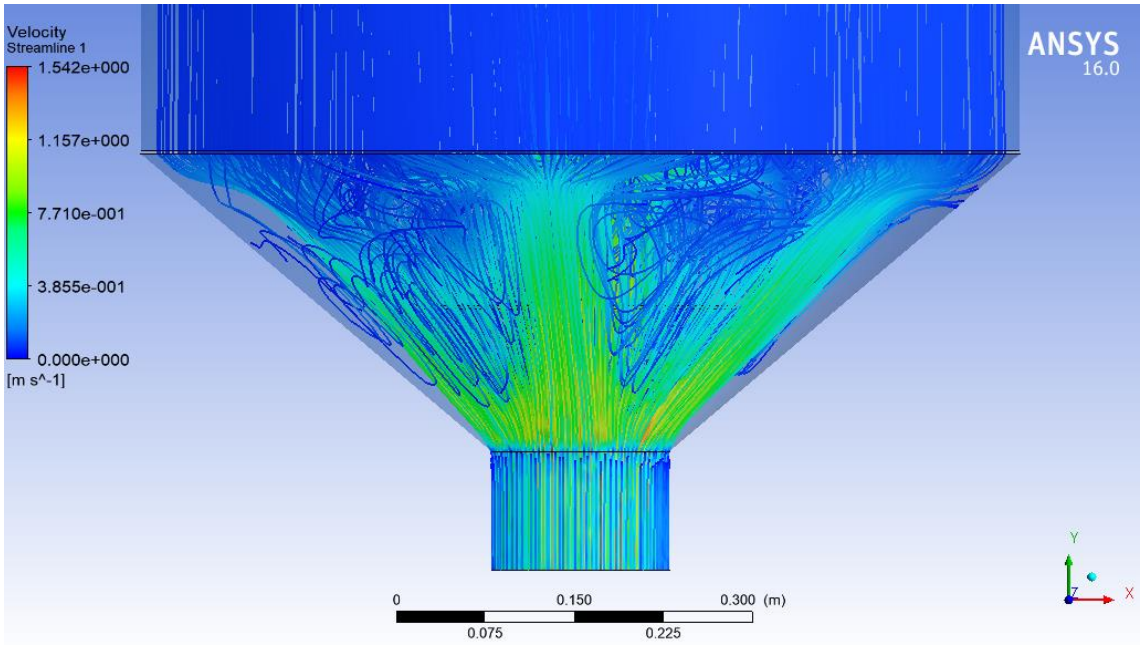

Figure 93. Velocity streamlines plot conical nozzle. Obtained from ANSYS by the author.

Well, as it was predicted, the dryer is facing some vorticity issues, at the same time we achieved the proposed: split the main air flow. It is also notorious the difference between the air distribution in the conical part between this model and with diffusor only (see Figure 90). Apparently after the diffusor in this model we have also a constant and uniform velocity, but regarding the reciprocate vortexes, do we have a uniform air distribution across the cross sectional area? We must then to verify this prediction, take a look at the top view of the dryer.

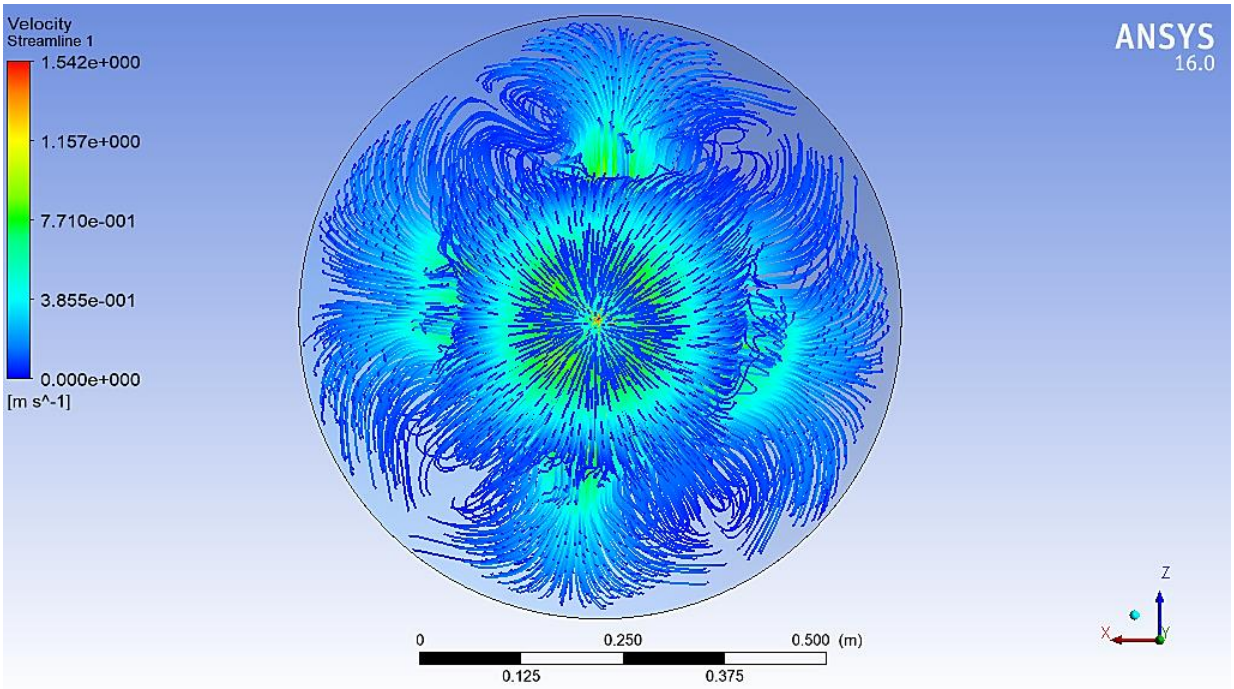

Figure 94. Velocity streamlines top view diffusor - conical. Obtained from ANSYS by the author.

As it was feared, the reciprocate vortexes create some non-desired blind spots where the evidence of air lack is quite big. Even though this distribution is better than the one we found in the square dryer, is also worse than the previous studied: Diffusor only.

11.1.3 Ring diffusor

Finally, we will perform the same analysis as to the previous models with the ring diffusor, so we can decide which type of dryer is more suitable for our purposes.

The ring diffusor dryer is meant to have three different rings, inner, mid and outed rings. Each one of these will have a different porosity, the inner will have less free space and the outer freer space, the mid ring will hold the average free space. By doing this we expect that the air will be a bit restrained in the inner ring and loose in the outer ring, therefore an improved peripherical distribution is expected.

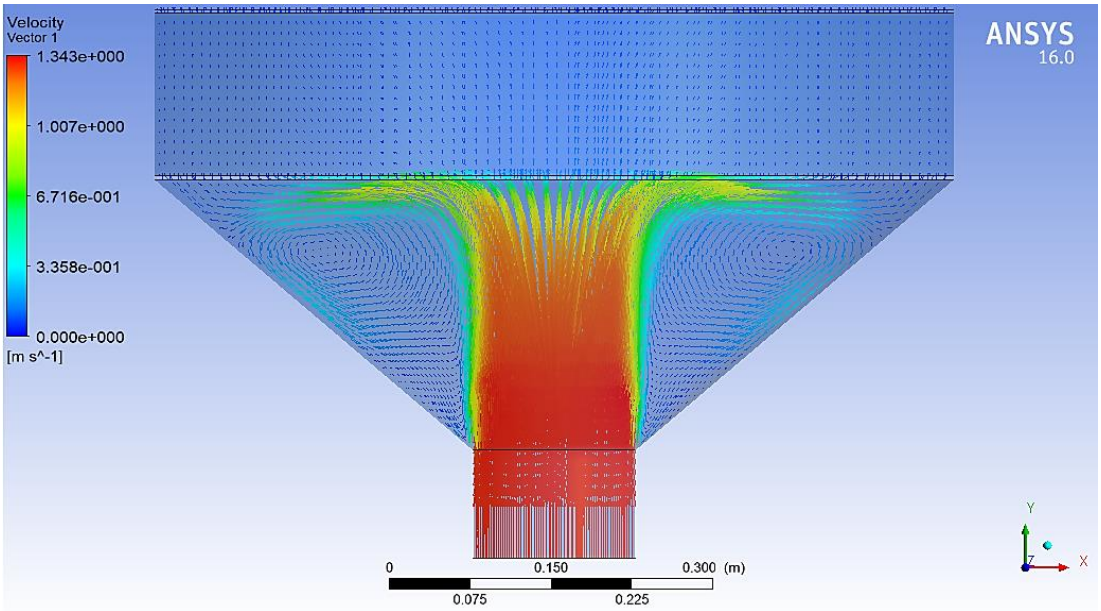

Figure 95. Velocity vectors ring diffusor. Obtained from ANSYS by the author.

In the Figure 95 we can appreciate that in the inner part of the dryer the breakthrough of the air is a bit different, let us say a bit more limited, this is due to the different porosities as explained before. We can see as well similar vortexes as in the first model which will improve the air distribution. So far it seems good, now let us take a look at the streamlines in order to get more information about this model and its performance.

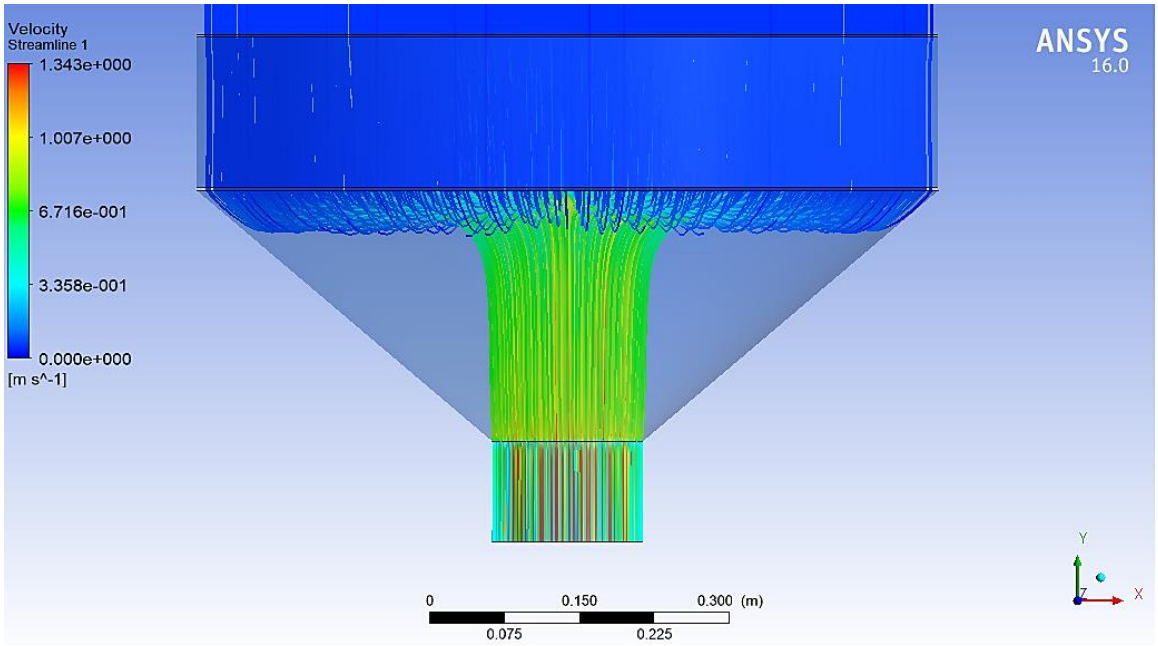

Figure 96. Velocity streamlines ring diffusor. Obtained from ANSYS by the author.

If we compare the Figure 96 and the Figure 90, we can see quite a similarity; the only small difference might be that the flowback charge in the inner ring is a bit higher due to the restriction

present in this part of the dryer. But it looks quite promising and for now it looks like after the ring diffusor a homogeneous profile is achieved. Now we will display the top view and analyze the streamline distribution from this point.

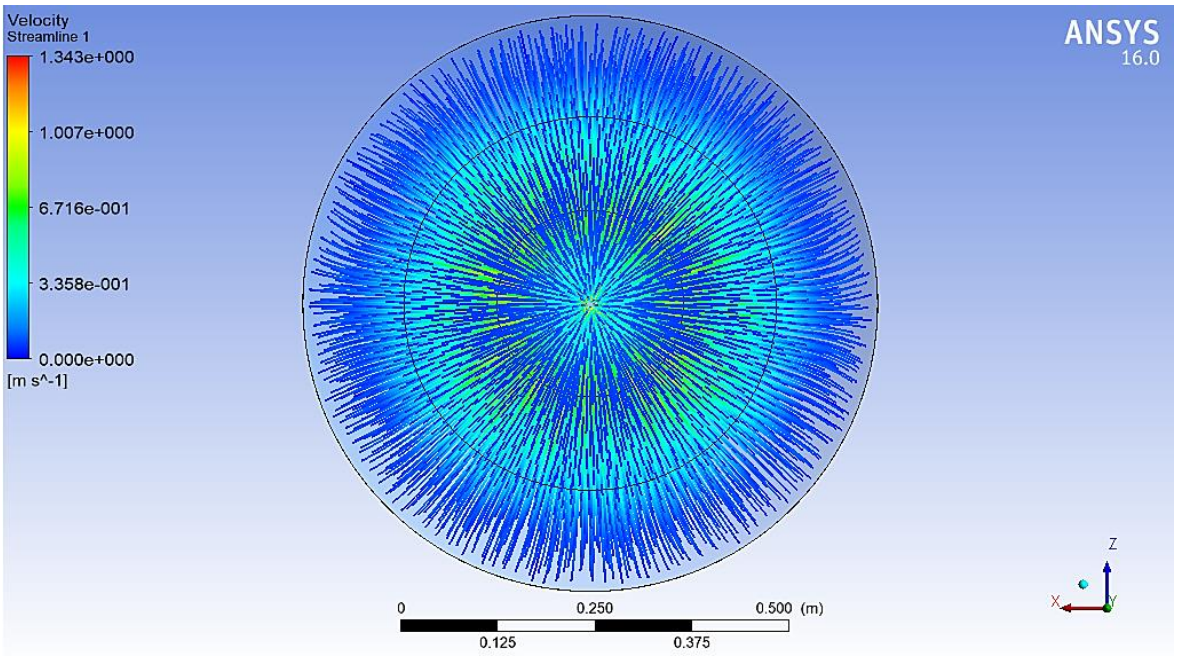

Figure 97. Velocity streamlines ring diffusor top view. Obtained from ANSYS by the author.

As displayed in the Figure 97, the streamlines are quite homogeneously distributed, quite similar to the first model. This is good but at the same time is a bit disappointing because we already achieved this behaviour with an easier solution.

11.2 Model choice

After analyzing the three states it was considered better to use the first one, the reasons are quite obvious: the distribution across the geometry is even and uniform as the third model but the first option is easier to manufacture and of course cheaper, and this fact will affect directly the selling price of the final apparatus; and if it is well remembered, this apparatus is intended to supply the needs of the small coffee growers which have low incomes and savings.

12. Construction

This chapter seeks to explain and show clearly the construction procedure of the dryer, even though the technical drawings are supplied, there are some matters that must been taken into account regarding the construction of the equipment. For instance, the welding order and position of dryer during the procedure to ensure the best possible results.

At the same time some calculations will be performed such as the buckling and stability control of the legs.

12.1 Body

The body construction is the most important because the whole performance depends on this point; the body construction will be as following.

1. Roll the main cylinder and weld as prescribed in the blueprint 002.
2. Weld the diffuser in the bottom part of the cylinder as shown in the blueprint 001 (element 13).
3. Turn the dryer upside down and weld the bottom tray at the shown position in the blueprint 001 (element 12).
4. With the dryer in the same position weld the middle tray and then the top tray at the shown position in the blueprint 001 (element 11).
5. Roll the cone and weld at the given measures as shown in the blueprint 002 sheet number 2.
6. Weld the cone to the body as shown in the blueprint 002, sheet number 2, section C.
7. Weld the nipple from the outside perimeter to the cone mouth as shown in the blueprint 002, sheet number 2, section C.
8. Perform the door cuts in the body as shown in the blueprint 002 sheet number 2.
9. Weld the elbow to the nipple as shown in the blueprint 002 sheet number 1.
10. Weld the loft geometry to the elbow as shown in the blueprint 002 sheet number 1.
11. Weld the loft geometry to the loft-fan connector as shown in the blueprint 002 sheet number 1.
12. Weld the leg support plate as shown in the blueprint 002 sheet number 1 detail H.
13. Weld the leg profiles to the support plates as shown in the blueprint 002 sheet number 1 detail H.
14. Weld the fixing pieces to the legs as shown in the blueprint 002 sheet number 8.
15. Construct the engine support to the fan geometry as shown in the blueprint 002 sheet number 6
16. Weld the fan system to the loft-fan connector as shown in the blueprint 002 sheet number 1.
17. Screw the furnace geometry to the fan cover.

12.2 Doors and hinges

1. Weld the hinge supports as shown in the blueprint 001.
2. On top of the hinge support, weld the first half of the hinge (hinge data on blueprint 006)
3. Roll the doors to the given dimension see blueprints 003 and 009
4. The second half of the hinge will be welded on the doors at different positions as shown in the blueprint 001.
5. Locate the handle and after knowing the trajectory of movement weld the lock.

12.3 Legs

The legs should be welded and located as explained in the section 12.1 points 12-14, but we would like to make sure that the legs will withstand the coffee load plus the weight of the apparatus, therefore a buckling and stability analysis shall be performed

12.1.1 Support Design

Now that the general dimensions, geometries, thicknesses and accessories of our dryer have been established, is time to proceed and perform the leg calculation and analysis. We would like the dryer to stand in the ground of course with the possibility to fix it by using bolts. Relying on previous expertise and experience in design of machinery it will be more than enough to use to use 3 UPN profiles (Figure 1) @120° each to give enough support to the apparatus.

The chosen profile for this application is a UPN 80 which has the following data:

$$I_x = 106\ cm^4$$
$$I_y = 19.40\ cm^4$$
$$A_S = 11\ cm^2$$

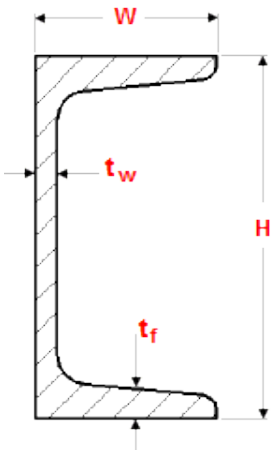

Figure 98. General dimensions of a UPN profile. Drawn in Solidworks by the author.

And the length of each leg is going to be $L_L = 600mm$ in order to be able to perform any operations in the air pipe elbow, fan, bolts, etc.

12.1.2 Buckling and Stability Calculations

We need to ensure ourselves that the legs are able to withstand the total weight of the structure and the coffee which will be held on the apparatus, for doing so we have the following data:

Mass of the dryer (ASTM A36)	96 kg
Mass of coffee in the different layers	140 kg
Total weight to withstand	2316 N
Weight per leg	771.7 N
Length of leg	600 mm

Table 5. Leg loading data.

Now, we need to calculate the critical force, this value represents the maximum load that one leg can withstand, in other words, if the real loading per leg exceeds the critical force value, the structure will collapse, or the legs will experiment buckling effect. We need to verify that the actual loading is lower than the critical force, for doing so we use the following statement:

$$F_{Cr} = n_i * \pi^2 * \frac{E * I_{min}}{L^2}$$

Where:

$$n_i = 1\ (Freedom\ degree)$$
$$E = 200\ GPa\ (ASTM\ A36\ Young\ modulus)$$
$$I_{min} = 19.40\ cm^4$$
$$L = 600\ mm\ (Length)$$

Computing the values:

$$F_{Cr} = 1 * \pi^2 * \frac{200000\ MPa * 19.40 cm^4 * \frac{(10mm)^4}{1cm^4}}{(600mm)^2}$$

$$F_{Cr} = 1063724.03\ N$$

$$F_{Cr} \geq Force\ per\ one\ leg$$

We can say then that the legs are going to withstand perfectly the weight of the loaded dryer, and of course the empty dryer as well, but just to be sure and check out the displacements in order to verify the safeness of the leg operation, we could perform a quick simulation for the piece with the real loading.

Performing a static analysis in one leg using a finite element method feature, we can see that the biggest displacement has a magnitude of $2.861e-003\ mm$ (see Figure 99)which is actually really low and acceptable for this design, at the same time there is non-buckling alert and the structural component in all the axis are conserved, therefore, we can say that the leg design fulfills our requirements.

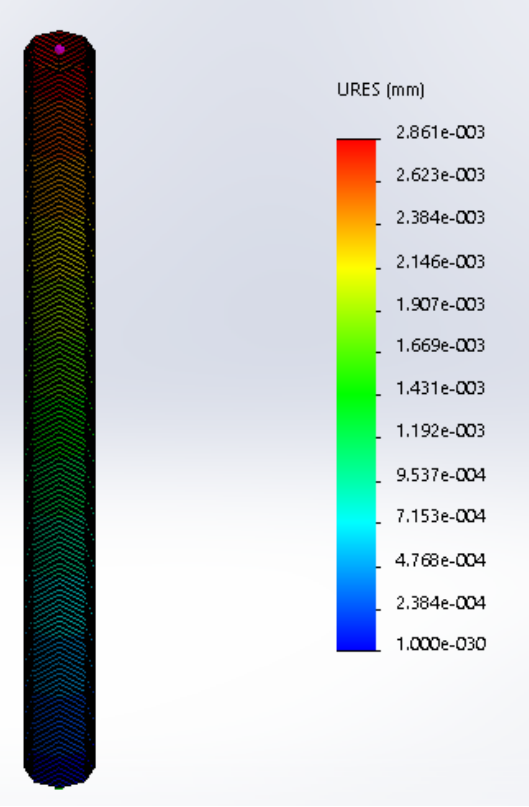

Figure 99. Simulation of the Loading of the legs. Obtained from Solidworks by the author.

Note: The software automatically change the geometry to a cylindrical shaped one with the aim of ease the meshing procedure, but the piece still have the same mechanical properties as the UPN profile while the analysis.

12.1.3 Welding calculations

If the load applied is not perfectly perpendicular to the fillet weld, the weld is in shear and its load carrying capacity is greatly reduced. Because of this reason, when designing welds, we always assume that the weld will be loaded in shear as seen below.

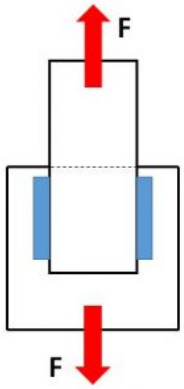

Figure 100. Welding forces. Drawn in Solidworks by the author.

For the calculation of the forces that the weld will withstand we shall take into account the following equation:

$$\tau_{allowable} = \frac{F}{A}$$

Where,

- $\tau_{allowable}$ is the maximum allowed shear stress on the weld.
- F is the force the weld can handle, in other words, the strength of the weld in N
- A is the effective area of the weld.

For our example we will use the data of the material Steel ASTM A-36, which has a tensile strength of 400-550 MPa. We are placing two (2) 100mm long lap welds on both sides of the joint.

If our two welds are 2mm fillets, then the shear strength (load carrying capacity) of the welds is calculated as follows.

First, we rearrange the formula provided above to solve for F.

$$F = A * \tau_{allowable}$$

To get A (effective area of the weld) we need to multiply the theoretical throat size (2mm) times the length (100mm) times 2 welds.

$$A = 0.002m * 2 * 0.1m$$

$$A = 0.0004m^2$$

We can now solve for F:

$$F = 0.0004m^2 * 550MPa$$

$$F = 220kN$$

Which is a really acceptable value since this is only for one leg, and, as it can be seen in the table 5, each leg should withstand 772N. Hence, we could say that the welding is quite safe.

12.4 Process flow diagram (PFD)

Now that we have all the documentation for the implementation of this coffee dryer we can then display the PFD of the process, we can also prepare a future PFD where a heat exchanger will be used to indirectly heat the drying air, but for now our solution which, is directed to the small coffee grower will use the flue gas for drying of the grain.

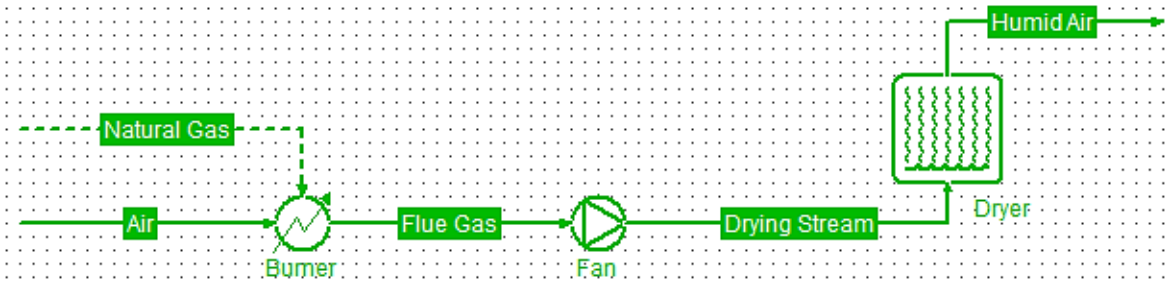

Figure 101. PFD of the designed process. Obtained from COFE by the author.

As it can be seen in the Figure 100, our process is quite simple, which is really good as for maintenance and construction costs. We must also include a fan on/off switch and a solenoid valve which will shut off the gas supply in case of an energy blackout.

As for future drying methods we propose the following process for further study and design in the coffee drying topic.

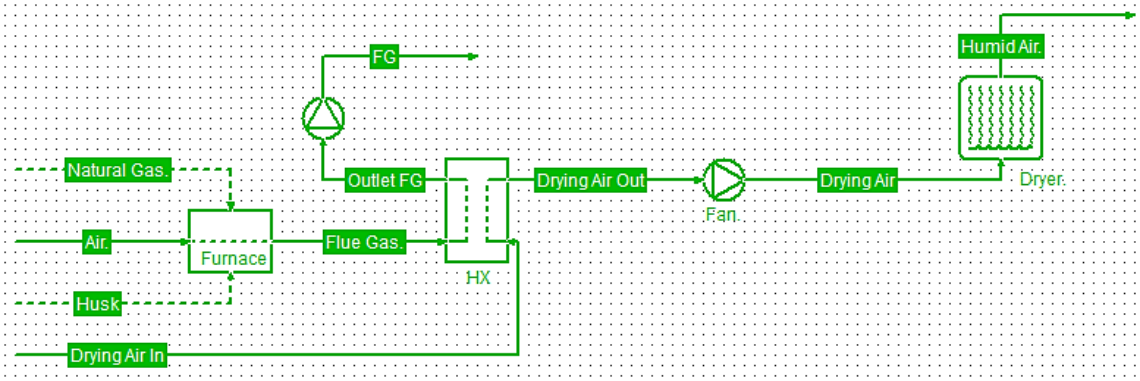

Figure 102. PFD of alternative pilot model for coffee drying. Obtained from COFE by the author.

The model displayed in the Figure 101 might have a better performance, but at the same time is more costly and for sure a small coffee grower would not be able to afford this drying method; on the other hand it might be interesting if it would be proposed as for middle and big coffee producers but it would be a complete different work.

13. General aspects

Let us make a very important statement, due to the multiple geometries which the trays hold, in the CAD model was impossible to recreate them, because for further display of the perforations the memory demand was quite high and eventually the model was immediately shut down. Reason why in the assembly blueprint and in the following snaps the perforations are not visible.

Nevertheless, in each individual construction blueprint of the trays and diffusor the required information for buying/manufacturing is provided.

Another important issue to highlight is related with the analysis of the circular dryer in the CFD Simulation. It was not explicitly explained how we performed the analysis, but the number of nodes, elements and mesh statistics are supplied; it is expected from the reader to develop some tacit mental procedure taking as an example the simulation explanation of the rectangular dryer, in other words, the circular dryer followed the same procedure as the rectangular one, of course, taking into account the different process parameters.

Having said all of the above, let us now display some general snaps from the dryer prototype already built and holding the components for its functioning.

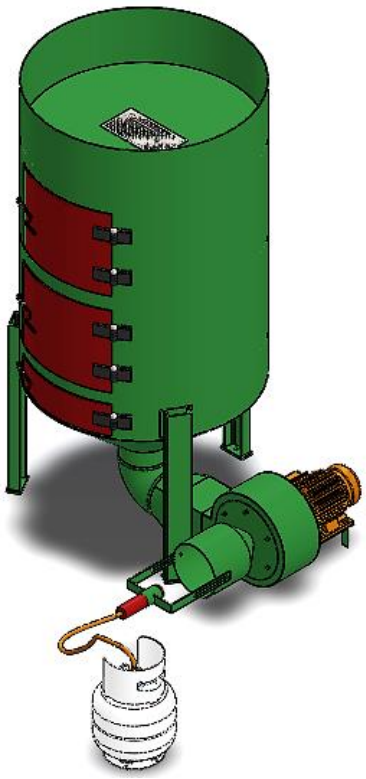

Figure 103. Snapshot of the new dryer. Drawn in Solidworks by the author.

As it is seen in the Figure 102 the new dryer holds a lot of similarities with the rectangular one, but of course, as it was developed across this entire document, this drier holds a more powerful and efficient performance.

One of the main concerns while setting up the dryer might be the buckling of the trays when they will be charged with coffee, but as a small reminder, the tray is 3mm thick and will hold in the worse case 62.5 kg, when the wet coffee is introduced in the first stage of the drying. Which is not that heavy. Therefore, we should not be concerned about warping of the plates.

It is also important as a remark that a gap of 12mm was left between the elbow, loft geometry, fan connector and fan case with the ground in order to solve the possible thermal dilatation issues.

14. Conclusions

As a main conclusion we could say that this entire project was solved smartly, all of the actions taken were done taking into account the main reason of the project itself: the coffee grower. The new dryer was designed properly, and the biggest issues of the square dryer were solved properly.

- The new dryer efficiently uses the drying air across its new geometry, we could see in the CFD simulations that the shape changed drastically the airflow distribution which is one of the most important aspects when it comes to drying. At the same time, the idea of including a diffusor helped to settle a uniform velocity across the drying sections and this, in addition to the uniform air improved the general drying process substantially.
- The performance of the square dryer is evidently lower, if we compare the plots of air streamlines, we will see that the circular shaped holds a better air distribution. Another matter which is related with the air distribution is not just the circular shape of the new dryer, but as well the bottom air inlet plays a really big role in the process; while in the rectangular dryer the air enters through one side and it crashes with some metal sheet, the circular dryer uses the airflow in all its "magnitude", and then the shape allows the air to do its work more efficiently.
- We had some doubts when it came to use the direct combusted air (flue gas) as drying flow, but at the same time we search to be pragmatic and practical, and, if the most specialized coffee tasters do not perceive issues in the taste or aroma related to the flue gas drying, then the most wise decision was to keep working as it does nowadays. It might be not the most accurate and fine way, but we have to consider the low price of production, and by adding some indirect heating media the prices would rise quite a lot (it would be an interesting topic to perform some study related with the penetration depth of "non-desired" gases across the parchment of the coffee and see how much its components penetrate this layer). Therefore, a new proposal using a heat exchanger was given, in which the air is heated indirectly, but for this project is out of boundaries because of its price and required equipment, it can be a good topic for further studies.
- The drying time was reduced significantly; from 21 hours we were able to lower the drying of the same amount of coffee to 17.4 hours. This means that, theoretically 17% of the drying time will be saved, reducing the general time in 3.6 hours, and this represents not only a really big saving in energy, gas, etc. But at the same time, it represents a really big improvement as for the amount of coffee which will be dried, the square dryer can make 3 and 1/7 cycles per day, while the circular dryer offers 4 complete cycles and it still has some time gap maybe for cleaning or charging new fresh coffee. As well, a uniform residual humidity distribution is expected.
- The work performed was quite extensive, the calculation of stage humidity removal and stage temperature calculation for the circular dryer was done. The CFD analysis for the square dryer was done with which an optimal design was done and the CFD analysis of the 3 different proposals of the circular dryer (distributers) were also executed. Two PFD's were also design for the implementation of the process and another one as for future expansion of the process and the whole new proposal was analyzed and calculates exhaustively to be able to be able to make a concise proposal which addresses correctly the problems cited

throughout the work. And last but not least, the technical drawings for manufacturing of the apparatus were also drawn so tests can be performed or why not, directly build it and set it into working.

As a general conclusion we could say that the entire project was a success, now it is only a matter of time and resources to build a real model and perform experiments on it or maybe also offer it as a solution for the coffee producers and let them test it and get their feedback.

Literature

1. BAKKER A., T.W.; LEREW, L.E.; DE BOER, S.F.; ROTH, M.C. Grain drying simulation. Michigan: Michigan state university, 1974. 80 p.

2. BROOKER, D.B.; BAKKER A., F.W.; HALL, C.W. Drying and storage of grains and oilseeds: An AVI book. New York: Van Nostrand Reinhold, 1992. 450 p.

3. CENKOWSKI, S.; JAYAS, D.S.; PABIS, S. Deep-bed grain drying: A review of particular theories. Drying technology 11(7):1553-1581. 1993.

4. CFC. Enhancement of coffee quality through prevention of mould formation: Appraisal report. Amsterdam: CFC, 1999. 44 p.

5. DOMÍNGUEZ, J.; PARRA, A. Estudio del potencial de secado con aire natural y energía solar de una región. Bogotá: Universidad Nacional de Colombia. Facultad de ingeniería, 1.982. 135 p.

6. FNC. Análisis de la encuesta sobre beneficio y calidades de café: Documento interno de la sección ingeniería agrícola. Manizales: Cenicafé, 1984.

7. JARAMILLO, B.G. Propiedades físicas del café pergamino. Bogotá: Universidad Nacional de Colombia. Facultad de ciencias, 1989. 190 p.

8. JARAMILLO R., A.; ARCILA P., J. Variabilidad climática en la zona cafetera asociada con el evento de La Niña y su efecto en la caficultura colombiana. Manizales: Cenicafé, 2009. 8 p. (Avances Técnicos No. 389).

9. JURADO C., J.M.; MONTOYA R., E.C.; OLIVEROS T., C.E.; GARCÍA A., J. Método para medir el contenido de humedad del café pergamino en el secado solar. Cenicafé 60(2):135-147. 2009.

10. LÓPEZ, J.; OSPINA, J. Ecuación de capa delgada para el café pergamino: Informe de año sabático. Chinchiná: Cenicafé, 1990. 183 p.

11. MONTILLA P., J.; ARCILA P., J.; ARISTIZÁBAL L., M.; MONTOYA R., E.C.; PUERTA Q., G.I.; OLIVEROS T., C.E.; CADENA G., G. Caracterización de algunas propiedades físicas y factores de conversión del café durante el proceso de beneficio húmedo tradicional. Cenicafé 59(2):120-142. 2008.

12. MONTOYA R., E.C.; OLIVEROS T., C.E.; ROA M., G. Optimización Operacional del Secador Intermitente de Flujos Concurrentes para Café Pergamino. Cenicafé 41(1): 19-33. 1990.

13. OLIVEROS T., C.E.; RAMÍREZ G., C.A.; SANZ U., J.R.; PEÑUELA M., A.E. Secador de túnel para café pergamino. Manizales: Cenicafé, 2006. 8 p. (Avances Técnicos No. 253).

14. PARRA C., A.; ROA M., G., OLIVEROS T., C.E. SECAFÉ: Modelamiento y simulación matemática en el secado mecánico del café. Revista brasileira de engenharia agrícola e ambiental 12(4):415-427. 2008.

15. PARRA C., A.; ROA M., G., OLIVEROS T., C.E. SECAFÉ: Recomendaciones para el manejo eficiente de los secadores mecánicos de café pergamino. Revista brasileira de engenharia agrícola e ambiental 12(4):428-434. 2008.

16. RIVERA, O.L.; VÉLEZ P., A. Evaluación de una secadora de café de 12 arrobas (para pequeños cafeteros). Medellín: Corporación Universitaria Lasallista. Facultad de ingeniería de alimentos, 1997. 166 p.

17. ROA M., G.; OLIVEROS T., C.E.; ÁLVAREZ G., J.; RAMÍREZ G., C.A.; SANZ U., J.R.; ÁLVAREZ H., J.R.; DÁVILA A., M.T.; ZAMBRANO F., D.A.; PUERTA Q., G.I.; RODRÍGUEZ V., N. Beneficio ecológico del café. Chinchiná: Cenicafé, 1999. 300 p.

18. ROSSI, J.R.; ROA, G. Secagem e armazenamento de produto agropecuari com uso de energia solar e ar natural. Sao Pablo: ACIESP, 1980. 293 p.

19. THOMPSON, T.L.; PEART, R.M.; FOSTER, G.H. Mathematical simulation of corn drying: A new model. Transaction of the ASAE 11(4):582-586. 1968.

20. TREJOS, R.R. Determinación de las curvas de humedad relativa de equilibrio y del calor latente de vaporización del café pergamino y trillado. Cali: Universidad del Valle. Departamento de procesos químicos y biológicos, 1986. 171 p.

21. WAGNER, R. Historia del café de Guatemala. Bogotá: Benjamín Villegas editores, 2003. 224 p.

22. WATSON, E; BESORE, J. Drying drawer and method of drying. Atlanta Georgia, 2009, US8245414B2.

23. WINGER, R; SMITH, D. Drying of grains as an economical issue. Wye, Kent. 1997. p 23.

24. YUNKER, J; STILL, T. Suppression of the coffee-ring effect by shape-dependent capillary interactions. Nature 476, 308-311. August 18 2011.

25. ZULUAGA, L; VILLEGAS, M. Secado solar: una realidad alternative. Revista del agro colombiano. Volumen 19 p. 17-21. Cali, Colombia .

List of figures and tables

List of figures

List of tables